

L.A. ORBELI INSTITUTE OF PHYSIOLOGY
NATIONAL ACADEMY OF SCIENCES, REPUBLIC OF ARMENIA

ARESTAKESYAN HOVHANNES VREZH

SPECIFIC EFFECTS OF MACROVIPERA LEBETINA OBTUSA
SNAKE VENOM ON CULTURED MYOCARDIAL CELLS

THESIS

submitted for the degree of candidate of biological sciences
on the specialty 03.00.09 – Human and Animal Physiology

Scientific supervisor: PhD, Z.I. Karabekian

YEREVAN 2017

Table of Contents

List of abbreviations used in thesis	4
Introduction	5
Chapter 1 Literature review	8
1.1. Myocardium	8
1.1.1. Morphological and physiological characteristics of myocardium	8
1.1.2. Proliferative and regenerative characteristics of cardiac muscle	20
1.2. Cell adhesion.....	25
1.2.1. Molecular mechanisms of adhesion in myocardium and epithelial cells...	29
1.3. Macrovipera lebetina obtusa snake venom.....	33
1.4. Models used in this study.....	37
1.4.1. NRCM as a model for the study of morphological, biochemical and electrophysiological characteristics of the heart.....	37
1.4.2. HeLa cells as a model for studying epithelial cells	38
1.5. Venom-cardiomyocyte studies.....	38
1.5.1. Cardiovascular effects of Crotalid and Viperid venoms	39
1.5.2. Hemodynamic effects of Viperid venoms	39
1.5.3. Mechanism of depressor action of Viperid venoms	46
Chapter 2 Materials and methods	51
2.1. Cells.....	51
2.2. Venom collection and desiccation	52
2.3. Venom stock solution preparation and further dilutions	52
2.4. Preparation of thermally-treated venom	52
2.5. Preparation of PLA2 inhibited venom	53
2.6. Preparation of metalloproteinases inhibited venom.....	53
2.7. Venom enzymatic activity testing.....	53

2.7.1. Verification of venom caseinolytic activity in vitro	53
2.7.2. Verification of venom phospholipase activity in vitro	54
2.8. Morphological characterization of NRCM, CF, and HeLa cells	54
2.9. Physiological characterization of NRCM	55
2.9.1. Fluo-4 AM loading	55
2.9.2. Recording and analysis of Ca ²⁺ transients/sparks in NRCM.....	55
2.10. MTT viability assay	58
2.11. Statistics	58
Chapter 3 Results	60
3.1. Correlation of MLO doses with morphological/structural changes on tested cells with viability	60
3.1.1. MLO venom effect on NRCM.....	60
3.1.2. MLO venom effect on CF.....	71
3.1.3. MLO venom effect on HeLa cells	75
3.2. Unraveling the mechanisms of MLO detaching effects	79
3.2.1. Effect of MLO+BPB mixture on NRCM	79
3.2.2. Effect of MLO+BPB mixture on CF	82
3.2.3. Effect of MLO+BPB mixture on HeLa cells.....	85
3.3. Effect of metalloproteinases inhibited MLO venom	88
3.3.1. Effect of MLO+EDTA-Na ₂ mixture on NRCM.....	88
3.3.2. Effect of MLO+EDTA-Na ₂ mixture on CF.....	91
3.3.3. Effect of MLO+EDTA-Na ₂ mixture on HeLa cells	94
Chapter 4 Discussion.....	97
Conclusions	102
Future directions	103
References	105

List of abbreviations used in thesis

ATP - adenosine triphosphate
ATPase - adenosine-triphosphatase
BPB - bromophenacyl bromide
CF - cardiac fibroblast
CM - cardiomyocyte
CMF-HBSS - calcium and magnesium-free Hank's Balanced Salt Solution
CNP - C-type natriuretic peptide
DMEM - Dulbecco's Modified Essential Medium
DNA - deoxyribonucleic acid
ECM - extracellular matrix
EDTA-Na₂ - ethylenediaminetetraacetic acid's sodium salt
Fluo-4 AM - non-fluorescent acetoxymethyl ester
KTS motif - Lysine-Threonine-Serine motif
LD₅₀ - lethal dose 50
MHC - major histocompatibility complex
MI - myocardial infarction
MLD-dependent integrin - Methionine-Leucine-Aspartate dependent integrin
MLO - *Macrovipera lebetina obtusa*
MP - metalloproteinase
MTT - methyl-thiazolyl-tetrazolium
NP - natriuretic peptide
NRCM - neonatal rat cardiomyocyte
NRS - normal rat serum
PEF - polyethylene film
PLA₂ - phospholipase A₂
RGD-dependent integrin - Arginine-Glycine-Aspartate dependent integrin
ROS - reactive oxygen species
SERCA-2 - sarcoplasmic reticulum Ca²⁺ ATPase
SR - sarcoplasmic reticulum
YBS - yolk buffer solution

Introduction

Relevance of the study. Studies of *Vipera* genus snakes' venom demonstrated a significant difference in the mode of action of their diverse components. Such divergence depends on the prey and the ultimate goal of specific envenomation. The initial analyses of venoms discovered identical families of enzymes and polypeptides among various types of snakes and common principals of their activity. However, a deeper analysis revealed the strict specificity of venom components unique to a given species and even sub-species of snakes. The habitat of a prey and the type of animal used as food greatly influences the composition of the venom. The specific composition of venom ensures certain kind of damages for the quick death of prey [1]. On the whole body level, the prey is being immobilized and disoriented, develops pain syndrome and hypotonic collapse. Destruction of multiple organs and organ systems occurs on the level of functional systems. On a molecular level, venom components act with high specificity on mechanisms of cellular activity of a prey. It is important to mention that the main action of venoms is not only in a direct interaction of venom component with its target but also in an induction of hyperactivity and the generalized reaction of the whole organism to the venom. As opposed to plant poisons, which mainly block a target function in a body of a prey, injected animal venom often recruits prey's defense mechanisms to fight against itself [2]. Many venom components act as bi- or multi-functional agents and depending on the effector site can exhibit enzymatic activity and/or serve as a ligand for different receptors and signaling systems [3].

The focus of our study is the venom of *Macrovipera lebetina obtusa* (*MLO*) living in Armenia and its effect on the cells of the myocardium. This species contains several sub-species, which are characterized by a very specific combination of components [4]–[7]. Along with common enzymes characteristic of *Vipera* species, *MLO* venom contains unique components specific for “obtusa” sub-species, such as disintegrin obtustatin [6]. This and some other components, at large, define the uniqueness of this venom. *MLO* venom contents metalloproteinases, phospholipase

A2, serine proteases, L-alfa amino acid oxidase, few kinds of disintegrins and some other active agents [6]. The cluster of *MLO* venom components, such as metalloproteinases, obtustatin, C-type lectins and few others are known as cell adhesion inhibition molecules, which are breaking up integrins and cadherins or bind to them [6], [8], [9]. Therefore, the adhesion affecting properties of *MLO* venom and its action on cell binding in tissue culture was of an interest.

The overarching objective of this study was to investigate the anti-adhesive actions of fermentative systems and active polypeptides of *MLO* snake venom. Specifically, we aim to examine the effect of active venom's molecules on the connection of cell with the extracellular matrix and intercellular connections. Additionally, we aim to examine the survivability of cardiomyocytes (NRCM) and other nondirect targets of the *MLO* venom, such as cardiac fibroblasts (CF) and epithelial HeLa cells. The necessity of such studies is substantiated by the basic mechanisms of the *MLO* snake venom's action. Among well-characterized effects of this venom is its hemolytic activity on erythrocytes; moreover effect on the vascular system, results in damage to histohematic barriers and leakage of plasma proteins into surrounding tissues; and finally, *MLO* venom affects hemostasis by aggregating platelets and activating different clotting proteins etc. Among the non-canonical effects of *MLO* snake venom the following processes need to be included – the destruction of cellular membranes, induction of pathologic inflammation, apoptosis, necrosis, ischemia of different organs and organ systems, as well as pre-digestion of prey's tissues.

The understanding of venom's specialized and general action mechanisms on the prey's organism is necessary for its potential use as a therapeutic or diagnostic agent. More importantly, it is necessary to understand the molecular responses of a prey, in order to synthesize easily obtainable and highly specified medications. Such studies usually transferred from *in vivo* investigations on the whole organism level to *in vitro* or even *in silico* studies. A special role is given to genetically modified animals (knockout mice, chimerical mice that express human MHC molecules, animals with

recombinant fluorescent target proteins, etc.) and to cultures of both primary and immortalized cells. This allows us to overcome the long process of “tuning” of the effective dose for prospective medication and allows us to identify the major side effects prior to animal testing.

The specific objectives of this project were:

1. Detecting the general effect of *MLO* snake venom on the morphology of cultured NRCMs, CFs, and model epithelial cells.
2. Identifying the morphological and physiological effects of non-lethal doses of *MLO* venom on investigated cell types.
3. Determining the effect of *MLO* venom exposure time on the adhesion properties of tested cells.
4. Correlating the dose and time dependent effects to detachment of *MLO*-treated cells with their subsequent viability.
5. Investigating the role of the PLA2 component of the *MLO* venom on the attachment and viability of tested cells.
6. Investigating the role of *MLO* venom metalloproteinases on the attachment and viability of tested cells.

Chapter 1 Literature review

1.1. Myocardium

The myocardium or cardiac muscle consists of highly organized and interconnected network of cardiac cells. There are two main types of cells in myocardium: cardiomyocytes and fibroblasts. They are mutually necessary for the work, but they don't carry out the same function. Volume-wise, the working myocardium consists of approximately 75% of cardiomyocytes due to their size, however, these cells make up 30-40% of the total cell number [10]. The remaining cells are mainly non-myocytes, specifically cardiac fibroblasts. Endothelial and vascular smooth muscle cells are also present, but in rather small amounts [11]. The fundamental contractile cell of the myocardium is the myocyte. The uniform contraction of heart cardiomyocytes is a prerequisite for the effective pump action of the heart. That in turn, provides an adequate blood flow to peripheral organs and tissues [12]. Ion channels that accurately control the transport of Ca^{2+} across the cellular membrane and into the sarcolemma are responsible for the contractility of individual cardiomyocytes [12]. Fibroblasts are present throughout the myocardium. They support cardiomyocytes and create connections between different strata of myocardial tissue, such that every cardiomyocyte is in close relation with a fibroblast. In general, fibroblasts participate in the cardiac development, the formation of the myocardial structure; cell signaling, the biochemical and electromechanical function of the heart tissue [13]–[20].

1.1.1. Morphological and physiological characteristics of myocardium

Cardiac muscle is striated, although the pattern is not as ordered as in skeletal muscle (Fig.1). There are several unique structural features characteristic of the myocardium which ensures its proper functioning.

Basement membrane: The basement membrane is the first boundary encountered when moving from the extracellular space to the intracellular space of

the myocyte (Fig.2). Type IV collagen, glycoproteins, laminin, fibronectin, and proteoglycans are the primary component of the basement membrane [21].

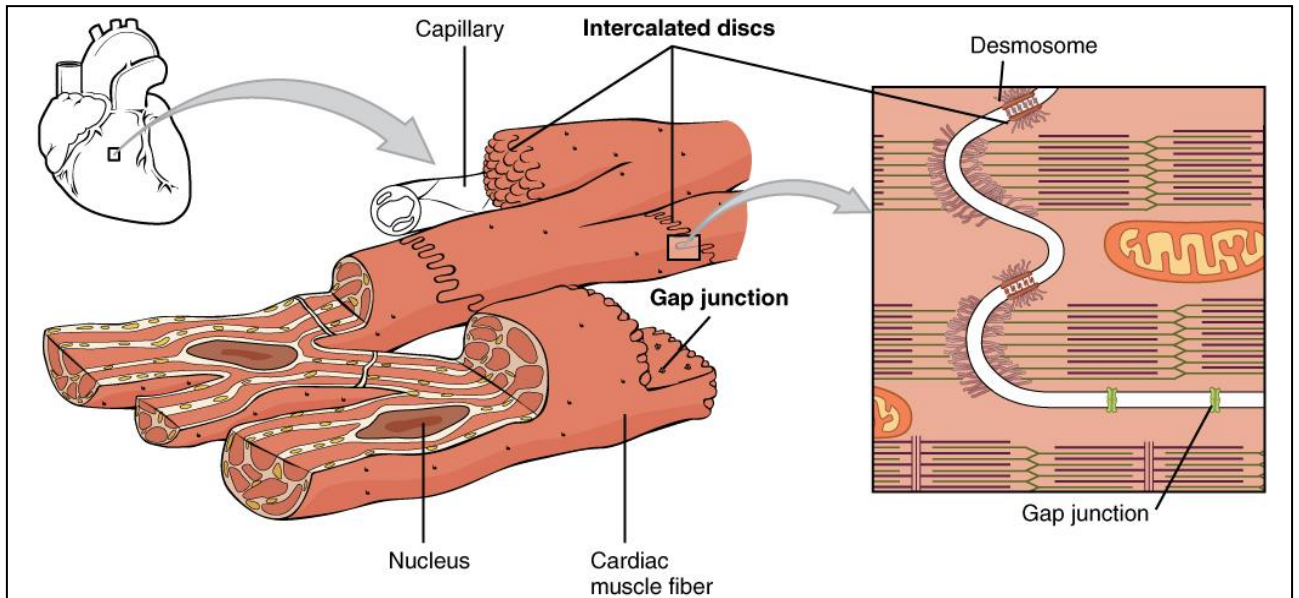


Figure 1. Schematic representation of cardiac muscle. Adapted from OpenStax™ Anatomy and Physiology [197].

The basement membrane gives an interface to the fibrillar collagen matrix of the extracellular space with anchoring fibers, which binds the basal lamina to the collagen underneath.

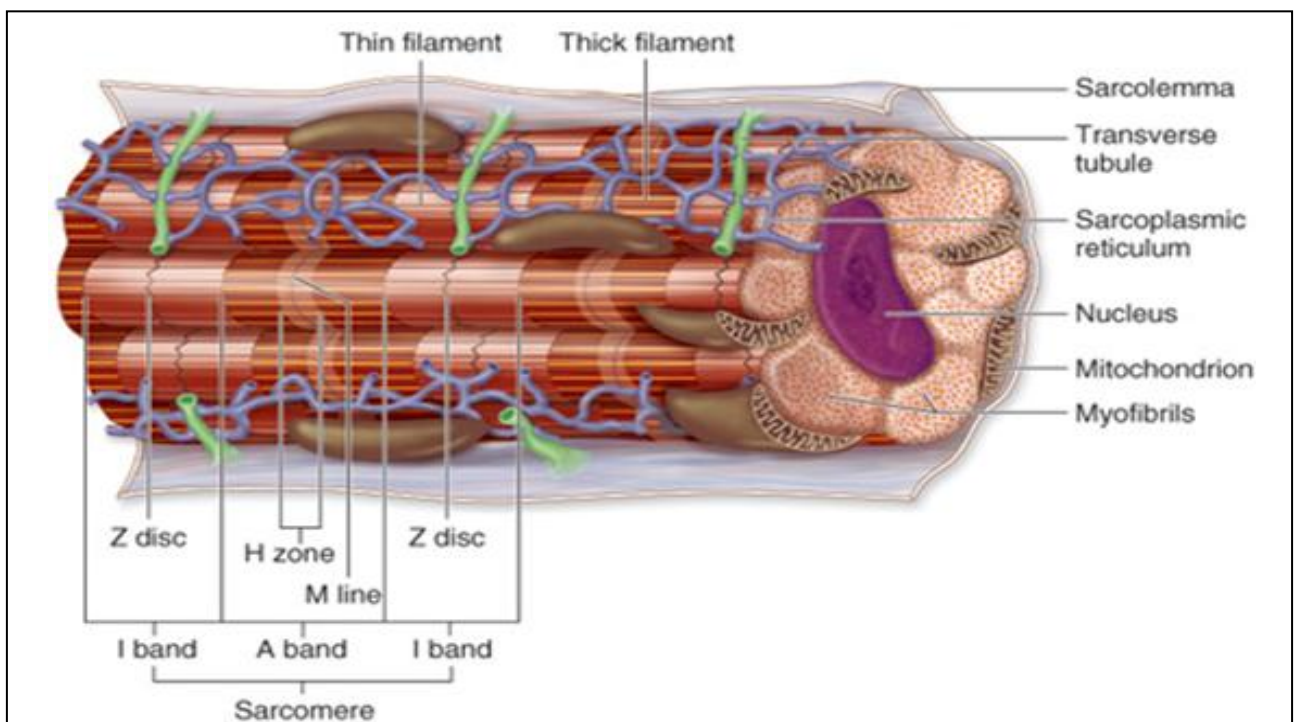


Figure 2. Structure of sarcomere within the body of cardiomyocyte. Adapted from OpenStax™ Anatomy and Physiology [197].

The function of the basement membrane is to create an initial barrier that will affect the exchange of macromolecules between the extracellular space and the myocyte. An additional function of the basement membrane is to provide an interface for myocyte adhesion and continuity with the extracellular matrix. Sarcolemma's membrane proteins include receptors, pumps, and channels. These proteins are essential to the contractile process of the myocyte. Below we present a summary of sarcolemmal proteins that participate in the propagation of the myocyte action potential and are therefore fundamental to the contractile process.

Sarcolemma: This is a specialized structure of the cardiomyocyte. The sarcolemma consists of a lipid bilayer, which has hydrophilic heads and hydrophobic tails. This allows for the interaction of the extracellular and intracellular environments, but due to its hydrophobic core, the sarcolemma is impermeable to charged molecules. Integrins are interwoven throughout the sarcolemma. Along with receptor transmembrane proteins, they bind the myocyte to the extracellular matrix and basement membrane. More importantly, integrins attach themselves to the intracellular side of the sarcolemma, forming an important collagen-integrin-cytoskeletal relation [22]. It has been shown that myocyte contraction and consequent ventricular ejection are due to the integrin interaction to the extracellular and intracellular spaces [22].

The intercalated disks and the transverse tubular system are the two specialized regions of the myocyte that are formed by the sarcolemma. The intercalated disks are specialized cell-cell junctions, which serve as a strong mechanical linkage between myocytes. Moreover, they create a path of low resistance, which allows for the quick conduction of the action potential between myocytes [23]. Transverse tubules, or T-tubules, are invaginations of the sarcolemma into the myocyte. Transverse tubules form a barrier between the intracellular and extracellular spaces. These extensions bring the L-type Ca^{2+} channel and the sarcoplasmic reticulum Ca^{2+} discharge system close to one another. Hence, the T-tubular system is an important structural component in excitation-contraction coupling.

As is the case with most lipid bilayers, the primary function of the sarcolemma is to provide a barrier for diffusion. Sarcolemma's membrane proteins include receptors, pumps, and channels. These proteins are essential to the contractile process of the myocyte. Below we present a summary of sarcolemmal proteins that participate in the propagation of the myocyte action potential and are therefore fundamental to the contractile process [24].

Sarcolemmal pumps and ion channels: A practical way to review the pumps and a channel of the myocyte sarcolemma is to look at them throughout the phases of the action potential.

A representative ventricular myocyte action potential is shown in Figure 3. The resting membrane potential, which is the fourth phase of the action potential, is maintained mostly by the inward K^+ rectifier. However, it is also controlled by the Na^+/K^+ adenosine-tri-phosphatase (ATPase), the Na^+/Ca^{2+} exchanger, and the sarcolemmal Ca^{2+} ATPase.

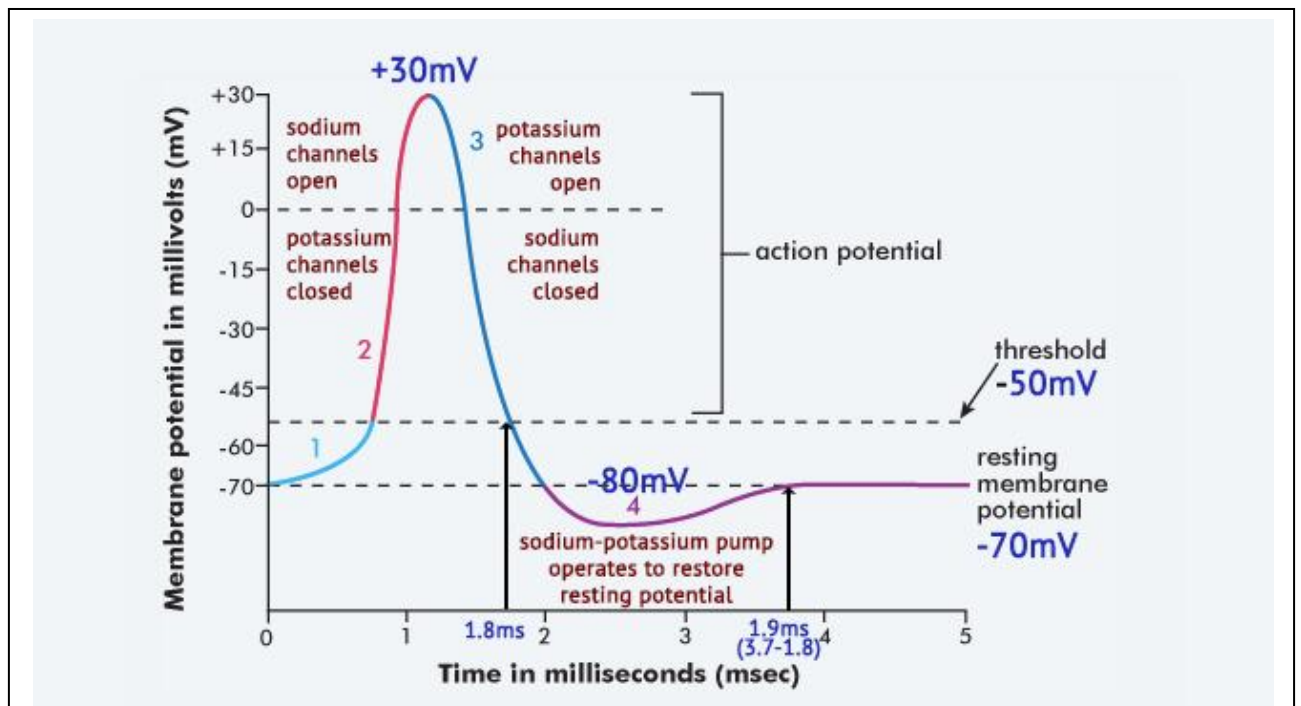


Figure 3. Typical action potential characteristics of ventricular cardiomyocytes. Changes in membrane potential are paralleled with the activity of ion channels.

The K^+ rectifier ensures the diffusion of K^+ ions into the myocyte. The Na^+/K^+ ATPase has two main functions: firstly, it creates a net outward current by exporting three Na^+ ions outside of the cell and allowing two K^+ ions into the cell. Secondly, it

is the site for digitalis binding. The $\text{Na}^+/\text{Ca}^{2+}$ exchanger and the sarcolemmal Ca^{2+} ATPase carry out the outward movement of Ca^{2+} ions from the myocyte. The $\text{Na}^+/\text{Ca}^{2+}$ exchanger is bidirectional and is the primary system for Ca^{2+} efflux from the myocyte [25], [26]. The relative amount of the $\text{Na}^+/\text{Ca}^{2+}$ ions carried across the membrane is determined by their concentrations on either side of the membrane. The removal of cytosolic Ca^{2+} maintains a balance of Ca^{2+} efflux and influx and ensures the maintenance of the resting potential.

The “fast Na^+ channel” carries the initiation or phase 0 of the action potential. When the membrane potential reaches the predetermined threshold voltage, the Na^+ channels activate ($<1\text{ms}$) and stay activated for 2 to 10ms; this is why they have assumed the name “fast” Na^+ channel. Once these channels are activated, Na^+ ions flow into the cell down their electrical and chemical concentration gradients. The influx of Na^+ through the “fast Na^+ channel” initiates the ionic processes responsible for the further stages of the action potential.

Early repolarization starts when the Na^+ channels are rapidly inactivated and two outward channels are slowly activated. The entry of Cl^- into the cell occurs because of the positive membrane potential, the Cl^- concentration gradient, and increased membrane permeability to Cl^- . Additionally, K^+ flows out of the cell down the K^+ electrochemical gradient. This brief efflux is carried by specific channels. As a consequence of these three events, we see a brief and small repolarization of the membrane potential during phase 1 of the action potential.

The influx of Ca^{2+} through the L-type Ca^{2+} channels determines the plateau, or Phase 2 of cardiac action potential [27], [28]. Additionally, a counterbalance is created by the outward flow of K^+ current through the “anomalous” K^+ rectifier [23]. Both of these channels are activated during the upstroke of the action potential and reach their peak of activity during the plateau phase. L-type Ca^{2+} channels also play a major role in excitation-contraction coupling, but this will be discussed in later sections.

Phase 3, also known as repolarization phase, occurs because of increased K^+ conductance through the delayed rectifier K^+ channels toward the end of the plateau phase the delayed rectifier K^+ channels are activated. This allows the K^+ ions to flow along the concentration gradient. Na^+ and Ca^{2+} and other inward currents are inactivated. Hence, the delayed rectifying K^+ current is responsible for the restoration of the membrane potential to the resting state. Increased gene expression for the K^+ channel was induced in adult ventricular myocyte preparations by means of an adenovirus transfer method [29]. As a result of this experiment, increased expression of the K^+ channel led to a significant shortening of phase 3 of the action potential and abbreviation of the excitation-contraction coupling process.

Myocyte cytoskeleton: The myocyte cytoskeleton links the extracellular environment and the contractile apparatus to one another [30], [31]. In particular, at the site where integrins enter the cytosolic compartment a number of cytoskeletal proteins, such as α -actinin, talin, and desmin, converge. When phosphorylated, these cytoskeletal proteins change their structural conformation, which in turn influences the myocyte geometry and function. Moreover, it has been shown that large cytoskeletal proteins provide viscoelastic properties to the myocyte and prevent overstretch of the myofilament apparatus. For example, the cytoskeletal protein titin [32], [33]. Tubulins are other important cytoskeletal proteins. Specifically, alpha and beta-tubulin participate in the myofibrillar assembly and the transduction of mechanical signals to the nuclear envelope [34]. It has been shown that the density and organization of beta-tubulin within the myocyte may directly influence the contractile performance of the myocyte [35]. Therefore, it is highly probable that the complex interaction of cytoskeletal proteins directly affects the form and function of the myocyte.

Sarcoplasmic reticulum: The body of cardiomyocyte is comprised of myofilaments, which are surrounded by, so-called, sarcoplasmic reticulum (SR) (Fig.4). The SR is equivalent of endoplasmic reticulum found in other cells. There are separate transverse tubular structures, which cross cardiomyocyte, called T-tubules.

The extracellular fluid surrounding the cell is connected to the lumen of the T-tubule. This guarantees the faultless propagation of action potential from ECM down the T-tubule. T-tubule crosses at the Z-line. Neighboring cardiac myocytes are joined via intercalated disks, a special end-to-end at structures. These connections always occur at a Z-line. Moreover, at these points, the cell membranes form a number of parallel folds and are tightly held together by desmosomes. All together, this results in strong cell-to-cell cohesion, and allowing the contraction to be transmitted from one myocyte to the next. Lastly, cardiomyocytes are physically connected to each other by gap junctions, which provide low resistance pathways for the spread of excitation from one cell to another.

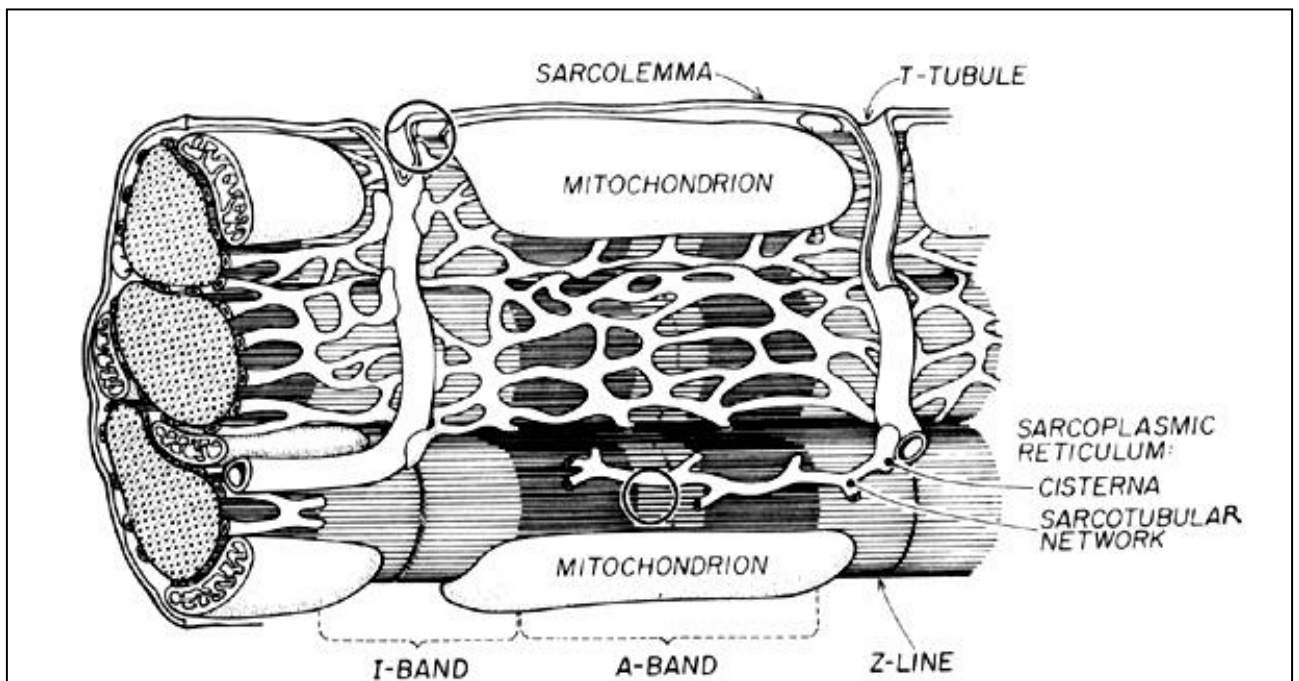


Figure 4. *T-tubules are directly connected to sarcoplasmic reticulum of cardiomyocytes. Adapted from Fundamentals of anatomy and physiology, 10th edition [198].*

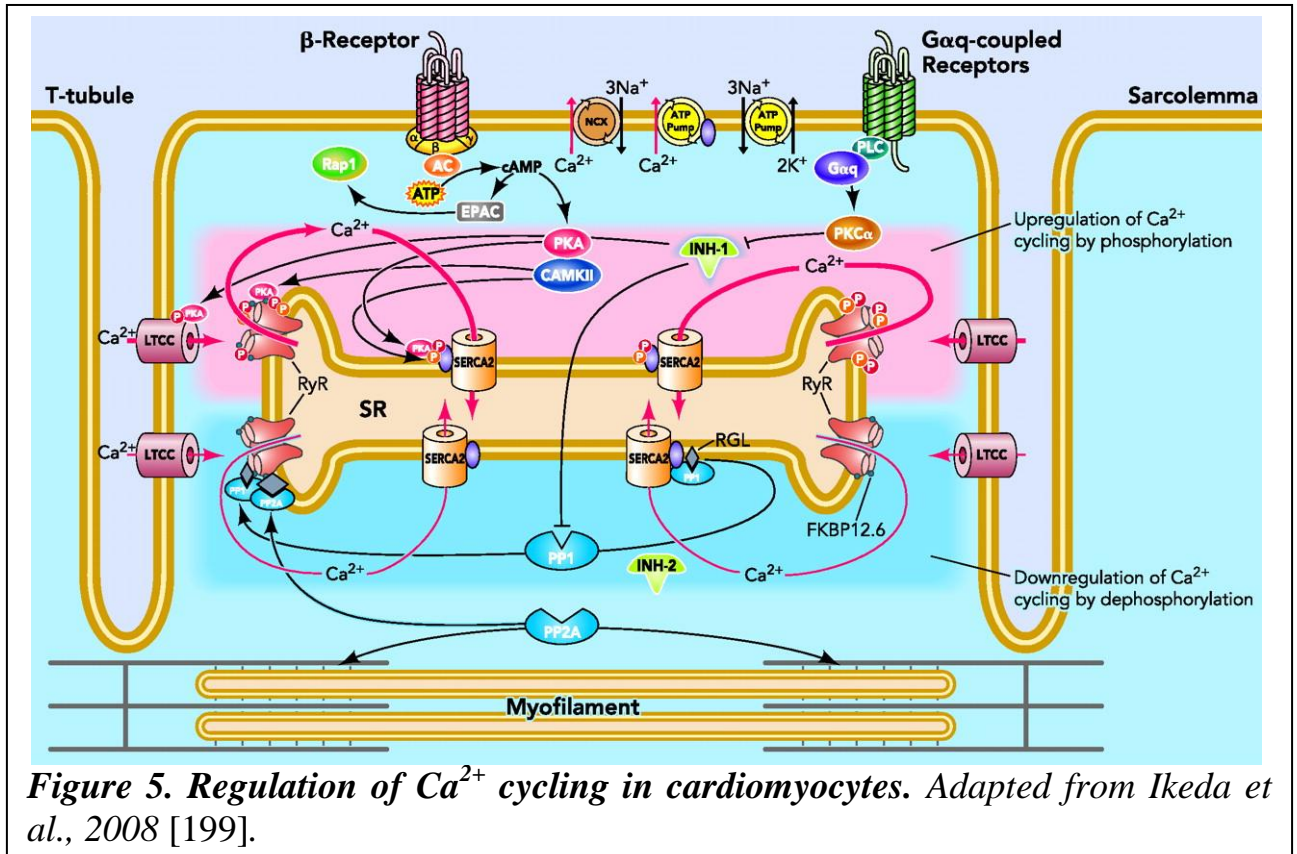
The sarcoplasmic reticulum (SR) is an organelle that is highly efficient in Ca^{2+} handling and specialized in the regulation of cytosolic Ca^{2+} concentration [36], [37]. It forms T-tubular system which are specialized structural regions of the myocyte positioned closely to the sarcolemma [38]. The SR is responsible for the Ca^{2+} source in excitation-contraction coupling [39]. It contains three important components that participate in the role of this organelle with respect to Ca^{2+} homeostasis: the

sarcoplasmic reticulum Ca^{2+} ATPase (SERCA-2), the regulatory protein of SERCA-2, phospholamban, and the Ca^{2+} release channel.

Sarcoplasmic reticulum proteins: SERCA-2, is a fundamental determinant of Ca^{2+} accumulation within the myocyte [23]. It is ATP-dependent Ca^{2+} pump distinct from that found in the sarcolemma. By utilizing 1mol of ATP, SERCA-2 transports back into the sarcoplasmic reticulum 2mol of Ca^{2+} , consequently decreasing cytosolic Ca^{2+} [36], [40]. Another system regulating intramyocardial Ca^{2+} concentration is the $\text{Na}^+/\text{Ca}^{2+}$ exchanger. This exchanger together with sarcolemmal Ca^{2+} ATPase, the uptake of Ca^{2+} can be altered by more than 100-fold during the excitation-contraction coupling process [41]. Another recently been recognized protein, Phospholamban, colocalized with SERCA-2 [42], and plays important regulatory function for SERCA-2. Upon phosphorylation, phospholamban facilitates SERCA-2 uptake into the sarcoplasmic reticulum, whereas dephosphorylation of phospholamban results in decreased sensitivity of SERCA-2 to cytosolic Ca^{2+} (Fig.5) [37]. Therefore, phosphorylation of phospholamban determines the rate and extent of Ca^{2+} removal from the cytosolic compartment. These mechanisms were proven in a genetically engineered mouse model, in which endogenous phospholamban had been increased by more than 2-fold, and significant changes were observed in the Ca^{2+} uptake process [43].

Specifically, a reduction in the affinity of SERCA-2 for Ca^{2+} occurred and caused a decline in the magnitude of the Ca^{2+} signal [43]. These changes in SERCA-2 function with phospholamban overexpression were translated into the diminished active relaxation of the myocyte [43]. Thus, phospholamban plays a critical role in the regulation of Ca^{2+} uptake in the sarcoplasmic reticulum, which in turn regulates the fundamental process of excitation-contraction coupling. The calcium release channel is found in dense populations at the interface between the sarcoplasmic reticulum and the T-tubular system of the sarcolemma [44]. This channel, also called the ryanodine receptor channel [39], [44], [45], is responsible for Ca^{2+} release from sarcoplasmic reticulum stores and is very sensitive to small changes in cytosolic Ca^{2+} .

A small but rapid influx of Ca^{2+} through the L-type Ca^{2+} channel will result in an immediate release of a large bolus of Ca^{2+} into the myocyte cytosolic space [23]. This large release of Ca^{2+} from the calcium release channel is responsible for engaging the contractile apparatus [44]–[46].



Contraction: Once the action potential reaches the myocyte, the wave of depolarization, particularly at the T-tubular system, activates the sarcolemmal voltage-sensitive L-type Ca^{2+} channels and initiates Ca^{2+} conductance [27], [28]. The result is a small but rapid influx of Ca^{2+} through the L-type Ca^{2+} channels, this, in turn, causes activation of the Ca^{2+} release channel, and as a result, a large amount of Ca^{2+} is released into the cytosol [27], [39], [44]–[48]. The Ca^{2+} that flows through the L-type Ca^{2+} channel is known as the trigger Ca^{2+} current [27], [41]. The amount of trigger Ca^{2+} is very small when compared to the amount of Ca^{2+} released from the sarcoplasmic reticulum; therefore, trigger Ca^{2+} does not have significant contribution in cross-bridge formation.

Once Ca^{2+} released from the sarcoplasmic reticulum, a series of interactions take place within sarcomere's contractile unit. Here we will use the sliding filament theory

to illustrate the interaction of various contractile proteins [27], [41], [49], [50]. Cytosolic concentrations of Ca^{2+} are low during resting conditions; the phosphorylation of troponin I decrease cytosolic Ca^{2+} affinity for troponin C, favoring a stronger interaction between troponin I and the actin molecule. Thus actin-myosin interaction is blocked because of the troponin-tropomyosin complex shifts toward the outer grooves of the actin filament. An increase in cytosolic Ca^{2+} leads to the binding of Ca^{2+} to troponin C, which in turn results in a shift of troponin I affinity from the actin filament to troponin C. Once troponin I is destabilized from the actin molecule a conformational shift of the troponin-tropomyosin complex occurs, leading it away from the actin-myosin binding site; subsequently we see a cross-bridge formation. After the cross-bridge is formed, the hinge regions found in the cross-bridge allow the myosin head to swing toward the thin filament. Once the myosin head attaches to the thin filament, it changes its conformation, resulting in the hydrolysis of ATP. A force is generated due to the conformational change in the cross-bridge. The generated force is used to move the thin filament relative to the thick filament. Once the ATP molecule is hydrolyzed, a new ATP molecule replaces it. The binding of new ATP causes the release of the existing cross-bridge and allows the formation of a new cross-bridge. With each cross-bridge cycle, the filaments are moved approximately 10nm, having an average velocity of 0.98mm/s [27], [51]. This process is highly dynamic and depends on several factors, including the action potential duration, the number of cross-bridge formed during each contraction, the amount of Ca^{2+} released from the sarcoplasmic reticulum, and the availability of ATP stores. The cycle of cross-bridge will be arrested only if the Ca^{2+} is removed from the cytoplasm by active, energy-dependent means or when the ATP stores are depleted.

Active relaxation: The function of SERCA-2 is responsible for the active. Two moles of Ca^{2+} is transported back into the sarcoplasmic reticulum for each mol of hydrolyzed ATP. The active relaxation process within the myocyte is controlled by SERCA-2 and phospholamban. There are other systems designed for the removal of cytosolic Ca^{2+} ; these include the $\text{Na}^+/\text{Ca}^{2+}$ exchanger, the sarcolemmal Ca^{2+} ATPase

and cytosolic Ca^{2+} binding proteins calmodulin and calsequestrin. Calmodulin binds to intracellular Ca^{2+} , forming a complex that can activate the sarcolemmal Ca^{2+} ATPase to extrude cytosolic Ca^{2+} . Calsequestrin locates and stores Ca^{2+} within the internal cardiac vesicular stores [36]. Lastly, it is worth to highlight that active relaxation is a process that is highly dependent on energy.

Myocyte contractility: Contraction occurs once the action potential has been successfully transduced and Ca^{2+} is released into the cytosolic compartment of the myocyte. Measuring contractile function at the single myocyte level has become possible over the past decade [52], [53]. On the isolated myocyte, it is possible to examine the modulating effects of the sarcolemmal receptor systems with respect to contractile performance in the absence of confounding factors. For example, more recently, the direct effects of β -adrenergic receptor stimulation, as well as modulating downstream factors in the β -adrenergic receptor transduction pathway, have been examined on isolated myocytes [54]. Specifically, a left ventricular myocardial biopsy specimen can be taken during cardiac surgery and can be used to isolate myocytes and measure contractile performance. It has been shown that by this method we can isolate viable human left ventricular myocytes, which properly respond to electrical stimulation (Fig.3). In addition, it has been shown that the left ventricular isolated myocyte preparations allow for the study of the contractile effects of β -adrenergic receptor stimulation. In terms of future implications, it is highly probable that these isolated left ventricular myocyte studies will generate important information regarding the mechanisms that regulate the excitation-contraction coupling process [55].

Contractile apparatus: The contraction of cardiomyocyte is provided by a contractile unit called the sarcomere. The sarcomere contains all the components of the contractile apparatus. It is composed of thick and thin interdigitating filaments and has a resting length of 1.8 to 2.4 μm (Fig.6) [41]. The main proteins of the contractile apparatus are myosin, actin, tropomyosin, and the troponin complex [41]. Interactions between those proteins occur in the presence of increased extracellular

Ca^{2+} , with utilization of ATP and results in changes in physical-chemical dynamics such as the development of tension within the myocyte. Myosin, the thick filament, is composed of a filamentous tail and a globular head region. This globular head contains the site for actin binding, as well as a catalyzing site for ATPase activity. Actin is the major contractile protein found in the thin filament. Having two forms, G, and F, F-actin is the backbone of the thin filament with G-actin working as a stabilizing protein. Each G-actin monomer has two myosin binding sites. The interaction between the myosin globular head and the G-actin monomer in the presence of ATP results in cross-bridge formation and sarcomere shortening.

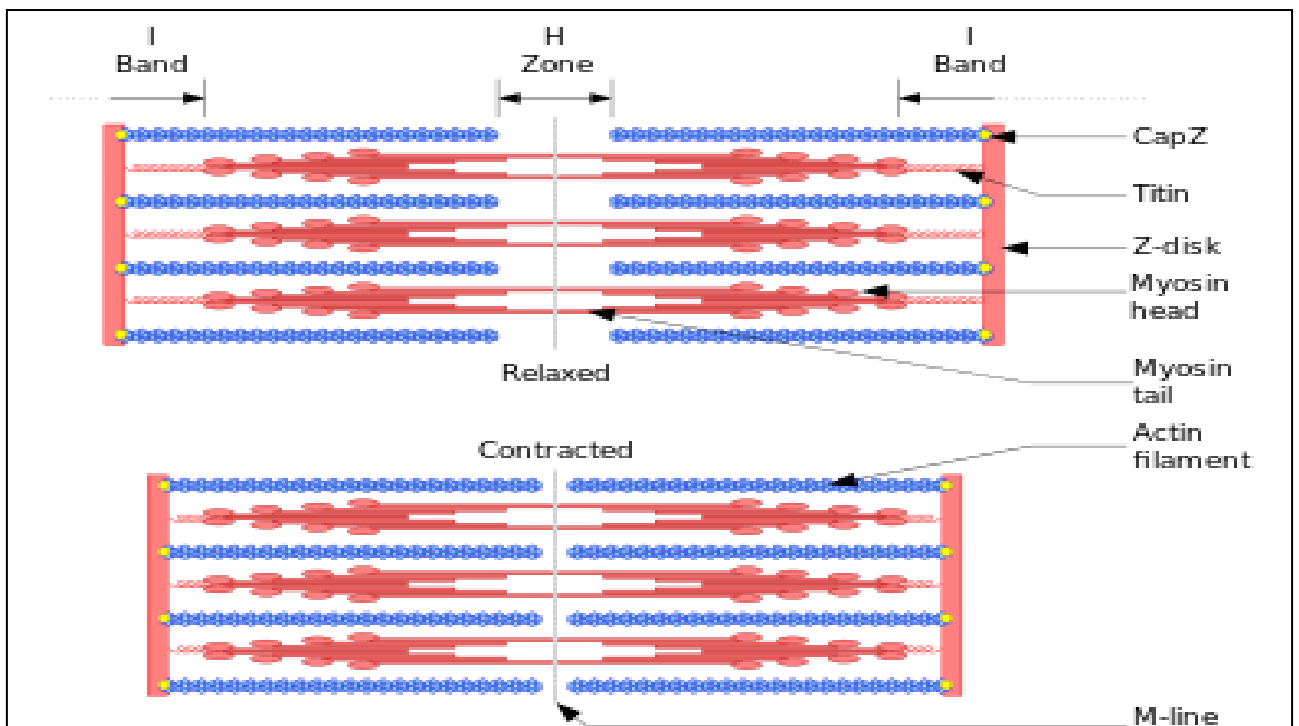


Figure 6. Sliding filament model of contraction. Muscle fibers in relaxed (above) and contracted (below) positions. Adapted from *Boundless Anatomy and Physiology* [200].

Tropomyosin is another protein found in the thin filament. This rigid molecule lies on either side of actin, adding rigidity to the thin filament. Tropomyosin influences actin-myosin cross-bridge formation by physically interdigitating between the actin-myosin cleft, thus preventing Ca^{2+} binding [23]. The troponin complex, also present in the thin filament, is composed of three proteins: troponin T, I, and C. Troponin is an important component in that it regulates the extent of cross-bridge formation, as well as contributing to the structural integrity of the sarcomere.

Troponin T binds the troponin complex to tropomyosin and anchors the complex to the thin filament. Under normal conditions, phosphorylated troponin I weakens the affinity of Ca^{2+} for troponin C. Ca^{2+} binding to troponin C results in a conformational change of the complex, with subsequent actin-myosin interaction, thus initiating cross-bridge formation.

Excitation-contraction coupling: The mechanism by which an action potential leads to contraction of the myocyte is called excitation-contraction coupling. Ca^{2+} is the fundamental ion that induces the excitation-contraction coupling complex. The excitation-contraction coupling complex occurs through the gradual increase of cytosolic Ca^{2+} levels, starting from nanomolar (100nmol/L) concentrations and terminating at micromolar (10mmol/L) concentrations [41]. Figure 6, adapted from Boundless Anatomy and Physiology, depicts the important components of the excitation-contraction coupling process.

Mitochondria: The myocyte requires storage of ATP in high amounts. Thus, the myocyte is rich in mitochondria- the organelles that carry this process; 40% of myocyte cell volume is occupied by mitochondria [23], this emphasizes the massive energy demands that the myocyte has. Phosphocreatine is a high-energy reserve molecule, which is also responsible for shuttling of phosphate to the cytosol [23]. In the cytosol, the concentrations of phosphocreatine and creatine are higher than that of adenosine diphosphate. This creates a rapid transport system of high-energy phosphate between the mitochondria and the cytosol. For example, in excitation-contraction coupling, the high-energy phosphate group of ATP molecule is transferred to phosphocreatine, which, in turn, diffuses through the cytosol to be reconverted to ATP for cell energy use. It has also been shown that mitochondria can take up large amounts of cytosolic Ca^{2+} , as well as buffer the cytosolic amounts of Ca^{2+} , thus protecting the myocyte from an overload of Ca^{2+} [23].

1.1.2. Proliferative and regenerative characteristics of cardiac muscle

Regenerative capacity - an evolutionary perspective: Far from a rare talent, it is common for adult organisms the regeneration of injured body parts is a common

ability of adult organisms ranging from tiny planarians to large mammals. In humans, hepatocytes increase cell size or divide to replace lost liver mass after surgical resection, and local stem cell populations continually renew tissues like hair follicles and intestinal epithelium. However, animals vary widely in their capacity to regenerate particular tissues. Invertebrates such as planarians and hydra, which can form whole animals from small segments, exhibit the greatest regenerative aptitude [56]–[58]. Mammals, by contrast, fail to regenerate crucial structures, including limbs, spinal cord, and cardiac muscle. However, certain vertebrates, including urodeles (e.g. salamanders) and teleost fish (e.g. zebrafish), retain the ability to regenerate these and other organs. It is thus of significant interest to understand the degree to which fundamental aspects of these organisms' biology, rather than or in addition to cardiac specific factors, allow them to repair their hearts so effectively. Although we briefly discuss certain non-cardiac influences on cardiomyocytes proliferation in this review, we refer interested readers to other, more thorough reviews of the comparative biology of regeneration and its mechanisms [59], [60].

Approaches to cardiac regeneration: Modern science is pursuing several strategies for myocardial regeneration. Cardiac stem cells are the population targeted in theory to be used for the increase of the cardiomyocyte pool. Cardiac stem cells can be circulating or local non-myocardial progenitors that have the ability to differentiate into cardiomyocytes [61], [62]. However, objective interpretation of lineage-tracing experiments finds insufficient evidence for stem cell populations harboring significant myocardial repair activity [63], [64]. This does not preclude applications of stem cells in heart regeneration therapies. Indeed, modern regenerative biology provides many techniques of tissue engineering that influence cell fate and generates cardiomyocyte-like cells or progenitors in vitro. However, to this date, transplanted stem cell populations provide very few benefits, if any, and have been shown to affect endogenous repair mechanisms by paracrine signaling [65], [66]. The use of pluripotent stem cell-derived cardiomyocytes for heart therapy is still far from clinical use as it still faces various challenges, with respect to cell

maturation, arrhythmogenesis, immunosuppression, and the need for scaling up [67], [68]. To avoid these issues, we need to be able to stimulate vigorous endogenous cardiac regeneration without adding exogenous cells or factors. This issue still remains unsolved. A possible way to achieve this goal could be the direct reprogramming of non-muscle cells into cardiomyocytes like cells by the means of injecting or treating the heart with certain factors. Recently, provocative demonstrations of the potential of this approach have been published [69]–[72]. The stimulation of cardiomyocyte proliferation, as described above, remains an attractive approach for regenerating the heart.

Lately, cardiomyocytes have been suggested as target cells for regenerative intervention. After birth, the mammalian heart mainly grows by cardiomyocyte hypertrophy, during which existing cardiomyocytes enlarge in size but do not proliferate. Most mature cardiomyocytes are poor targets for cell division and contribute minimally, due to their increased DNA content and proliferated contractile structures. However, cardiomyocyte cells proliferate rapidly during the fetal development, and a few days after birth [73]. Moreover, some teleost fish have the ability to use cardiomyocytes division to regenerate portions of their hearts after injury. Additionally, some urodele amphibians have also been reported to have the same ability to varying degrees [74]–[76]. It has been reported that neonatal mice exhibit some level of cardiac regenerative capacity as well [77]. The aim of this is to emphasize that cardiomyocytes do harbor some endogenous proliferative capacities after all, albeit in different contexts and to different degrees.

Nowadays, the major investigations in the field try to answer the following question: how, and to what extent this endogenous regenerative capacity can be enhanced to recover muscle mass and restore the function after injury. To address these questions, all accessible contexts and species of cardiomyocyte proliferation should be investigated [78].

The adult human heart does not have significant regenerative capacity upon injury of the heart tissue. Human hearts do scarring and hypertrophy, rather than

generating new functional muscle. However, this can often lead to fatal arrhythmias or heart failure. The explanation for this ineffective cardiac regeneration in mammals lies within the low proliferative capacity of adult cardiomyocytes. However, considering that mammalian cardiomyocytes proliferate during fetal and neonatal development, along with the fact that both adult zebrafish and neonatal mice regenerate cardiac muscle after injury, it has been suggested that latent regenerative potential exists.

So, the primary goals in cardiovascular research nowadays include detecting the molecular and cellular mechanisms that induce cardiomyocyte proliferation throughout our lifespan, explaining why proliferative capacity diminishes in adult mammals and designing methods to boost this proliferative capacity [78].

A major cause of mortality and morbidity is heart failure, which usually results from a myocardial infarction (MI) event [79]. The limited proliferative capacity of cardiac muscle impedes the functional recovery of the infarcted myocardium, resulting in a failing human heart. Unlike skeletal muscle, cardiac muscle has no vigorous, natural mechanism for regeneration. Instead, cardiac injury followed by fibrotic scarring and hypertrophic remodeling of the myocardium [80]. Consequently, the modern medicine puts focus on rapid reperfusion after ischemic cardiac injury. This is done to minimize cardiomyocyte death and to pharmacologically aid the chronically weakened organ [57], [81]. Theoretically, a more permanent and promising solution would be the design of therapies for myocardial regeneration or reconstitution [78].

The heart has been considered a post-mitotic organ for a very long time [82]. Although it has been shown that adult human cardiomyocytes can be replaced at a very low yet noticeable rate, this native regeneration rate is not sufficient to compensate for the tissue damage caused by Myocardial Infarction [83], [84]. Therefore, a number of approaches should be designed that lead to cardiac regeneration [78].

Cardiac regeneration in neonatal mammals: Different injury models have been studied to measure the regenerative capacity of adult mammalian hearts and all of these have failed to show significant proliferation rates [85], [86]. For almost a century, analyses of postmortem histological specimens in children have suggested an opportunity of a regenerative window [87], [88]. Inspired by these studies, Robledo decided to explore cardiac regeneration in rat infants in 1950s, but he observed only incomplete regeneration after injury, which was caused by myocardial burns in rats, 4-7 days after birth. More recently, cases of corrective heart surgeries in infants [89] and myocardial infarction (MI) of a newborn child have been reported [90], suggesting that human neonatal heart also has the ability to functionally recover and may have a higher regenerative potential. Recently, it has been reported, that neonatal mice have regenerative capacity; this has been shown in various injury models, including ventricular resection [77], MI [91], cryo infarction [92], [93], and clamping [94], [95].

Porrello et al. Neonatal reported [77], [96] heart regeneration studies in mice in resection and MI models. According to these studies, there is a time window immediately after birth when the mammalian heart displays a robust regenerative response. Neonatal animals exhibit increased cardiomyocyte proliferation and angiogenesis upon undergoing resection or MI surgery. In both MI and the ventricular resection model, during which 15% of the ventricular apex is resected, the lost tissue is substantially restored within 3 weeks, although some scarring may occur [77]. The regenerative response in neonatal mouse injury is initiated with rapid clotting, which is followed by inflammatory cell infiltration to the injury site, epicardial activation, and initiation of cardiomyocyte proliferation. In the MI model, ligation of the left anterior descending coronary artery routinely induced ischemia soon after birth. The infarction model initially induces myocyte necrosis and collagen deposition. However, 95% of lost tissue is replaced within 3 weeks, showing minimal fibrosis, and cardiac function resumes to normal 9 months after surgery [96]. Porrello et al. (2013) and others have used genetic fate mapping to show that the major source

of cardiomyocyte repopulation is pre-existing cardiomyocytes that re-enter the cell cycle [91], as in zebrafish [97], [98]. Interestingly, soon after birth, there is a steep decline in heart's potential to regenerate since this robust regenerative response is not elicited in mice injured at postnatal day 7 or day 14 [95].

When Andersen et al. (2014) [99] reported widespread scarring and limited regeneration following neonatal ventricular resection; a controversy arose in the field. Hence, Bryant et al. (2014) conducted a systematic analysis of technical considerations in the surgery, showing that experimental discrepancies, such as the varying size of apical resection, leads to varying regenerative response, including some degree of scarring at 21 days post operation [94]. Several different groups have demonstrated clear evidence for myocardial regeneration after ventricular resection in neonatal mice [77], [94], [100]. In contrast, there is no significant increase in cardiomyocyte proliferation following cryoinjuries, whereby transmural cryoinjury fails to elicit a regenerative response, while non-transmural cryo-injury models exhibit full recovery [101]. However, carefully controlled experiments with a consistent choice of injury type in neonatal mice are currently not of high importance [95].

1.2. Cell adhesion

Cell adhesion is the process by which cells interact and attach to a surface, substrate or another cell, mediated by interactions between molecules of the cell surface. Cell adhesion occurs from the action of transmembrane glycoproteins, called cell adhesion molecules. Examples of these proteins include selectins, integrins, syndecans, and cadherins [102]. Cellular adhesion is essential in maintaining the multicellular structure. Cellular adhesion can link cells in different ways and can be involved in signal transduction [102]. Cell adhesion is crucial for the assembly of individual cells into the three-dimensional tissues of animals. Cells do not simply “stick” together to form tissues, but rather are organized into very diverse and highly distinctive patterns. A variety of cell adhesion mechanisms are responsible for assembling cells together and, along with their connections to the internal

cytoskeleton, determine the overall architecture of the tissue. Thus, cell adhesion systems should be regarded as mechanisms that help translate basic genetic information into the complex three-dimensional patterns of cells in tissues [40].

The functional units of cell adhesion are typically multiprotein complexes made up of three general classes of proteins; the cell adhesion molecules/adhesion receptors, the extracellular matrix (ECM) proteins, and the cytoplasmic plaque/peripheral membrane proteins. The cell adhesion receptors usually transmembrane glycoproteins that mediate binding interactions at the extracellular (EC) surface and determine the specificity of cell-cell and cell-ECM recognition. They include members of the integrin, cadherins, immunoglobulin, selectin, and proteoglycans (for example syndecans) superfamilies. At the EC surface, the cell adhesion receptors recognize and interact with either other cell adhesion receptors on neighboring cells or with proteins of the ECM. ECM proteins are typically large glycoproteins, including the collagens, fibronectins, laminins, and proteoglycans that assemble into fibrils or other complex macromolecular arrays [103]–[109].

The adhesive elements that stably connect cells together play essential roles in overall tissue organization and the proper physiological function of the tissue and organ. Numerous kinds of stable adhesion elements are found in an organism. Here only those relevant to our study are presented. Those are:

- ***Cadherins and cell-cell adherence junctions.*** One of the most important and ubiquitous types of adhesive interactions required for the maintenance of solid tissues is that mediated by the classic cadherins adhesion molecules. Cadherins are transmembrane Ca^{2+} -dependent homophilic adhesion receptors that are well known to play important roles in cell regulation and cell sorting during development [110]. However, they continue to be expressed at high levels in virtually all solid tissues. There are many members of the classic cadherins family (which is a subset of the larger cadherins superfamily), but E-cadherins in epithelial tissues has been the most studied in the context of stable adhesions. Continued expression and functional activity of E-cadherins are required for cells to remain tightly associated in the

epithelium, and in its absence, the many other cell adhesion and cell junction proteins expressed in epithelial cells are not capable of supporting intercellular adhesion. In its capacity to maintain the overall state of adhesion between epithelial cells, E-cadherin is thought to act as an important suppressor of epithelial tumor cell invasiveness and metastasis [111], [112]. A loss of E-cadherin expression or function leads to enhanced cell invasiveness in cell culture, and E-cadherin deficiencies or mutations correlate with the invasiveness and metastasis of certain human tumors. E-cadherin gene knockouts in mice cause lethality at a very early stage [113], making it difficult to investigate its tumor suppressor role in whole organisms. This latter finding is not very surprising, given the fundamental role for E-cadherin in the formation of epithelial tissues.

To exhibit functional adhesion activity, cadherins must form complexes with cytoplasmic plaque proteins, called catenins, and with the actin cytoskeleton [104], [114]. α -catenin is required for cadherin-mediated cell adhesion, and since it has actin-binding activity, it probably functions to link the cadherins to the actin cytoskeleton [115]. Normally, β -catenin must also be required for adhesion, because it is a necessary intermediate in the linkage of α -catenin to the cadherin cytoplasmic tail [116]. This finding, along with observations that tyrosine phosphorylation of β -catenin correlates with diminished adhesion in response to growth factors and cell transformation [117], has inspired the hypothesis that β -catenin acts as a regulatory component of the complex. β -catenin also participates in signal transduction and developmental patterning, suggesting that it serves to couple physical adhesion to signaling events during morphogenesis.

- ***Desmosomal junctions.*** The desmosomes are the most conspicuous adhesive elements in epithelia and cardiac muscle. They are linked to the intermediate filament cytoskeletal network (cytokeratins in epithelia and desmin filaments in the heart). Together the desmosomes and intermediate filament cytoskeleton form a contiguous network throughout the tissue that engenders it with high tensile strength. The adhesion receptors of the desmosomes are members of the cadherins superfamily,

called desmogleins and desmocollins, for which there are a variety of isoforms with distinct tissue-specific patterns of expression [118]. The desmogleins and desmocollins are linked to the intermediate filament network by several cytoplasmic plaque proteins, including the desmoplakins and plakoglobin. Desmoplakins share sequence similarity with intermediate filament proteins and seem to interact directly with them. Plakoglobin binds to the cytoplasmic tails of certain desmogleins and desmocollins and seems to be essential for the formation of the desmosomal plaque and attachment of cytokeratins filaments [119]. Plakoglobin may have other important functions; it has high sequence similarity to β -catenin and can also transduce developmental signals. It is also sometimes found in adherens junctions in association with cadherins, probably on the place of β -catenin.

- ***Occluding junctions.*** One of the most physiologically important properties of tissues is their capacities to create selective permeability barriers. Cells are often organized into specialized structures that create interfaces between compartments, which serve to regulate the movements of cells, macromolecules, small solutes, and ions. A few common examples include the control of leukocyte traffic across endothelia and epithelia, the selective absorption of nutrients by the epithelium of the gastrointestinal tract, the maintenance of proper electrolyte balance in the nervous system by the blood-brain barrier, and the electrical insulation of axons by myelin. The adhesive element most important for the formation of permeability barriers in tissues like epithelia and endothelia is a tight junction or zonula occludens. The tight junction actually serves two interrelated roles in these tissues: to regulate the permeability characteristics of the paracellular space between adjacent cells and to divide the surface of the cell into two functionally and biochemically distinct regions that interface with either one of the two physiological compartments [120].

The importance of maintaining these occluding barriers for the well-being of the organism is obvious. Nevertheless, tight junctions are remarkably plastic and diverse structures. Their permeability properties vary from tissue to tissue, ranging from the exclusion of whole cells to macromolecules to the selective permeability to protons

and ions. They are also often subject to rapid physiological regulation [121]. The molecular basis of tight junction diversity and regulation is not well understood, but there has been significant progress in the elucidation of its molecular composition and structure. An integral membrane protein, called occludin, probably contributes to the formation of the EC contact and the occluding barrier [122]. Occludin interacts with two cytoplasmic plaque proteins, ZO-1 and ZO-2. Their functions are uncertain, but they may play a role in assembling occludin or localizing it to the specific site at the boundary between apical and basolateral cell surfaces. Several cytoskeletal associated proteins, cingulin, the 7H6 antigen, and actin, also localize to the region of the tight junction [123].

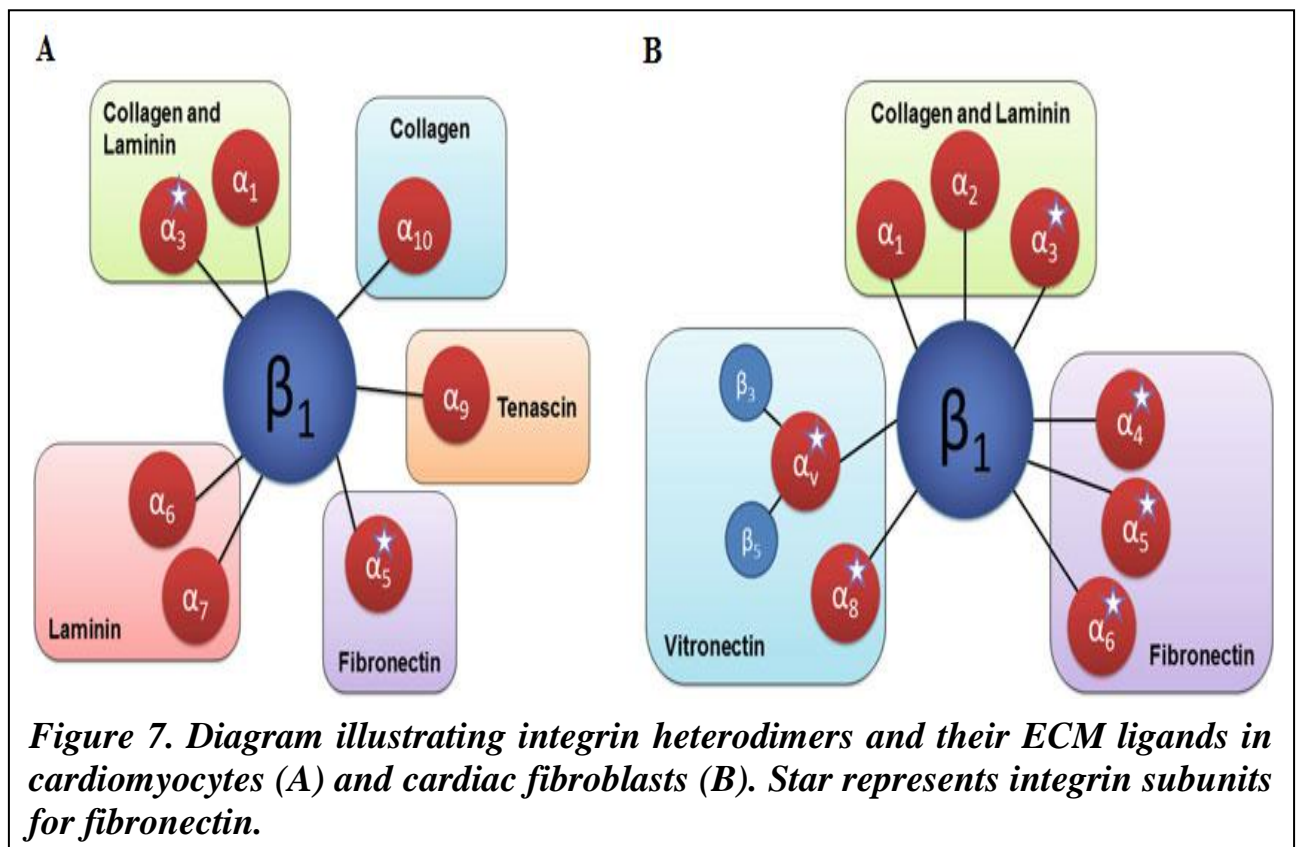
- ***Cell-ECM attachments and the basement membrane.*** The attachment of cells to the ECM is also crucial for the maintenance of tissue integrity. Cells attach either directly to components of the collagen-rich interstitial matrix or to the basement membrane, a more distinct sheath of the ECM that surrounds many kinds of tissues. Basement membranes cover the basal surfaces of virtually all epithelia; surround the surfaces of muscle fibers, and ensheath nerves. Basement membranes are comprised of two distinct layers. The basal lamina, immediately adjacent to the cells, contains a variety of adhesive ECM glycoproteins, including collagen IV, laminin, fibronectin, proteoglycans, and many others [107]. The reticular lamina is produced by fibroblasts of the underlying connective tissue and contains fibrillar collagens. Cells use a number of different adhesion receptors to attach to the ECM, including a family of cell surface proteoglycans called syndecans. Of course, the most prominent of the ECM adhesion receptors are the integrins, a large family of heterodimeric transmembrane proteins with different α and β subunits [105].

1.2.1. Molecular mechanisms of adhesion in myocardium and epithelial cells

Adhesion properties of each cell types are also slightly different. Extracellular matrix provides a structural, chemical, and mechanical support that is essential in cardiac development, growth, and responses to pathophysiological signals.

Transmembrane molecules named integrins to ensure an active communication of environmental cues with subsequent intracellular events [124]–[126]. Integrins are expressed in all cells, including heart cells. Integrins are noncovalently associated heterodimeric transmembrane proteins which are critically important for functional and structural maintenance of cardiac myocytes network and their interaction with supporting fibroblast layers. They participate in multiple critical processes including adhesion, extracellular matrix organization, signaling, survival, and proliferation [127].

Heart muscle consists of highly organized and interconnected network of cardiac cells. Integrins are critically important for functional and structural maintenance of cardiac myocyte networks and its interaction with supporting fibroblast layers (Fig.7).



Extracellular matrix provides a structural, chemical, and mechanical substrate that is essential in cardiac development, growth, and responses to pathophysiological signals. Integrins are transmembrane receptors responsible for dynamic interaction

between intracellular events and extracellular/environmental cues (Fig.8) [124]–[126].

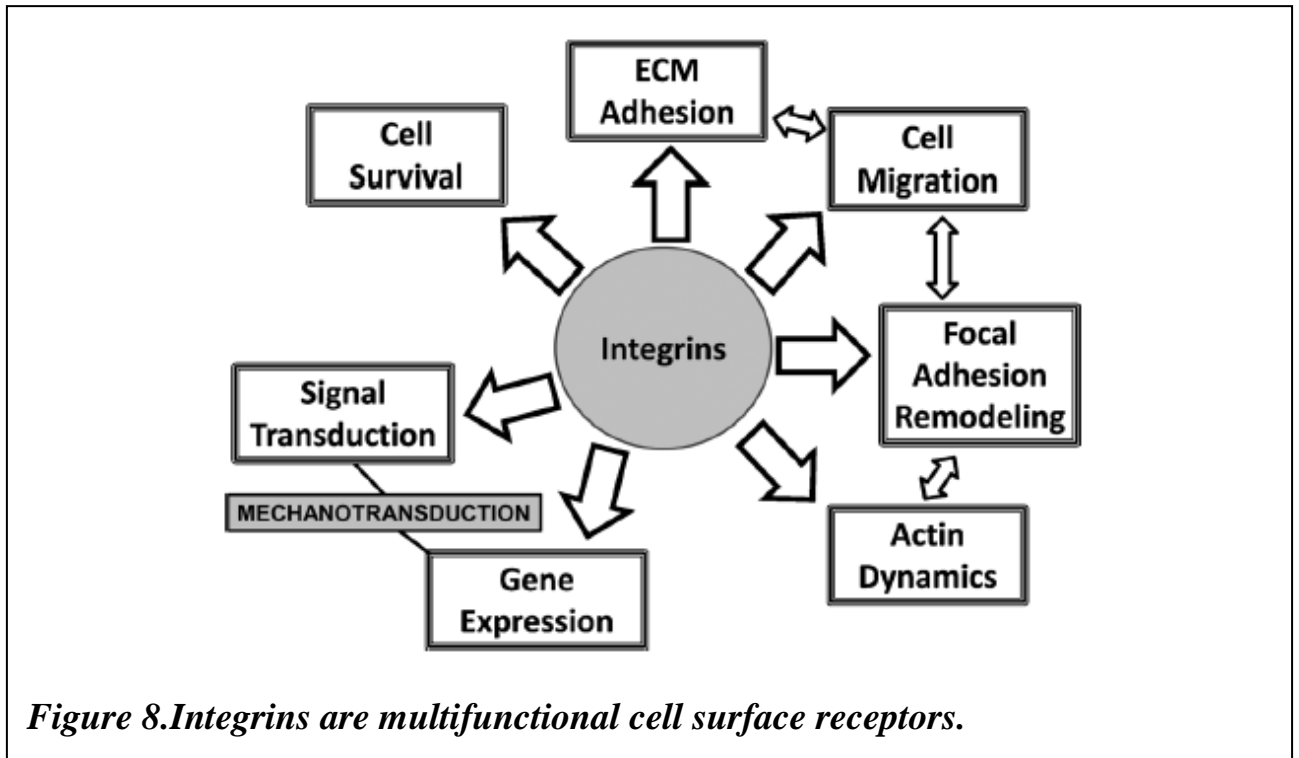


Figure 8. Integrins are multifunctional cell surface receptors.

Cell adhesion molecules are surface proteins involved in modulating intercellular communication among a wide variety of different cell types. Several major families of adhesion molecule receptors have been identified and characterized; these include the integrins, cadherins, selectins, membrane associated proteoglycans, and the immunoglobulin superfamily members. VCAM-1 (or CD106) and ICAM-1 (or CD54) are two members of the immunoglobulin gene superfamily that are critical in the recruitment and infiltration of inflammatory cells to sites of injury. VCAM-1 binds circulating monocytes and lymphocytes expressing the integrins $\alpha 4\beta 1$ and $\alpha 4\beta 7$ [128]–[130], whereas ICAM-1 is the counter-receptor for several leukocyte $\beta 2$ integrins (e.g., lymphocyte function–associated antigen [CD11a/CD18] and Mac-1 [CD11b/CD18]). The interaction of ICAM-1 with leukocyte integrins also plays an important role in leukocyte trafficking and the initiation of antigen-specific immune responses [108], [131]. Myocardial CAM gene expression is upregulated in inflammatory states such as ischemia/reperfusion and myocarditis [131]–[135]. Elevated CAM expression is temporally associated with leukocyte sequestration and

infiltration into myocardial tissues. In cardiac inflammation, resident cells (e.g., endothelial cells, myocytes, fibroblasts, and smooth muscle cells) and infiltrating leukocytes release cytokines capable of transcriptionally activating CAM genes and, as a consequence, promote leukocyte sequestration and transmigration. The importance of myocyte ICAM expression in neutrophil adherence and subsequent myocardial injury has been shown by several groups [136]–[138]. Although ICAM and VCAM are constitutively expressed in a few cell types, they are readily induced by proinflammatory stimuli such as IL-1, TNF, LPS, and phorbol esters [128], [130], [131], [139], [140]. Control of CAM expression is largely due to an increase in mRNA production, and several specific mechanisms responsible for the transcriptional activation of CAM genes have been investigated [140]–[143]. Both ICAM and VCAM genes contain sequences in their promoter regions that are recognized by the NF- κ B/rel and AP-1 transcription factor families [142], [143]. Deletion analysis has demonstrated that these sites are necessary for both cytokine or LPS induction of these adhesion molecules [142], [143]. Although CAMs have been extensively investigated in both vascular tissue and in endothelial cells, there are few reports available concerning CAM regulation by cytokines in myocardial cells (myocytes and non-myocytes). Furthermore, in the investigations that have been reported, the signal transduction pathways underlying CAM induction have not been identified. Previous reports indicate that cytokines such as TNF- α and monocyte chemoattractant protein-1 induced a dose-dependent induction of ICAM mRNA and protein in neonatal cardiac myocytes [138], [139]. Among the important stimuli in the production and release of cytokines in several cell types is hypoxia [144]–[147]. Moreover, hypoxia and/or reoxygenation have been shown to induce ICAM and E-selectin in endothelial cells [148], [149]. However, little is known about (1) the mechanisms of adhesion molecule regulation in cardiac myocytes and fibroblasts by hypoxia and cytokines and (2) the potential interaction of these two variables that are known to be involved in the inflammatory myocardial injury. Because hypoxia and cytokine release are components of acute and chronic myocardial ischemia, we

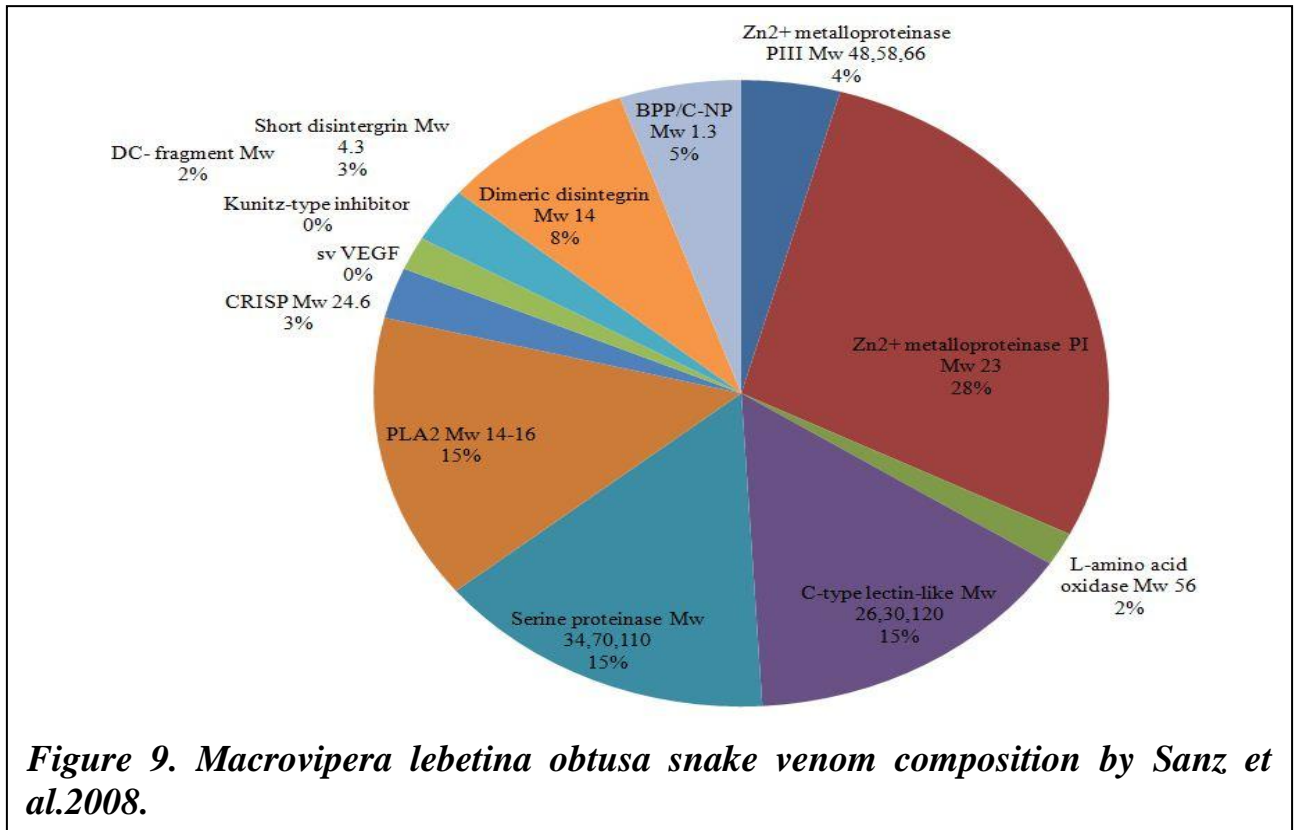
investigated the induction and the regulation of cardiac myocyte and fibroblast ICAM and VCAM expression by hypoxia and cytokines in an established cell culture model.

1.3. *Macrovipera lebetina obtusa* snake venom

Most animal poisons (venoms) are an evolutionally optimized mixture of highly specialized enzymes and physiologically active polypeptides, aimed at killing and digestions of a prey. Snake venoms contain up to several dozen different enzymes designed for destruction of cellular structures of a preys' organism or trespassing functions of individual organs or organ systems. The action of venom is exaggerated by the fact that many of its components carry out two or more functions [150]. Importantly some venoms trigger cascades of host enzymatic reactions, which means that even the smallest amounts of venom can result in the development of severe pathologies. The evolution of snakes and their venoms is greatly affected by a specific biocenosis. As of today, venoms can be roughly classified into three groups: neurotropic, hemotropic and mixed. It is important to mention that all venoms have neurotropic and hemotropic effects, however, one manifestation is usually more prevalent than another is. In such snakes as a cobra, belonging to Elapidae family, the venom is mostly neurotoxic (damages neurons). Thus, one of the venom toxins (cobratoxin) prevents muscle contraction and causes muscle paralysis. Among affected muscle are those responsible for breathing. Consequently, a prey stops breathing and dies.

The venom of snakes from *Viperidae* family acts differently. *Viperidae* snake venom contains hemorrhagic proteases, characterized with haemo coagulatory and necrotizing properties, peptide hydrolases, hyaluronidases, and phospholipases which are injected into the bloodstream during the bite. *M. lebetina* species of *Viperidae* genus has the largest living area. It includes Northern Africa, Cyprus, Turkey, Middle East countries such as Iran, Afghanistan, as well as **Armenia**, Azerbaijan, Dagestan, and parts of Central Asia, specifically Turkmenistan, Uzbekistan, Tajikistan [151]. *MLO* venom possesses all properties of hemotropic venoms (Fig.9) [151]. This includes hemorrhagic damage of blood, vessels, total clotting of blood throughout

circulatory system (called disseminating intravascular clotting [DIC] syndrome) with the following thinning of blood and hemolysis (Table 1).



Each of these processes is defined by many agents within the venom, which act together to cause a particular damage. Hemorrhagic damage of vessels caused by *Macrovipera lebetina* venom delivered by metalloproteinases PI and PIII (svMP-PI and svMP-PIII) and disintegrins of several types. Blood coagulation is caused by serine and thrombin-like proteases. Erythrocyte hemolysis is a result of the interaction of venom's phospholipase A2 (PLA2) with host tissue factor, which is released upon destruction of blood vessels. In addition, L-alpha amino acid oxidase of blunt-nose viper created a local high concentration of H₂O₂ and consequently large amounts of reactive oxygen species (ROS). Along with the described events, amino acids are transforming into keto acids causing the starvation of cells. The aforementioned processes initiate apoptosis and/or necrosis of neighboring cells [152]. Free disintegrins (both, dimeric VLO4, VLO5A, VLO5B, and obtustatin) are involved in blocking of integrins and other adhesion molecules, thus limiting platelets and other cells formability to stick together and to the injured vessel walls [153].

There is a very specific minor component in *MLO* venom -C-type natriuretic peptide (CNP) [6]. CNP in human organism is involved in the maintenance of electrolyte-fluid balance and vascular tone; as its name suggests, it promotes

natriuresis and diuresis resulting in loss of sodium and water thereby lowering blood volume and blood pressure.

Table 1. Components of MLO snake venom and their effects on a prey.

Type of Compound	Action on the body
Arginine esterases	believed to predigest prey
Bradykinin-potentiating peptides (BPP)	pain, hypotension, immobilize prey
C-type lectins	modulate platelet activity, prevent clotting
Cysteine-rich secretory proteins (CRiSP)	believed to induce hypothermia, immobilize prey
Disintegrins	inhibit platelet activity, promote hemorrhaging
Hyaluronidases	increase interstitial fluidity, aiding the dissemination of venom from the bite site
L-amino acid oxidases (LAAO)	cell damage/apoptosis
Metalloproteinases (MPr)	hemorrhage, myonecrosis, believed to predigest prey
Myotoxins	myonecrosis, analgesia, immobilize prey
Nerve growth factors	believed to cause cell apoptosis
Phosphodiesterases (PDE)	believed to cause hypotension, shock
Phospholipase A2's (PLA2)	myotoxicity, myonecrosis, damage to cell membranes
PLA2-based presynaptic neurotoxins	immobilize prey
Purines and pyrimidines	believed to cause hypotension, paralysis, apoptosis, necrosis, immobilization of prey
Serine proteases	hemostasis disruption, hypotension, immobilize prey
Three-finger toxins (3FTx)	rapid immobilization of prey, paralysis, death

CNP was first purified and identified, in 1990 some 10 years after the discovery of atrial natriuretic peptide. CNP is the most widely expressed natriuretic peptide. It was discovered in the brain, chondrocytes, and endothelial cells. CNP acts as a local paracrine or autocrine regulator, then cleared rapidly from the circulation and present at traced concentrations in plasma.

Endogenous and exogenous CNP may offer protection from myocardial infarction and cardiac remodeling injury. Ventricular hypertrophy, necrosis, inflammation and functional impairment of cardiac tissue induced by coronary artery ligation is reduced in mice overexpressing CNP in cardiac myocytes [154]. Chronic CNP infusion administered post-myocardial infarction (MI) attenuates cardiac fibrosis and increases survival [155].

Because we deal with cardiomyocytes, the action of this component (CNP) of *MLO* venom was in the field of our interest. What may be the action of CNP part of venom on cultured cardiac cells without a vascular environment? Is there a direct interaction between cardiac myocytes and CNP-related to contractile activity? It is known, that *MLO* venom cause tachycardia in preys, but this phenomenon related directly to cardiac cells functioning is not enough elucidated.

Venoms are designed to act exclusively in physiological media of prey's organism. But first, any of components will not harm snake itself. So poisonous glands, in addition to destructive enzymes, secreted inhibitory substances or create acidic media to prevent self-digestion or there may be inhibitors in snake blood [156]. Despite the dried venom keeps its activity for a very long time (years), diluted venom must be used in few hours. Not dried freshly milked venom even in refrigerator can't be stored even for a week due to autolysis. When venom is ejaculated from glands, activated proteases digest each other. Venoms or their certain components could be inactivated for investigative needs too. There are different methods and reagents for venom inactivation *in vitro*. The simplest method is the thermal destruction of thermally labile components, e.g. metalloproteinases. Metalloproteinases contents Zn^{2+} ion in their enzymatically active site and loose it when the temperature of venom solution is more than $70^{\circ}C$. Another enzyme of snake venom, phospholipase A_2 has 6 or 7 disulfide bonds and may be inactivated only when venom solution is boiled for 10-15 minutes. Thermal inactivation is not enough selective method and different enzymes may be not only inactivated but denaturated too. In some cases in highly protonated, acidic media, the enzymatic activity of snake venom components may be stopped in a reversible manner. This method of inactivation is not usable for injections and any investigation *in vivo*. When the acidic solution is injected in an experimental animal organism, it is diluted by blood or tissue liquids and loose it's inhibiting properties. The more suitable method is biochemical inhibition by specific kinds of molecules, which may bind with enzyme active site and block it. One of the most known inhibitors of PLA_2 is bromophenacyl bromide (BPB). BPB irreversibly

binds to the PLA₂ active site and keeps inhibiting effect even after venom injection [157]. Ethylenediaminetetraacetic acid or its sodium salt (EDTA-Na₂) often is used to bind bivalent ions in media [158]. A certain concentration of EDTA-Na₂ if incubated with venom solution can bind Zn²⁺ ions which are located in MPs active site. Without Zn²⁺ ion in the active site, MP can't exercise its enzymatic activity. In such, incubated with EDTA-Na₂ solution, Ca²⁺ ions are bind too. All Ca²⁺ dependent enzymes may be inhibited in EDTA-Na₂ treated solution and it must be taken into account for *in vitro* experiments. When injected into animals via different routes, Ca²⁺ dependent enzymes may bind it from tissue liquids and blood, but MPs activity do not restore. This method is good to investigate venom activity excluding MP effects on the organism or any kind of cultured cells.

1.4. Models used in this study

1.4.1. NRCM as a model for the study of morphological, biochemical and electrophysiological characteristics of the heart.

Various animal models are accepted for examination of cardiac physiology and cardiac diseases for a long time now. These models were primarily developed to study different surgical and pharmacological interventions in the intact heart. The development of intact muscle preparations came much later, which allowed direct manipulation of the heart muscle. Unfortunately, these models do not provide an easy access to the core of the muscle; hence, specific recordings or treatments cannot be performed. Moreover, the large size of these preparations hinders the electrophysiological examination of the myocardium, preventing appropriate control of membrane potential during voltage-clamp experiments. The aforementioned constraints have led to the development of single cardiomyocytes isolation techniques. An additional advantage of using isolated cardiomyocytes is the ability to select cells from different areas of the heart, including the atria, left and right ventricles, the conductive system or a specific region of the heart following myocardial infarction. In addition, isolated cells are a good solution for experiments designed to visualize the cellular structure and specific locations of intracellular

molecules. Lastly, isolated cardiomyocytes allow the study of intracellular Ca^{2+} homeostasis, cellular mechanics, and protein biochemistry [159]. Ca^{2+} homeostasis is often investigated by assessment of the contractile activity of cardiomyocytes' monolayer. In this study, such data was collected from a monolayer of rat neonatal cardiomyocytes, visualized by a Fluo-4 AM fluorescent indicator of Ca^{2+} release and recorded by confocal microscopy.

1.4.2. HeLa cells as a model for studying epithelial cells.

HeLa cells we used as a model of a mammalian epithelial cell. HeLa cells were first isolated in 1951 from Henrietta Lacks' cervical cancer [160]. They were immortalized by George Gey, become the first, and widely used human epithelial cancerous cell line. They are characterizing with rapid duplication properties (every 18 hours) and serve as test cells for many different purposes.

1.5. Venom-Cardiomyocyte studies

Snake venoms have a variety of deleterious effects on almost every organ system. In most cases of snake venom poisoning, the circulatory disturbance is one of the most frequently encountered events. Since a single snake venom contains a variety of enzymes as well as non-enzymatic components of different biologic activities, it is not difficult to appreciate the complexity of cardiovascular changes produced by different snake venoms.

Some attempts have been made to define the relationships between the direct effects of snake venoms on the cardiovascular system and those which may be caused by auto-pharmacological substances liberated from the tissues by the venom. During recent years, attempts have also been made to determine which component or components of snake venoms are responsible for these effects. In the course of these investigations, many important data, this indicated the complexity of the vascular response, have been obtained.

1.5.1. Cardiovascular effects of Crotalid and Viperid venoms

Crotalid venoms are characterized by the richest source of overall enzymatic activities among snake venoms: proteolytic enzyme activity in crotalid venoms has been shown to be the most potent among snake venoms so far examined. The viperid venoms have lesser amounts of proteinases, while the elapid and sea snake venoms either have very little or no proteolytic enzyme activity [161]. Venoms that are rich in proteinases produce marked tissue destruction and also deleterious effects on the cardiovascular system. However, what role the proteinases play in these deleterious effects is still not fully understood. The auto-pharmacologic substances released by snake venom enzymes could contribute towards the circulatory shock produced by crotalid and viperid venoms. These substances include bradykinin, histamine, 5-hydroxytryptamine, and prostaglandins. Again, to what extent each of these substances may be responsible for the cardiovascular changes produced by different venoms is still an unsolved problem. In addition, some of the viperid and crotalid venoms contain coagulant or procoagulant enzymes, which may produce intravascular clotting and thus contribute to the cardiovascular changes, even leading to sudden death. Apart from such enzyme activities, the crotalid and viperid venoms may contain some toxic principles which affect the cardiovascular system either directly or through central regulatory mechanisms.

1.5.2. Hemodynamic effects of Viperid venoms

Russell's Viper (Vipera russellii) Venom. The action of Russell's viper venom on the circulatory system was extensively studied by Chopra and Chowhan, 1934. A small dose of the venom (0.05-0.1mg/kg) injected intravenously into a cat produced a slight initial rise in blood pressure followed by a gradual fall amounting to 20-30mmHg. With larger doses (0.2- 0.5mg/kg), the fall was more pronounced and the blood pressure remained permanently at a lower level. Rapid administration of large doses produced a sudden fall in blood pressure and the animal sometimes died suddenly of convulsions and heart failure. Using heparin and other anticoagulants proved that the sudden death produced by Russell's viper venom is due to

intravascular clotting. The same conclusion was also reached by Ahuja et al., 1946 [162]. If the dose of the venom was gradually increased, the animals developed a sort of tolerance to it. Once the blood pressure had reached its lowest level after a dose of the venom, further administration of much larger doses did not produce any effect on the blood pressure. These authors summarized their experimental results as follows:

In the case of viper venom, the hemorrhagic phenomena appear at the outset of the poisoning and are very extensive in character. Death is preceded by spasmodic and irregular respiration, convulsions and asphyxia indicating the involvement of the vagal center owing to the deficient blood supply. Daboia (Russell's viper) venom has a marked tendency to produce thrombosis and gangrene at the site of the bite and death is due to secondary shock. The systemic blood vessels, especially the peripheral ones, are found to be contracted and those of the splanchnic area are widely dilated as in histamine shock. That the nervous centers are not much affected is shown by the fact that in decerebrated animals exactly the same results are produced. The symptoms of shock in daboia poisoning are not due to reflex impulses but are due to the local dilatation of the capillaries of the splanchnic area. There is enormous engorgement of the abdominal viscera and that the collapse goes hand in hand with hyperemia of the splanchnic area (chiefly the gut) is shown by the fact that if the mesenteric arteries are clamped, quite large doses of the venom do not produce any marked effect on the blood pressure. The paralytic action of the venom seems to be confined to the capillaries only. In the perfusion experiment, it was observed that the veins and arteries are not dilated; on the other hand, they show a tendency to constrict. The paralytic action of the venom on the capillaries was observed to be similar to that of histamine since the venom does not give any fall of blood pressure after large doses of histamine and vice versa. Drugs like ether and chloroform which depress the capillaries potentiate the action of the venom. Under the microscope, fine capillaries of the frog's omentum were seen to dilate widely when exposed to the action of Daboia venom. Adrenalin and pituitrin, which tone up the capillaries, and glucose, gelatine, and gum-saline, which increase the total volume and the viscosity

of the blood, tend to revive the blood pressure. The hemorrhagic tendency and enormous leakage of the plasma from the capillaries are further supported by the fact that the coagulation time is increased and the red cell count is also increased after large doses of the venom. From the above data, it was justified in concluding that the venom has a paralytic action on the capillaries which increases the leakage, thus producing symptoms similar to that of shock. Death is secondary to shock and life can be saved if the shock can be overcome early.

Vick et al. (1967) also reported that a lethal dose (0.5mg/kg, intravenous) of Russell's viper venom produced an immediate and irreversible decline in arterial blood pressure. Pulse pressure narrowed and heart rate decreased as arterial pressure fell. No terminal signs of hypoxia were exhibited with this venom. Respiration was not affected during the initial post injection period, but after approximately 10 min respiratory movements ceased abruptly and profound bradycardia was noted. Progressive hypoxia-induced changes in EKG were noted and at the time of death electrical disassociation leading to the cardiac arrest was seen. Evisceration prevented the initial hypotension and bradycardia. A rather slow progressive decline in arterial blood pressure occurred over a 15-30 min period. Vagotomy did not prevent the sharp fall in arterial blood pressure noted in the intact animal; however, bradycardia was prevented and a significant increase in heart rate occurred. Since surgical removal of the viscera prior to envenomation prevented the initial fall in blood pressure, Vick et al. (1967) concluded that Russell's viper venom produces a pooling of blood in the hepato-splanchnic bed of the dog. Apparently, these authors did not consider the possibility of intravascular clotting by this venom.

The circulatory action of the venom of *V russellii jormosensis*, a subspecies of Russell's viper, was studied in rabbits. This venom, like Indian daboia venom, has a coagulant action and produces intravascular clotting upon intravenous administration. When a sub-lethal dose (0.05-0.1mg/kg) was injected into rabbits intravenously, an immediate fall in mean arterial blood pressure and an increase in heart rate were observed. Subsequent injection of the same dose did not produce significant changes

in either blood pressure or heart rate. However, after a dose of 0.5mg/kg, the blood pressure fell suddenly to the zero line within a few minutes and no recovery was observed. Injection of adrenaline, transfusion of normal saline, or artificial respiration failed to restore the blood pressure. Section of both vagi and atropinization did not in any way alter the venom action. On the other hand, in the animals pretreated with heparin (25mg/kg), no sudden death was observed even with 5mg/kg of the venom. The arterial blood pressure fell to a very low level and finally, the animals died of circulatory failure after several hours.

The hemodynamic effects of this venom were further studied after heat treatment (at 80°C, for 30 min) which destroyed the coagulant and most other enzyme activities of the venom. The heated venom did not produce sudden death even at large doses (5-10mg/kg); as in the heparin-pretreated animals, it produced an immediate and irreversible fall in the arterial blood pressure and the animals died of circulatory failure within several hours. The hypotensive action of the venom was not affected by the heat treatment; a dose as small as 0.05mg/kg of the heated venom still produced a transient fall in the arterial blood pressure. With 0.1-1.0mg/kg, the hypotensive effect was more pronounced and long lasting; the heart rate increased as the blood pressure fell. However, with lethal doses (5-10mg/kg) bradycardia took place and arrhythmia appeared prior to cardiac arrest. With small doses (0.5-1.0mg/kg), the pulmonary arterial pressure decreased slightly as the systemic blood pressure fell, whereas with large doses (5-10mg/kg) a transient and slight rise followed by a fall was observed. Regardless of whether a small or large dose was administered, the volume of the small intestine was markedly increased when the blood pressure fell. The liver volume also increased slightly, whereas the kidney volume showed a decrease followed by an increase. The limb volume decreased after a transient increase. The portal vein pressure decreased and, in some cases, was followed by an increase. Intracisternal injection of 0.1mg/kg of the heated venom caused a rise in the systemic blood pressure. With 1.0mg/kg, the rise in blood pressure was followed by a gradual decline to the zero line. Neither, elimination of the brain circulation nor cutting of the

carotid sinus and depressor nerves altered the hypotensive effects of the heated venom. It was concluded that the cause of death by Russell's viper venom is at least twofold: (1) the coagulant enzyme is responsible for the acute sudden death due to intravascular clotting, and (2) the thermostable vasculotoxin produces a sustained hypotension leading to delayed circulatory failure. The cause of hypotension by the vasculotoxin is not central in origin and is due to peripheral vasodilatation, especially in the splanchnic area.

Vipera ammodytes Venom. Intravenous injection of *Vipera ammodytes* venom (4.5mg/kg) in rats produced a rapid fall in the arterial blood pressure followed by respiratory failure [163]. Severe cardiac disturbances did not appear until the animal was in hypoxia. A basic protein fraction from *V. ammodytes* venom produced similar effects, but it required a larger dose (22.5mg/kg, intravenous). After injection of a smaller dose, the initially depressed arterial blood pressure recovered to the normal level, but after a certain delay coma and death followed. By isoelectric focusing and preparative disc electrophoresis, this basic fraction yielded three homogeneous proteins [163]. In the rat, neither the crude venom nor the basic protein fraction (both in the concentration of 100ug/ml) produced neuromuscular block after prolonged stimulation. Since no labeled crude venom and only traces of the basic protein fraction were found in the brain, the respiratory depression could be caused by anoxia of the central nervous system due to the arterial hypotension [163], although it had been claimed that this venom contained a neurotoxic fraction which was devoid of hemorrhagic activity, but produced paralysis of extremities and respiratory failure in mice.

Vipera palestinae Venom. Intravenous injection of a maximum sub lethal dose of *Vipera palestinae* venom or its separated neurotoxic fraction, viperotoxin [164], into cats, produced an immediate and sharp fall in blood pressure [165]. This reduction in blood pressure continued throughout the duration of the experiment in most of the animals and was associated with progressive peripheral vasodilation. The pulse pressure diminished progressively to a very low amplitude. The action potentials of

the cervical sympathetic chain disappeared completely within 30s of injection. The voltage of electrocorticograms was also diminished in all leads, and sometimes entirely abolished for short periods 3 min after the injection of venom or neurotoxin. The neurotoxin showed no cardiotoxic or ganglionic blocking action. When administered to spinal cats, it produced a slight transient rise in blood pressure, probably due to a moderate vasoconstriction. From these results, the authors concluded that the primary circulatory shock produced by *V. palestinae* venom is correlated with its neurotoxic components, which cause depression of the central autonomic vasoregulation mechanism. The hemorrhagic component of *V. palestinae* venom does not produce circulatory shock and has no influence on the sympathetic nerve potentials. This fraction produces bleeding in experimental animals, which eventually leads to death.

Echis carinatus and Echis coloratus Venoms. The circulatory effects of *Echis carinatus* (saw-scaled viper) venom are similar to those of Russell's viper venom. A slight initial rise followed by a gradual but marked fall in blood pressure was produced by a dose of 0.2mg/kg of *Echis* venom injected intravenously into a cat. When larger doses (0.5-1.0mg/kg) were administered, a marked and permanent fall in blood pressure was observed. The volumes of the intestines, spleen, and the kidneys were definitely increased, while the limb vessels remained unaffected or even contracted. The fall in blood pressure does not appear to be central as it was obtained in decerebrated and designated animals. It is not cardiac in origin as the venom did not produce any marked effect on the heart. The fall is almost entirely due to the dilatation of the blood vessels of the abdominal viscera, since in eviscerated animals or when the splanchnic circulation had been excluded there was hardly any fall in blood pressure. The *Echis* venom is rich in hemorrhagins which are at least ten times stronger than those of the Indian doboia venom, and it also has a strong coagulant action [166]. These authors, as well as Kornalik and Pudlak (1962) [167], attributed the cause of death to the effect on clotting mechanism. Ahuja et al. (1946) [168] studied the action of heparin on this venom injected in rabbits and stated: (1) that

comparatively a much larger quantity of heparin is required to counteract the toxic effect of *Echis* venom than that of Russell's viper venom, and (2) that when the dose of *Echis* venom injected is increased to 20 times the minimal lethal dose, some of the animals show paralysis of the limbs and respiratory failure, as against the convulsive seizures seen with smaller doses. They felt that with higher doses, a toxic fraction other than the one responsible for intravascular coagulation increase from sub-lethal to a lethal dose, against which heparin is ineffective. Using columns of Sephadex G 100, Zaki et al. (1970) have separated five protein fractions from *Echis carinatus* venom. One of these fractions (Fraction 4) is lethal to mice. In rabbits, this fraction increased capillary permeability and caused a fall in blood pressure followed by death. The effects of this fraction could be completely abolished by the antihistaminic drug, promethazine. The circulatory shock caused by the whole venom was delayed to a great extent by the antihistaminic drug and to a greater extent by the antihistaminic drug together with an anti-serotonin drug.

As in envenomation by *Echis carinatus*, hemorrhage associated with intravascular clotting is a prominent feature of *Echis coloratus* envenomation. Injection of *E. coloratus* venom into mice or guinea pigs caused widespread hemorrhage, afibrinogenemia, and severe thrombocytopenia [169]. Neurotoxic activities were also observed in association with a diffuse breakdown of the blood-brain barrier [170].

The effect of *E. coloratus* venom on the brain capillaries of the mouse was further studied electron microscopically using horseradish peroxidase as a tracer [171]. It was demonstrated that the envenomation resulted in the breakdown of the blood-brain barrier manifested by leakage of the peroxidase through the capillary wall. The peroxidase penetrated both by endothelial pinocytosis and through opened tight junctions between the endothelial cells. The envenomated mice showed hemorrhages and intravascular fibrin clots in the lungs and kidneys, but not in the brain. Although neurologic manifestations were observed in the absence of bleeding

in the brain, fractionation of this venom by column chromatography did not yield a separate neurotoxin [172].

Bitis arietans Venom. Intravenous injection of the venom of *Bitis arietans* (puff adder) in doses of 0.05- 0.3mg/kg produced after a latent period of 10-20s a gradual and marked fall in the blood pressure of cats that persisted for 30 min or more and then returned to near normal levels. Repeating the injection of the venom caused a further fall in blood pressure that reached a very low level and resulted in circulatory shock and death [173]. The crude venom was fractionated on Sephadex G-100 into five main fractions, of which only fraction 1 was lethal to mice at a dose of 1ug/g intraperitoneal, producing hemorrhagic lesions in both the lungs and kidneys. Fractions 1 and 2 produced hypotension when injected in doses of 25-50ug/kg in cats. Other fractions did not produce any significant effect on the blood pressure. When equal concentrations were used, fraction 1 was the most powerful depressant of the isolated rabbit heart, while fraction 2 was the most potent in increasing capillary permeability and producing hypotension. The hypotensive effect of the venom or its fractions was not antagonized by pretreatment with hexamethonium, cyproheptadine, propranolol, atropine, indomethacin, or trasyloi. The authors concluded that at least three factors contribute to the circulatory shock caused by the venom: (1) a direct inhibitory effect of the vascular smooth muscles resulting in vasodilation of the arterioles; (2) a direct depressant action on the myocardium; and (3) an extensive increase in- vascular permeability that was also unmodified by pretreatment with antihistamines, antiserotonergic, or agents which inhibit kinins or prostaglandins. Vick et al. (1967), using dogs, showed that evisceration did not prevent the hypotensive effect of *Bitis arietans* venom, but eliminated the bradycardia. They suggested that the venom did not produce a marked pooling of blood in the hepatosplanchnic bed; however, pulmonary pooling might be responsible for the hypotension.

1.5.3. Mechanism of the Depressor Action of Viperid Venoms

Mode of Hypotensive Action. Viperid venoms, in general, have a pronounced hemorrhagic activity and some of them are also blood-coagulating agents. Clinically, hypovolemic shock may be caused by extravasation of blood into soft tissues and various internal organs. Circulatory failure or bleeding is the frequent cause of death in viper bites. Although clear evidence of disseminated intravascular clotting (D.I.C.) was rarely found in clinical cases of viper bites, intravascular clotting has been proven to be the cause of sudden death of animals following inoculation of sufficiently high doses of these so-called coagulating venoms [162], [168].

Like crotalid venoms, most viperid venoms do not kill the animals as a result of central or peripheral neurotoxic effects. Certain viperid venoms [172] or their partially purified protein fractions [174], [175] have been claimed to contain proteins with neurotropic action. However, direct evidence to show the distribution of such a neurotoxic protein in the central nervous system after envenomation is still lacking. Most claims that certain "neurotoxins" are present in certain viperid venoms were usually based only on the signs and symptoms manifested by the envenomated animals. Moreover, there is no clear-cut evidence that "curarizing" toxins are present in certain viperid venoms. It is possible that the venoms affect the central nervous system indirectly as a consequence of anoxia resulting from the arterial hypotension [163]. Alternatively, the neurotoxic effects may be attributed to hemorrhages in the brain. However, in the absence of the latter, the breakdown of the blood-brain barrier due to damage of the capillary basement membrane may be responsible for the neurotoxic action of venoms of certain vipers, such as *Echis coloratus* [170]. On the other hand, the venom of *Vipera palestinae* and its purified neurotoxic protein, viperotoxin, have been claimed to act primarily on medullary vasopressor centers leading to lethal circulatory failure [165]. However, it remains to be proven that such a basic protein can pass through the blood-brain barrier in sufficient quantity to produce such central effects.

The fall in blood pressure produced by most viperid venoms is not central in origin since in decerebrated or designated animals, or after elimination of the brain circulation, exactly the same results are produced. As in the case of most crotalid venoms, the cardiac function is not significantly affected by the later stage [163]. The initial arterial hypotension appears to be due to peripheral vasodilatation, especially capillary dilatation in the splanchnic area, since the volume of the intestines is markedly increased, while the limb vessels remain unaffected or even contracted. That the blood accumulated in the abdominal viscera has also been shown by the fact that in the eviscerated animals or when the splanchnic circulation has been excluded, injection of Russell viper's venom, as well as of *Echis carinatus* venom, produces little or no fall in blood pressure. As described previously (B. I), the site of initial decrease in peripheral resistance produced by most crotalid venoms appears to occur in the skeletal muscle vasculature rather than in the splanchnic circulation. There is so far no explanation for such differences between venoms of these two groups.

Venom components responsible for the hypotensive action. So far no purified toxin responsible for the hypotensive action has been isolated from viper venoms, except viperotoxin from *Vipera palestinae* venom [164]. A basic protein fraction, which produces a rapid fall in the arterial blood pressure, has been isolated from *Vipera ammodytes* venom [163], but this fraction is a mixture of three proteins and is less active than the crude venom.

The role played by kinin-releasing enzymes (kininogenases) in the hypotensive effect of viperid venoms is apparently much less important as compared with crotalid venoms, since viperid venoms have in general much lower kinin-forming activity than crotalid venoms. In line with this contention is the finding that heat treatment (80°C for 30 min) did not appreciably affect the hypotensive activity of Russell's viper venom. Apparently, this venom contains a heat stable toxin which may act on the capillary vascular bed, especially in the splanchnic area.

Circulatory shock with internal hemorrhage is the frequent cause of death in viper bites. In experiments on animals, administration of crotalid and viperid venoms

produces a precipitous fall in systemic blood pressure, followed by a partial recovery, but eventually, the pressure falls again, terminating with cardiac arrest. Artificial respiration fails to maintain the blood pressure.

The initial hypotensive crisis after crotalid and viperid envenomations is not primarily cardiac in origin, but mainly due to vasodilatation leading to a profound decrease in peripheral vascular resistance. Although opinions of different authors conflict, the site of initial decrease in peripheral resistance produced by most crotalid venoms appear to lie mainly in the skeletal muscle vasculature, whereas most viperid venoms produce capillary dilatation in the splanchnic area rather than in the skeletal muscle. So far no explanation for such differences has been produced.

Although disseminated intravascular clotting is rarely found in viper bites, intravascular clotting has been proved to be the cause of sudden death of animals following injection of high doses of "coagulating venoms." The occasional onset of pulmonary hypertension may be related to the production of thromboembolism in the pulmonary vascular bed.

After the initial changes, venom shock is characterized by prolonged hypotension, a decrease in cardiac output, hypovolemia, and hemoconcentration. This secondary shock may be caused by extravasation of plasma or blood into soft tissues and various internal organs. So far, no single component has been identified that may be responsible for the circulatory changes produced by the crude venom. The basic protein toxins isolated from venoms of certain species of rattlesnakes, including the myocardial depressor protein (MDP) from *C. atrox* venom, produce myocardial depression and thus contribute to the overall circulatory collapse produced by these venoms.

The auto pharmacologic substances (bradykinin, histamine, serotonin, prostaglandins, etc.) released by venom enzymes, such as proteinases and phospholipase A, could also contribute toward the circulatory changes produced by crotalid and viperid venoms. However, to what extent each of these substances may be responsible for the circulatory changes produced by different venoms is an

unsolved problem. The peripheral vasodilatation and increase in capillary permeability could be due to the combined effects of these auto pharmacologic substances.

Crotalus durissus terrificus venom is unique among crotalid venoms in containing a potent neurotoxin (crotoxin) which produces respiratory paralysis rather than circulatory failure.

Viperotoxin isolated from *Vipera palestinae* venom has been claimed to act primarily on medullary vasopressor centers leading to circulatory failure. It remains to be proven that viperotoxin can pass through the blood-brain barrier in sufficient amounts to produce such central effects.

Chapter 2 Materials and methods

2.1. Cells

Primary rat neonatal cardiomyocytes were obtained according to the previously published protocol [176], [177] with modifications. Briefly, beating hearts were excised from 1- and 2-day old Sprague-Dawley rats, rinsed in a cold, calcium- and magnesium-free, Hank's Buffered Salt Solution (CMF-HBSS), and then minced into $\sim 1\text{mm}^3$ pieces. Tissue pieces were incubated overnight at 4°C in fresh CMF-HBSS containing 0.1mg/ml trypsin. The next day, heart tissue was washed with fresh CMF-HBSS and treated with 0.5ml normal rat serum (NRS). The tissue was then collected in Leibovitz's medium containing 1500U ($\sim 4\text{mg/ml}$) collagenase II and shaken for 30 min at 37°C . The cells were then gently triturated, passed through a cell strainer to remove any undigested pieces, and centrifuged for 5 min at 17.5G . The pellet was resuspended in Dulbecco's Modified Essential Medium (DMEM) supplemented with 10% NRS and pre-plated in the 100mm tissue culture dish for an hour to minimize the presence of fibroblasts, which attach more rapidly than myocytes. Unattached cells were then collected, counted and plated in a fibronectin, laminin, or gelatin-coated multiwell cell culture plates at a density of 10^5cells/cm^2 followed by incubation at 37°C in a 5% humidified incubator for at least 24 hours without being disturbed. Myocytes were then kept under standard culture conditions in DMEM, supplemented with 5% NRS, 10U/ml penicillin and $1\mu\text{g/ml}$ streptomycin. Media was changed every other day. Around day three after cell plating, cardiomyocytes form an interconnected confluent network that exhibited rhythmic spontaneous contractions.

Primary rat neonatal cardiac fibroblasts were obtained in parallel with the NRCM isolation. Specifically, the population of cells that rapidly attached during the pre-plating stage of NRCM isolation was cultured for about 7 days . During that time, cells were re-seeded $2\text{-}3$ times to remove accompanying NRCM and, hence, enrich the population of cardiac fibroblasts.

Epithelial cells: HeLa cells were maintained according to the suggested protocol (DMEM supplemented with 10% Human Serum, 1x Pen/Strep) and seeded in a tissue culture treated multiwell plates at a maximum density of 2×10^5 cells/cm².

2.2. Venom collection and desiccation

Venom was milked manually as followed. The membrane (polyethylene film, PEF) was stretched over a glass Petri dish. The snake was held behind its head, and the firmness of the grip brings its fangs to the fore. The snake was stimulated to bite through the thin PEF membrane covering the collecting vial, and the pressure was applied to the venom glands. The venom was collected in the vial. The membrane was removed and then the vial was placed in desiccators for drying. Silica gel was used as a desiccant. Venom was kept at a low level of humidity and low temperature. Fresh venom solutions, prepared daily, were used in experiments.

2.3. Venom stock solution preparation and further dilutions

The crude venom of *MLO* was collected from local *Macrovipera lebetina obtusa* snakes and stored in the form of lyophilized powder. Powdered *MLO* venom was reconstituted with sterile double distilled water to achieve a stock solution of 1mg/ml and was filter sterilized. This *MLO* stock solution was diluted with complete growth media right before experiments to obtain 0.1ug/ml; 1ug/ml; 10ug/ml; 20ug/ml; 50ug/ml; 100ug/ml working concentrations.

2.4. Preparation of thermally – treated venom

To generate a solution of thermally denatured *MLO* venom, 1mg of dry venom was diluted in 1ml pre-warmed sterile water. The 1mg/ml solution was vigorously mixed (Vortex) until complete dissolving. Then the tube with the stock solution was placed into boiling water and kept there for 30 min. Thermally denatured *MLO* snake venom stock was diluted with complete growth media right before experiments to obtain 0.1ug/ml; 1ug/ml; 10ug/ml; 20ug/ml; 50ug/ml; 100ug/ml working solutions.

2.5. Preparation of PLA2 inhibited venom

BPB was used to inhibit the PLA2 of whole *MLO* venom: BPB neutralized venom was prepared as follows. BPB stock solution of 1mg/ml was prepared prior by diluting it in 1ml of sterile distilled water and was stored at 4°C. On the day of experiments, 20 units of 1mg/ml solution of venom were mixed with one unit of 1mg/ml BPB solution and incubated at 37°C, for 2 hours with periodic mixing, to allow time for BPB to interact with PLA2 and inhibit this enzyme of *MLO* venom. The resulting *MLO+BPB* mixture was diluted with complete growth media immediately before experiments to obtain 0.1ug/ml; 1ug/ml; 10ug/ml; 20ug/ml; 50ug/ml; 100ug/ml final concentrations. The described ratio of venom to BPB was established by estimating the enzymatic activity of PLA2 in whole *MLO* venom (based on molecular weight of the venom and the venoms PLA2 fraction).

2.6. Preparation of metalloproteinases inhibited venom

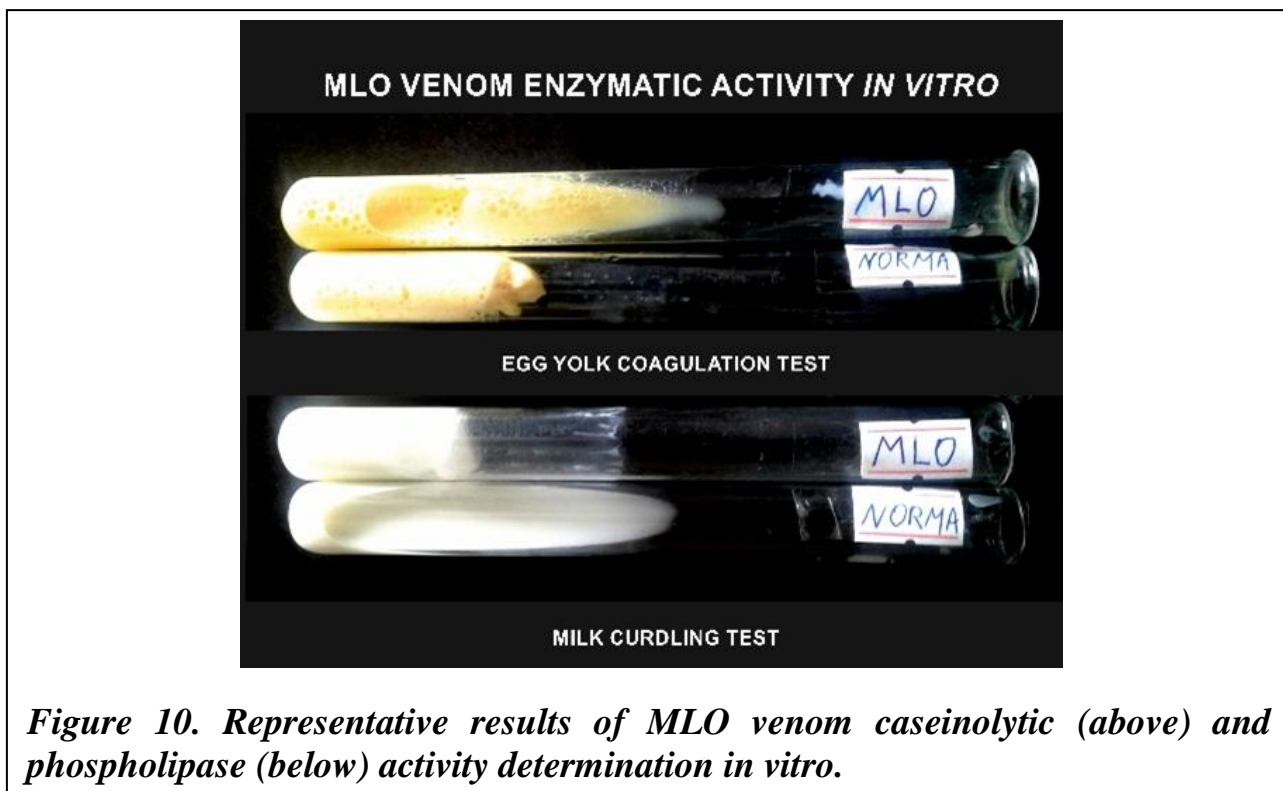
EDTA-Na₂ was used to inhibit metalloproteinases of whole *MLO* venom. The mixture was prepared as follows: 1mg of dry EDTA-Na₂ was added to 1mg of lyophilized venom and diluted in one milliliter of pre-warmed sterile distilled water. This stock solution was thoroughly mixed until complete dissolving of both reagents and incubated in the 37°C water bath for 2 hours to allow inhibition to take place. *MLO+ EDTA-Na₂* stock was diluted with complete growth media immediately before experiments to obtain 0.1ug/ml; 1ug/ml; 10ug/ml; 20ug/ml; 50ug/ml; 100ug/ml working solutions.

2.7. Venom enzymatic activity testing

2.7.1. Verification of venom caseinolytic activity *in vitro*.

We used our simple and effective test for caseinolytic activity of the venom in the assay of milk curdling *in vitro*. *MLO* venom was added to fresh milk at the ratio of 1:5000. At this ratio fresh venom leads to milk curdling when incubated for 30 minutes at 38°C (in 100% of cases). The control test tubes were filled with pure whole milk, without preservatives. Monitoring of pure milk under the same

conditions serves as an internal control and eliminates the errors associated with its spontaneous curdling (Fig.10). Each condition was tested in triplicates.



2.7.2. Verification of venom phospholipase activity *in vitro*.

Venom phospholipase activity was determined by the simplified method of chicken yolk coagulation in vitro [178], [179]. Fresh chicken egg yolk was mixed with phosphate buffer (pH 7.4) at the ratio of 1:1 (Yolk Buffer Solution, YBS). Snake venom was added at to YBS at the ratio of 1:5000. The mixture was incubated in at 38°C for 30 min. Next, the tubes with YCS/venom mixture were placed in boiling water for 15 minutes. Control mixture (without the venom) curdles up and changes the color to a lighter shade of yellow (Fig.10). However boiling of YBS/venom mixture does not lead to coagulation and the yolk retains its bright yellow color, which indicated the presence of active phospholipase in the venom. Each condition was tested in triplicates.

2.8. Morphological characterization of NRCM, CF, and HeLa cells

In order to determine the qualitative effects of *MLO* crude venom on the morphology of the cultured cells, we used phase-contrast microscopy to monitor cell

attachment. All tested cells were seeded at least 24h prior the experiments to obtain 90% confluent monolayers. Considering different proliferative properties of tested cells, NRCM were seeded at 2.5×10^5 cells/cm² and CFs were cultured at 1×10^4 cells/cm², HeLa cells were plated at 3.2×10^4 cells/cm² considering growth properties of each cell type. All experiments were conducted with monolayers reaching ~90% of confluency by the day of treatment. The morphological changes were assessed at 1 and 24 hours after addition of *MLO* venom. All other parameters were kept identical.

2.9. Physiological characterization of NRCM

Physiological characterization of contracting monolayers of NRCM consists of two main steps:

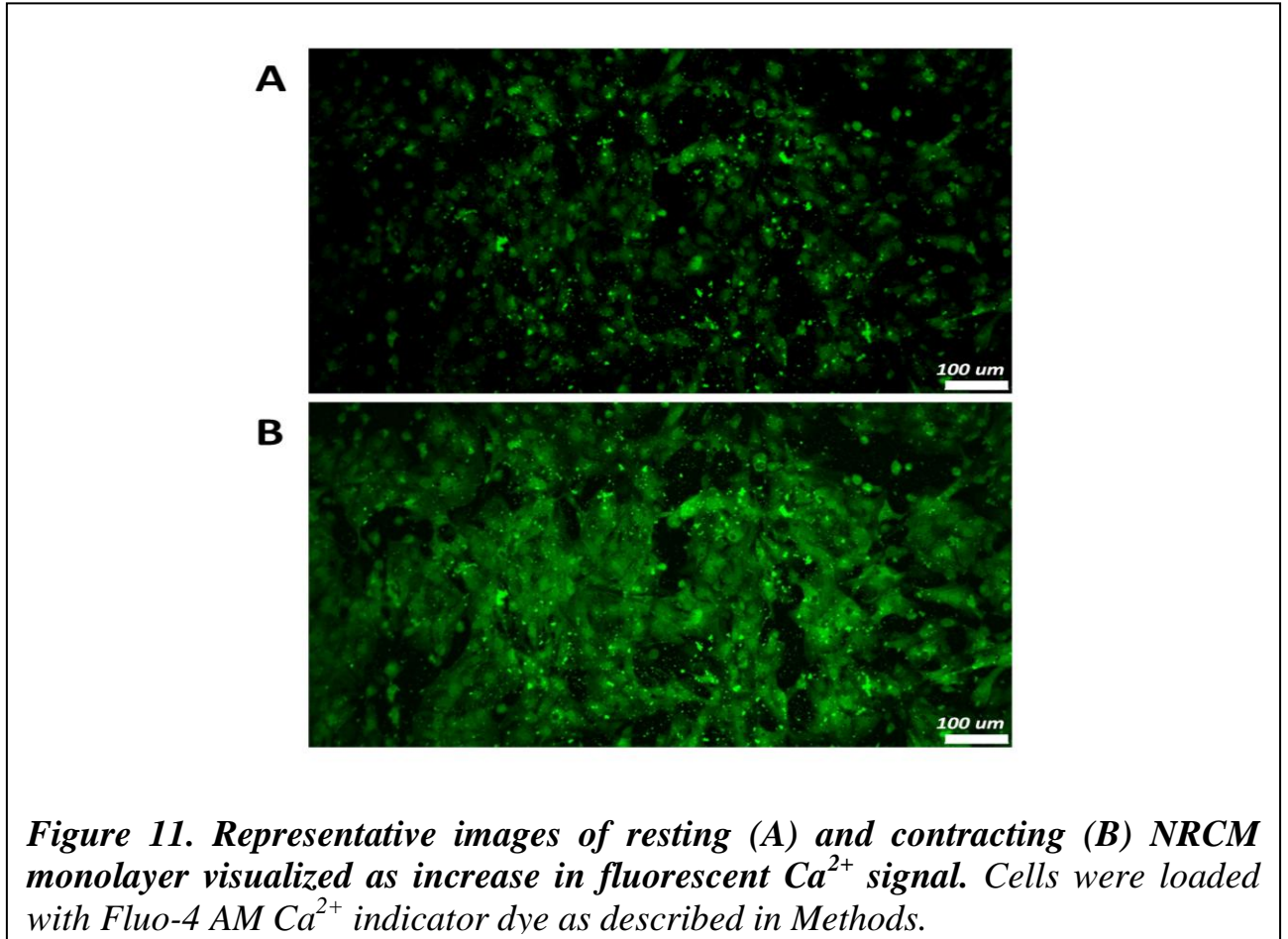
2.9.1. Fluo-4 AM Loading

Ca²⁺ release in the contracting monolayer of cardiomyocytes was imaged using fluorescence laser scanning confocal microscopy. Unless otherwise specified, loading of NRCM was performed as follows: complete media was removed, monolayers were washed with PBS, and then cultures were loaded with Fluo-4 AM (10µg/ml; Molecular Probes) in either Tyrode or phenol red-free DMEM in order to avoid color associated interference of fluorescent signals. The cultures were incubated at 37°C for 45 min. The excess of Fluo-4 was removed by washing the monolayers with PBS, after which cells were placed in phenol red free media and analyzed immediately under a confocal microscope (Fig.11). Changes in contractile activity of the cells were recorded as Ca²⁺ transients' traces.

2.9.2. Recording and analysis of Ca²⁺ Transients/Sparks in NRCM

The changes in the contractile activity of NRCMs we examined as changes in intracellular calcium levels using laser scanning confocal microscopy (Leica DMI8 Inverted TCS SPE Laser scanning confocal). As fluctuations in the intensity of calcium indicator Fluo-4. Unless otherwise specified, loading of NRCM was performed as follows: the complete media was removed and the cultures were loaded

with Fluo-4 AM (10ug/ml; Invitrogen) in Tyrode at room temperature for 20-40 minute. Afterward, cells were placed in fresh Tyrode solution and imaged immediately under a confocal microscope. The following parameters were extracted from calcium transient signals: spontaneous beating rate, amplitude (F1/F0) and peak. The beginning of the upstroke was defined by the initial deflection from baseline.



Investigation of Ca^{2+} fluorescence was done using confocal imaging with a TCS SPE laser scanning system (Leica Microsystems, Germany). Images were taken with a $\times 63$ oil immersion objective (numerical aperture (NA) = 1.4). Fluo-4 was excited by 488nm line of an Argon laser and emission signals over 505nm were collected. The fluorescent signals represent the relative level of intracellular $[Ca^{2+}]_i$ and fluorescence intensity indicates the amount of released $[Ca^{2+}]_i$. We utilized a line scan mode for recording Ca^{2+} transients as sparks in fluorescence. The confocal pinhole was set to render spatial resolutions of $0.4\mu m$ in the horizontal plane and $0.9\mu m$ in the axial direction. Ideally, the detector gain is set at around 700 (no digital

gain). Line-scan images were acquired at a sampling rate of 1.54 or 1.92ms per line, along with the longitudinal axis of the cell. Each line comprises 512 pixels spaced at 0.14 μ m intervals. After a sequential scanning, a two-dimensional (2D) image of 512 \times 1000 lines or 512 \times 2000 lines were generated and stored for later analysis (Fig.12A). It is not recommended to scan a cell in the same line region for a prolonged time because exposure to laser causes photobleaching of fluorescent dye [180]. Once the fluorescent images (static and timeline) were collected, the changes in recorded contractile activity of the cells were analyzed using ImageJ program (Fig.12B).

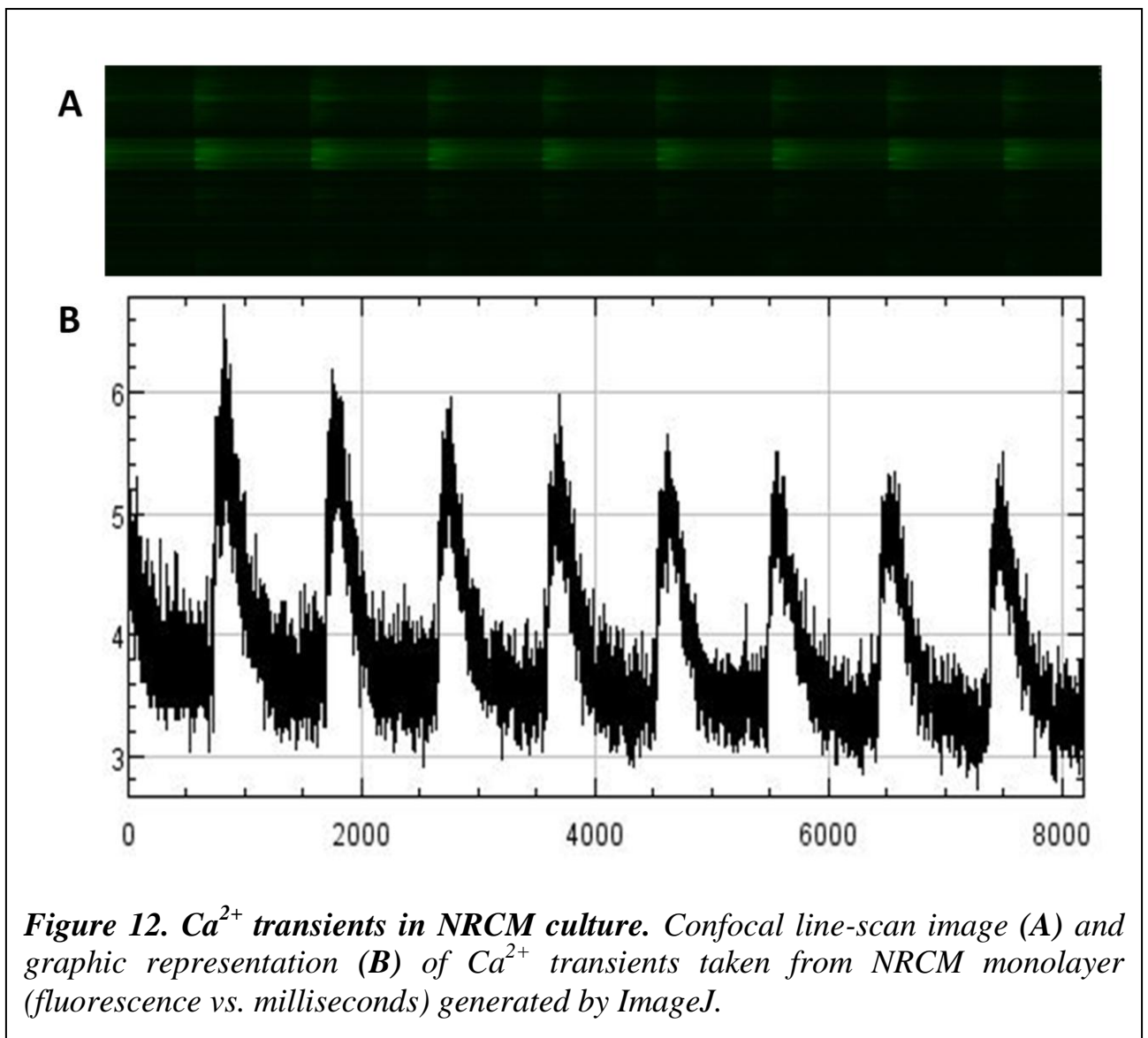


Figure 12. Ca^{2+} transients in NRCM culture. Confocal line-scan image (A) and graphic representation (B) of Ca^{2+} transients taken from NRCM monolayer (fluorescence vs. milliseconds) generated by ImageJ.

2.10. MTT viability assay

A standard methyl-thiazolyl-tetrazolium (MTT) colorimetric assay (Cat. #L11939) was used to assess cell metabolic activity [181]–[183]. Briefly, cells were seeded in multiwell microplates at 2×10^5 cells/cm² initial concentration for NRCMs and 1×10^4 cells/cm² for CFs. When the cultured cells form a confluent monolayer they were treated with different venom concentrations and incubated for 24h. Thereafter, the cultured cells were treated with MTT reagent and incubated for 3 hours until purple precipitate became visible. After incubation, the culture medium was removed, and MTT solvent (0.4uM HCl, 10% TritonX100 in isopropanol) was added to the wells, to dissolve formazan crystals. The plate was shaken for 20 min at room temperature to ensure complete dissolving of formazan crystals. The optical density was measured at 570nm and referenced at 620 nm wavelength using HiPo MPP-96 Microplate Photometer (Biosan). Recorded data were quantified using provided Quant Assay software.

2.11. Statistics

MTT assays for NRCM, CF, and HeLa cells viability and attachment experiments included three independent experiments with all conditions run in triplicates. To measure the degree of cells' detachment, at least five different view fields were analyzed (Fig.13).

Areas covered with cells were quantitated and related to the areas from which cells detached upon exposure to intact *MLO* snake venom, or thermally-inhibited venom, or PLA2 inhibited venom (BPB-treated), or metalloproteinases inhibited venom (EDTA-Na₂-treated) at all indicated concentrations and time points.

For quantitative analysis of calcium transients, each *MLO* concentration was applied to three different coverslips and Fluo-4 recordings were collected from four to five different fields. All values are expressed as mean \pm SE, with $p \leq 0.05$ considered statistically significant (*), $p \leq 0.01$ considered statistically very significant (**), and $p \leq 0.001$ considered statistically the most significant (***)

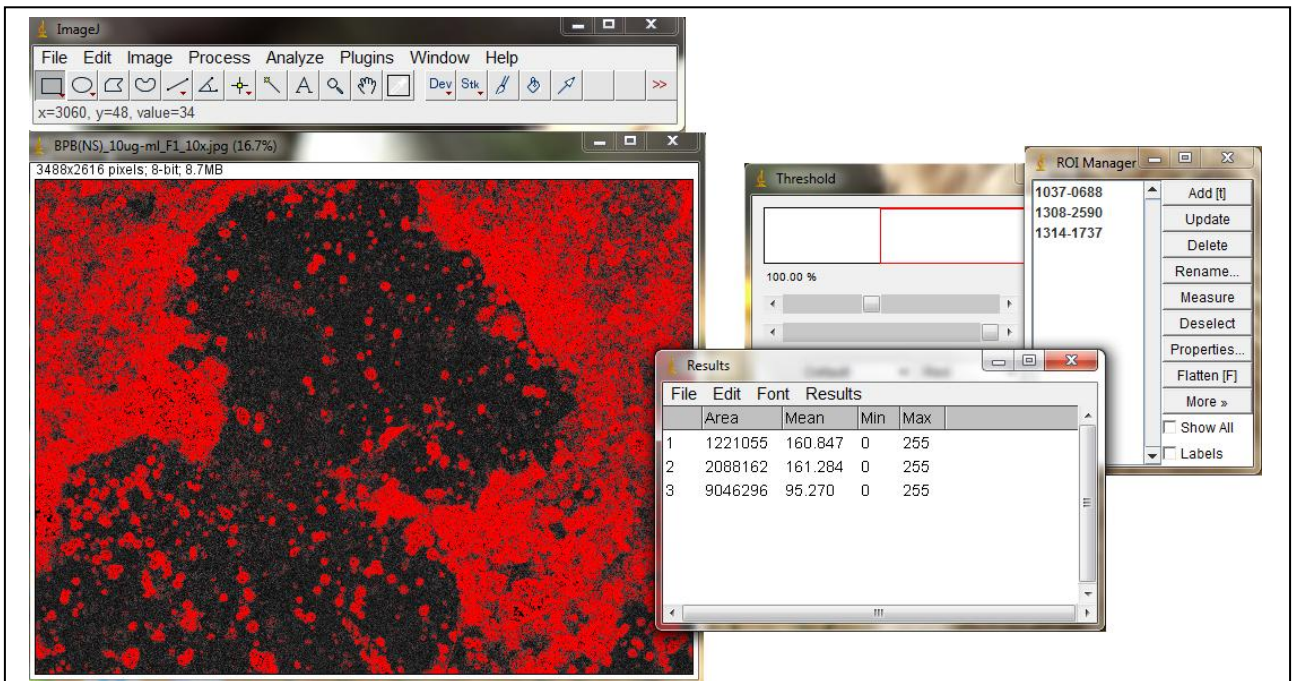


Figure 13. Sample of attachment/detachment areas counting using ImageJ.

Mean values are expressed as a percentage of vehicle control. Statistical analyses were performed using Student's t-test (MS Excel). Representative traces and images are shown.

Chapter 3 Results

3.1. Correlation of *MLO* doses with morphological/ structural changes on tested cells with viability

It is known that *MLO* snake venom affects different organs and organ systems. To better understand its effects on cardiovascular system, we decided to assess its effect on cultured cardiomyocytes and other major cells of cardiac muscle. The initial experiments were designed to evaluate the effects of whole *MLO* venom on NRCMs, CFs and HeLa cells (Fig.14).

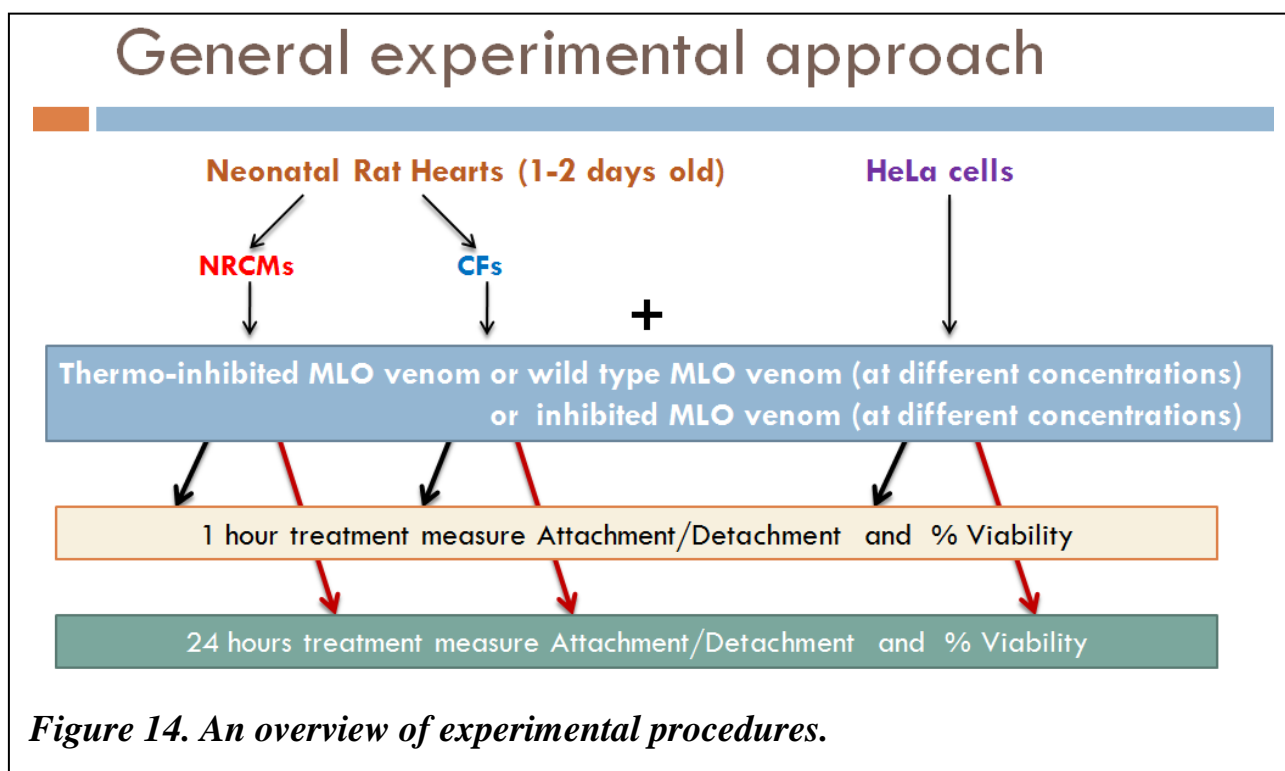


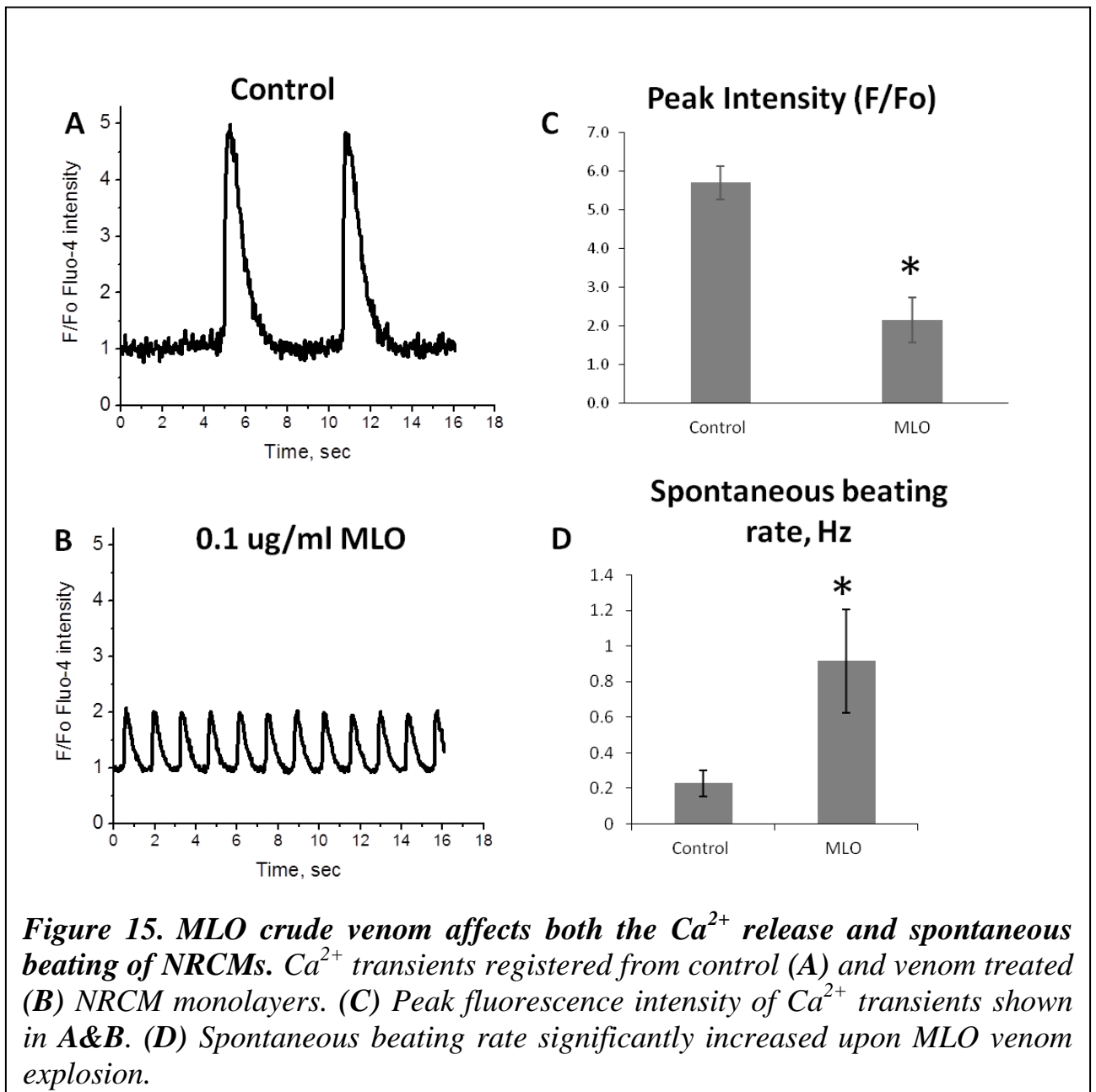
Figure 14. An overview of experimental procedures.

3.1.1. *MLO* venom effect on NRCM

The *MLO* venom was added to the cultured NRCM at the following final concentrations of 0.1ug/ml; 1ug/ml; 10ug/ml; 20ug/ml; 50ug/ml; 100ug/ml to discover possible reactions such as detachment/reattachment, changes in contraction frequency, action potential amplitude, etc.

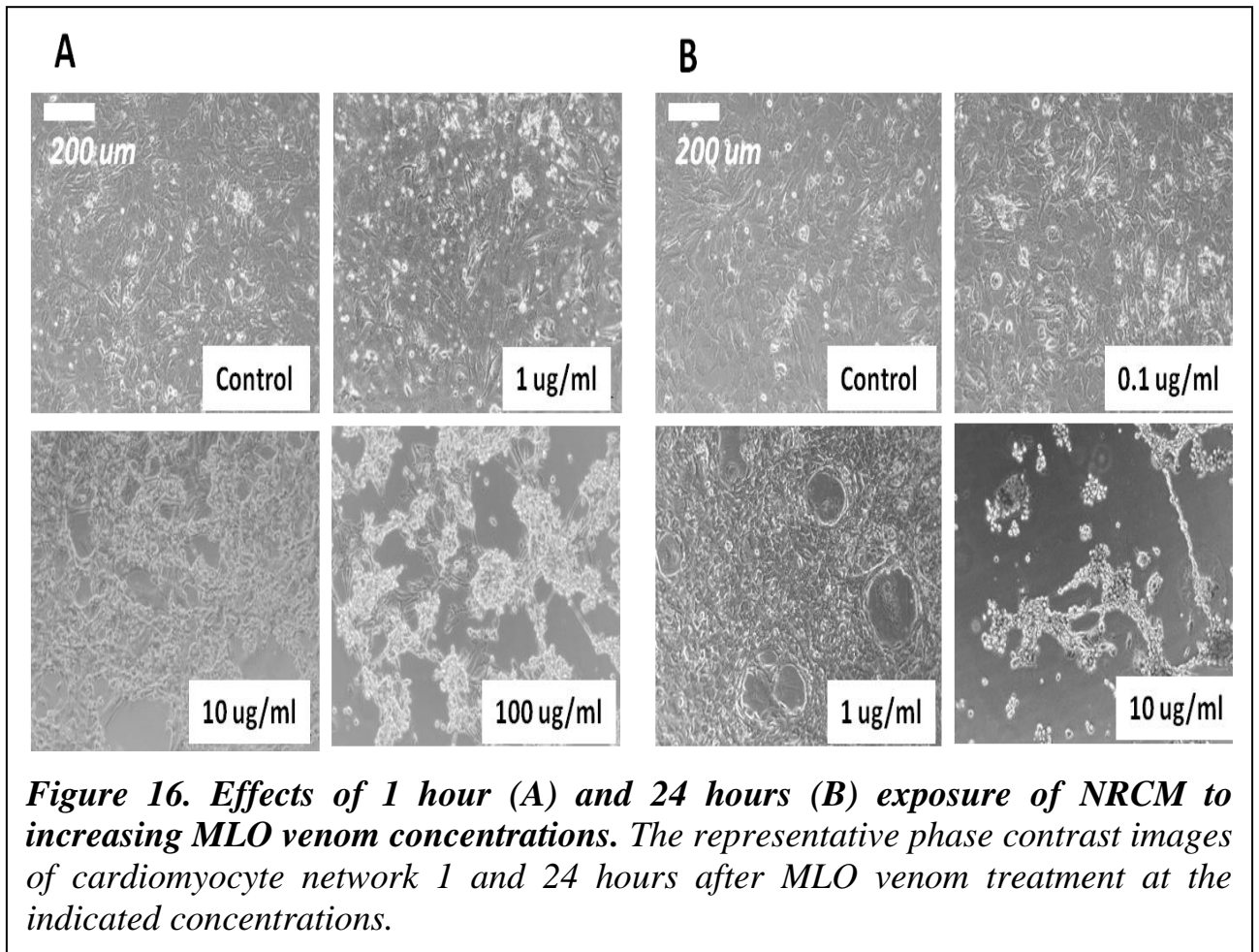
Figure 15A illustrates action potentials registered from unmanipulated control NRCM monolayer, whereas Figure 15B shows similar measurements taken from a monolayer of cells treated with the lowest 0.1ug/ml concentration. A detailed kinetic

analysis of calcium transients revealed associated changes in amplitude and duration of calcium transients. Interestingly even the lowest dose of venom caused a dramatic change in NRCM contraction amplitude (Fig.15B), decrease in Ca^{2+} release (peak fluorescence intensity Fig.15C) and a significant increase in NRCM spontaneous beating rate and (Fig.15D). As expected, increased beating frequency led to shorter durations and significantly decreased amplitude (F/F₀) of calcium transients due to the action of bradykinin-potentiating/C-type natriuretic (BPP/C-NP) peptide in *MLO* venom.



Initially, NRCM detached from culture plates as contracting clumps and later (in about 30 min) cells dissociated from each other. After 1-hour, the detached clumps and single-beating cells stop contracting and the monolayer largely disengaged.

At the lower “clinically relevant” concentration of *MLO* (from 0.1ug/ml to 10ug/ml) the NRCM monolayers remain attached which allowed investigation of *MLO* effect at the later time points. Therefore, monolayers were assessed 1 and 24 hours post venom exposure (Fig.16A and 16B respectively).



Attachment properties of NRCM were affected by *MLO* venom in a dose-dependent manner. In addition time exposure also has an effect on NRCMs attachment to the substrate and to cell-to-cell contact. Longer exposures times result in higher detachment even at the same *MLO* venom concentrations (Fig.16A vs Fig.16B). In order to quantitatively evaluate the detaching effects of *MLO* venom on NRCMs, areas covered with cells were compared with those w/o cells after exposure to *MLO* venom. As demonstrated in Figure 17A the attachment of NRCM was affected by

MLO crude venom starting at 1ug/ml concentration and reaching 100% detachment at 100ug/ml concentration (for 1hour).

In order to differentiate between the cytotoxic effect of *MLO* venom (causing cell death) and its effect on attachment properties of NRCMs, the viability of described cultures was assessed by MTT viability assay.

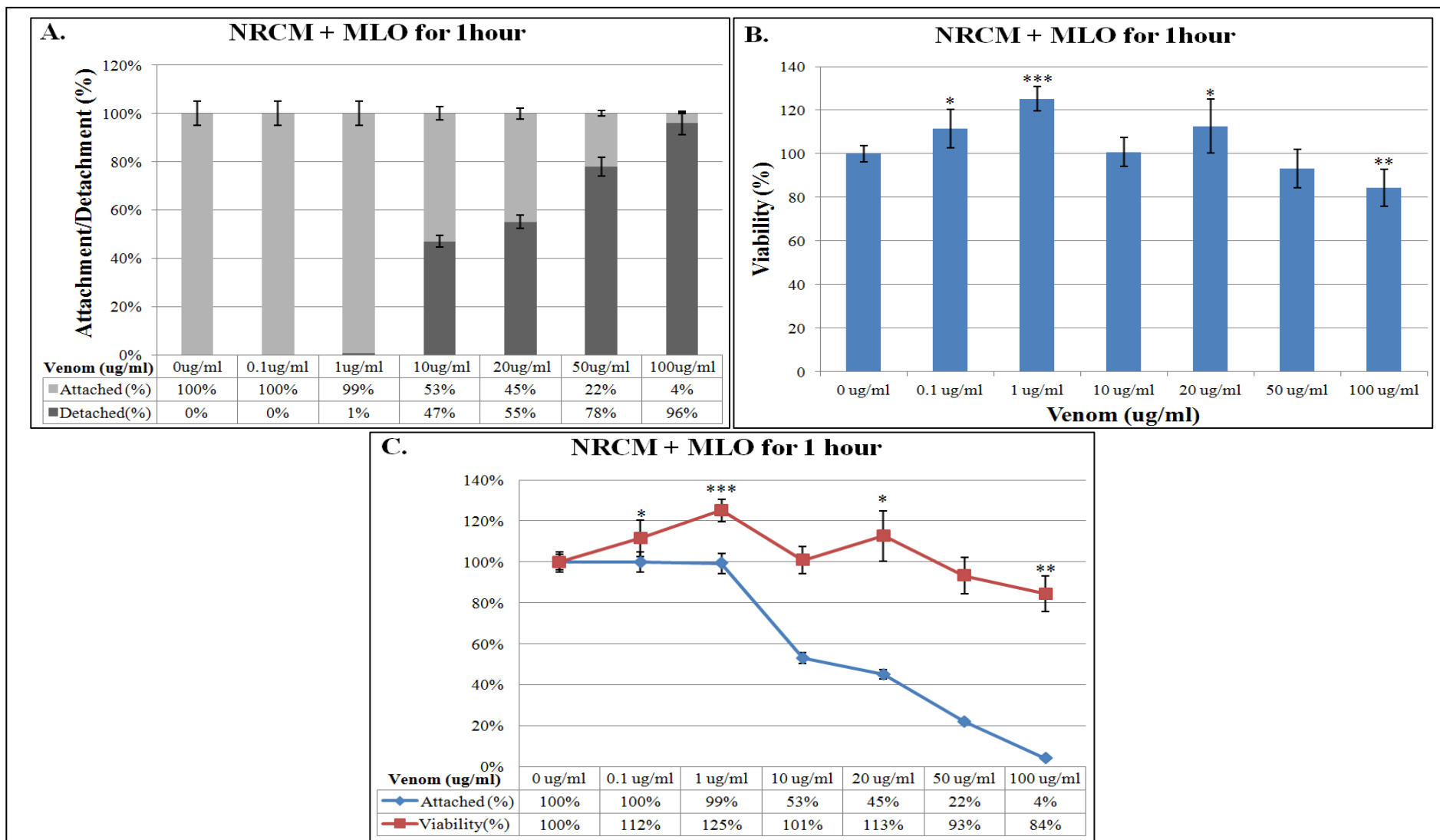


Figure 17. Attachment and Viability of NRCM is affected by MLO in a dose- and time- dependent manner. (A) The ratio of covered areas (dark gray columns) to uncovered areas (light gray columns) of NRCMs cultured for 1 hour at indicated concentrations. (B) Effect of MLO venom on NRCMs viability after 1 hour of treatment. (C) Attachment (blue line) and Viability (red line) of NRCMs treated with indicated concentrations of whole venom were assessed after 1 hour of treatment.

To properly assess cells' survivability, exclude all non-relevant effects of cell manipulations and set baseline observable facts, we conducted a series of experiments where all three cell types were exposed to thermally-inhibited *MLO* venom at different concentrations. Boiling *MLO* venom for 30 min ensures denaturing of all venom enzymes but does not rid of other non-proteinaceous elements. Therefore we assessed both the viability and the attachment of cells treated with fully denatured-thermolysed *MLO* venom at all experimental concentrations (Fig.18-20). Monolayers of NRCMs, CFs, and HeLa cells treated with thermo-destroyed *MLO* venom for 1 and 24 hours post exposure, remain attached and otherwise unaltered (data not shown). The same cultures were assessed by MTT viability assay. The results demonstrated that all attached cells were still alive and non-affected by other elements of thermally-inhibited venom, which could influence the level of cells survivability. The viability of the NRCMs remained similar after 1 hour (Fig.18A) and 24 hours of treatment (Fig.18B). Similar results were obtained with CFs and HeLa cells (Fig 19A&B and 20A&B respectively). Importantly these phenomena correlated with 100% attachment of all cells treated with thermally-inhibited *MLO* venom (NRCM - Fig.18C&D, CF - Fig.19C&D, HeLa - Fig.20C&D).

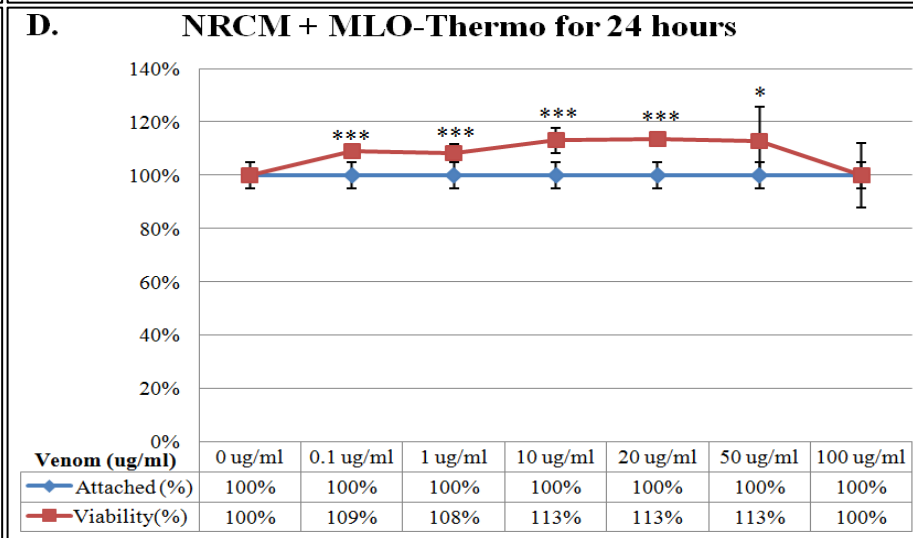
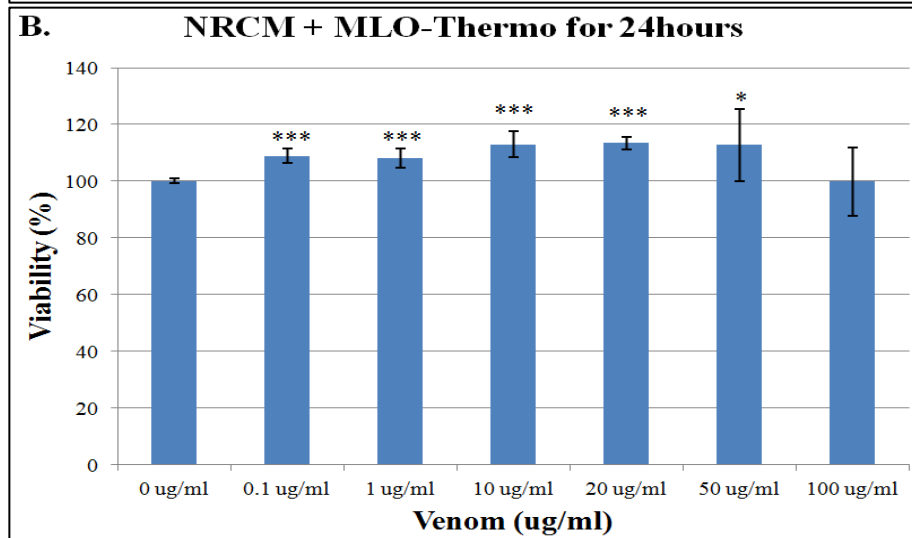
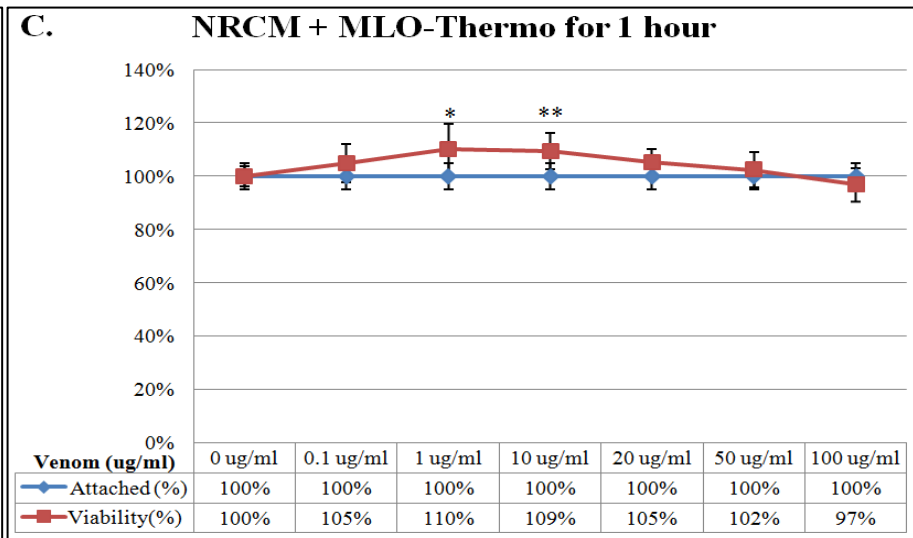
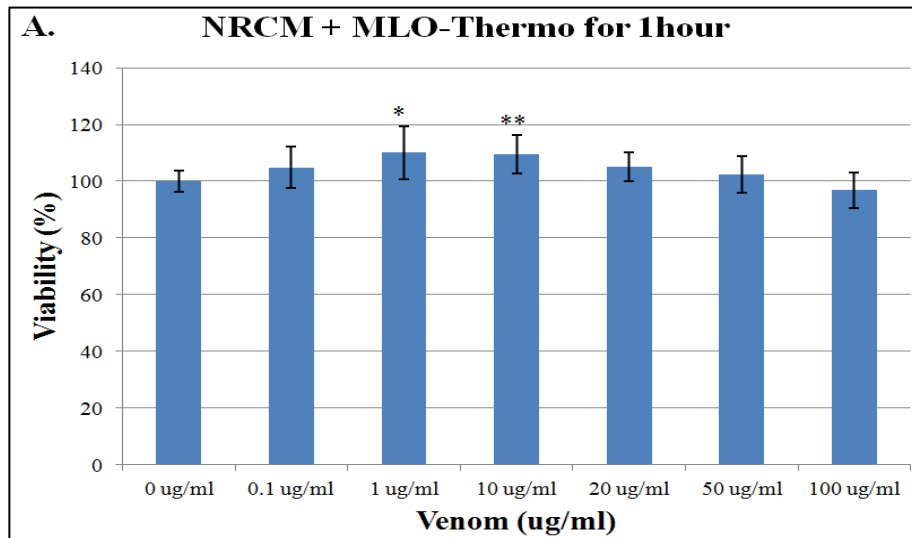


Figure 18. Attachment and Viability of NRCMs treated with indicated concentrations of thermally treated MLO venom. Effect of MLO venom on NRCMs viability after 1 (A) and 24hours (B) of treatment. Attachment (blue line) and Viability (red line) of NRCMs treated with indicated concentrations of thermally treated venom were assessed after 1 (C) and 24hours (D) of treatment.

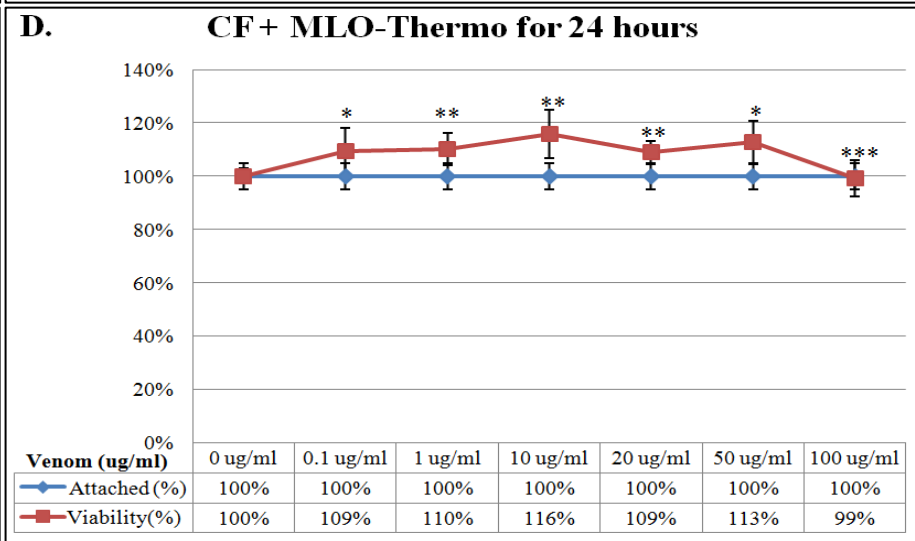
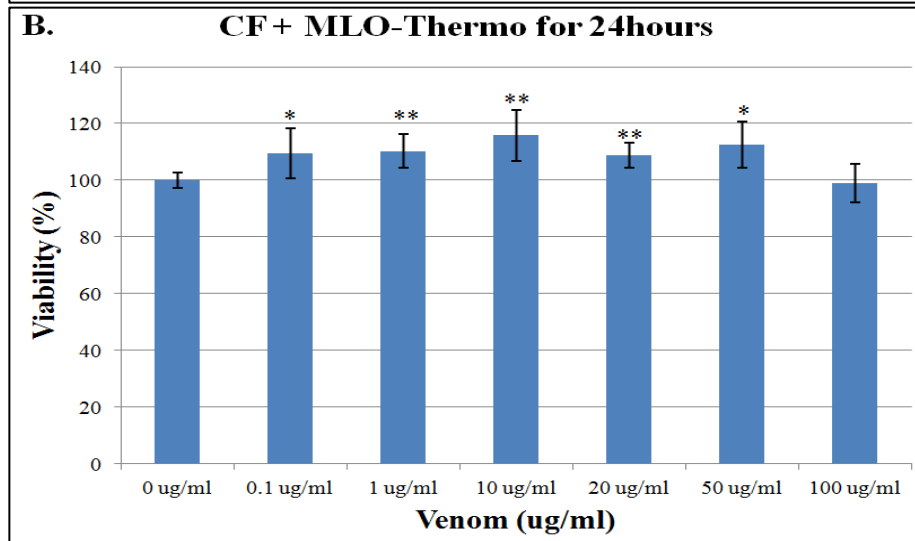
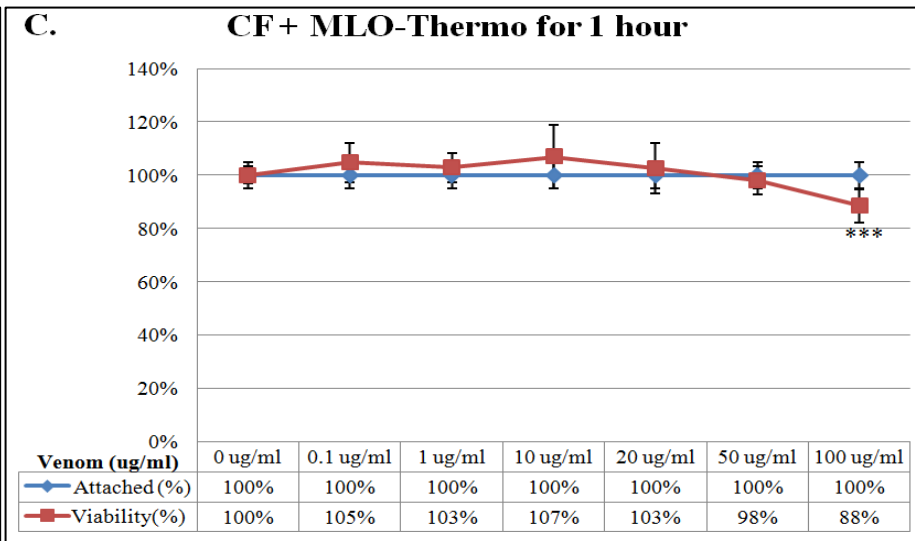
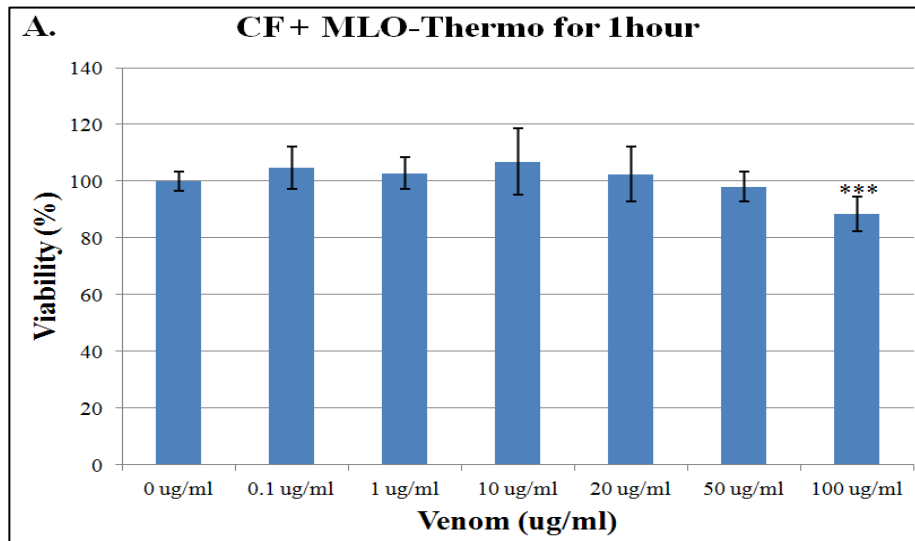


Figure 19. Attachment and Viability of CFs treated with indicated concentrations of thermally treated MLO venom. Effect of MLO venom on CFs viability after 1 (A) and 24hours (B) of treatment. Attachment (blue line) and Viability (red line) of CFs treated with indicated concentrations of thermally treated venom were assessed after 1 (C) and 24hours (D) of treatment.

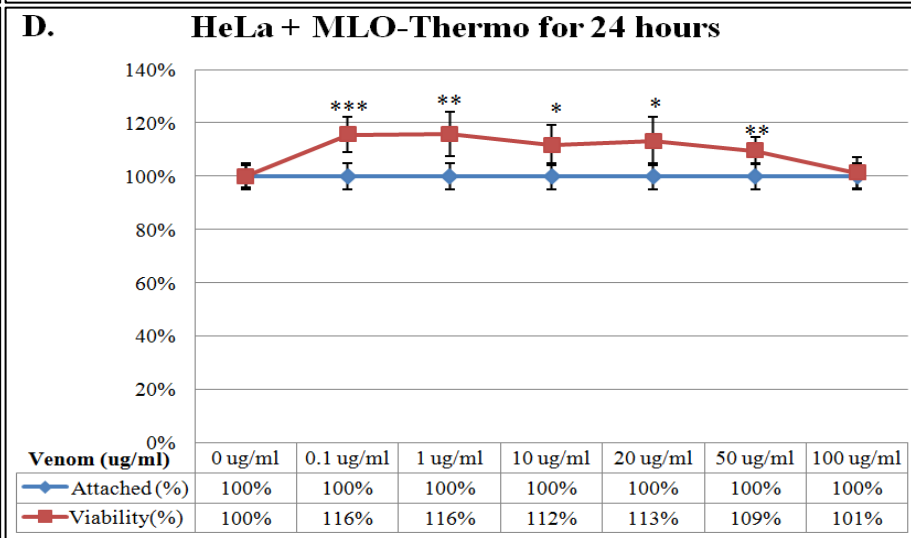
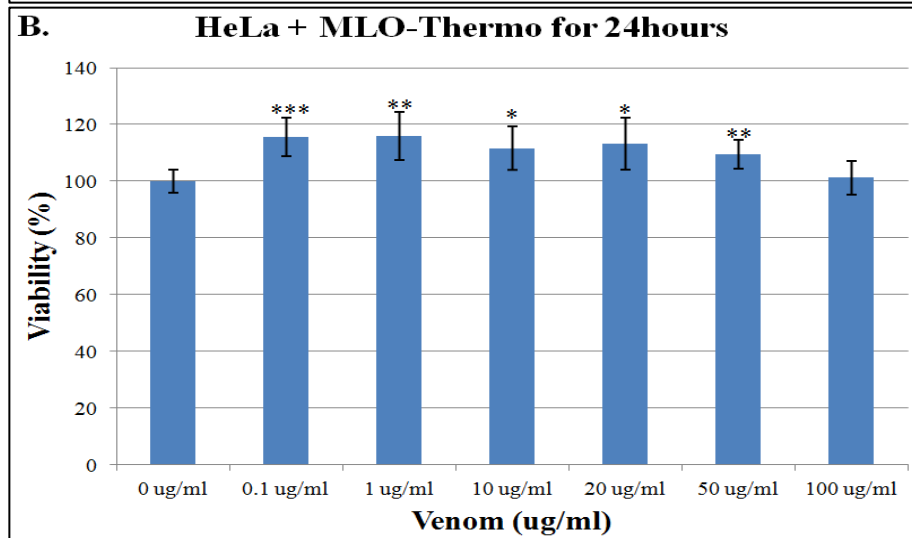
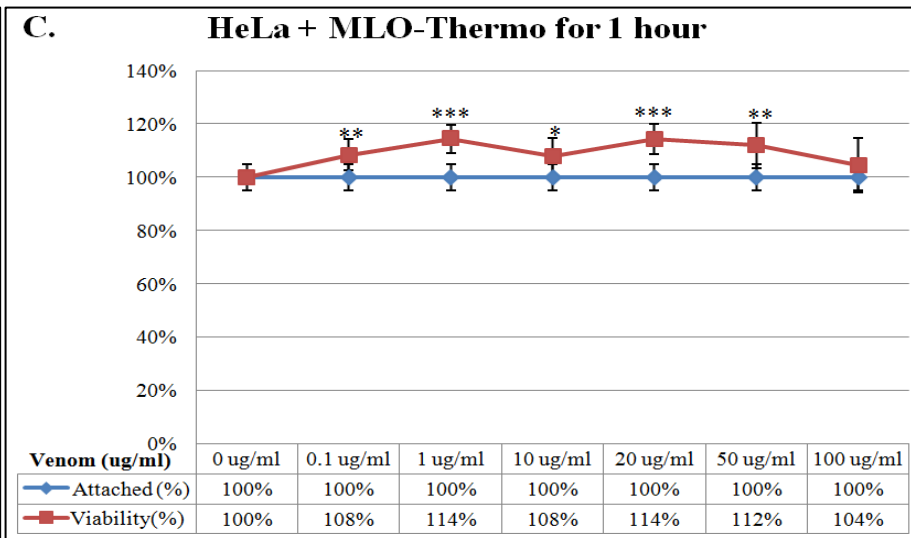
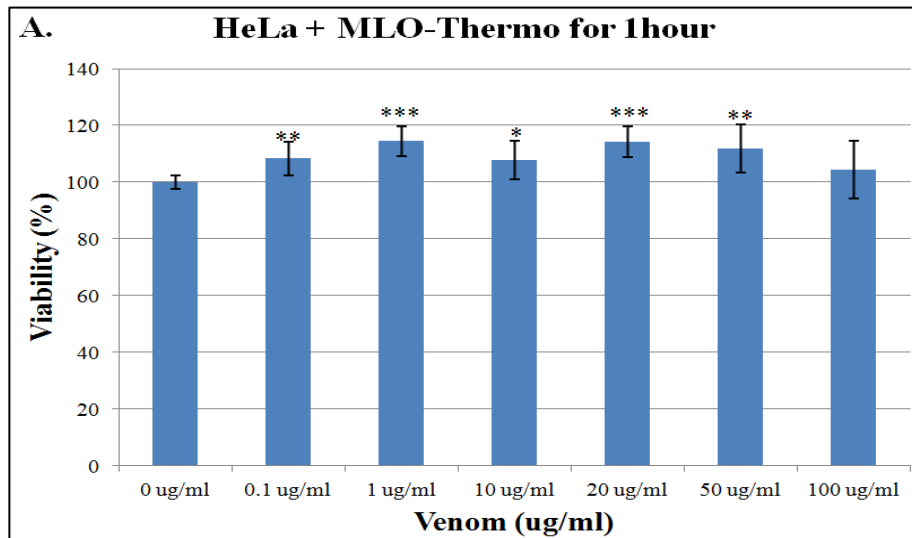


Figure 19. Attachment and Viability of HeLa cells treated with indicated concentrations of thermally treated MLO venom. Effect of MLO venom on HeLa cells viability after 1 (A) and 24hours (B) of treatment. Attachment (blue line) and Viability (red line) of HeLa cells treated with indicated concentrations of thermally treated venom were assessed after 1 (C) and 24hours (D) of treatment.

Next, we tested the effects of native (un-manipulated) *MLO* venom on the viability of NRCMs, CFs and HeLa cells. NRCMs treated with venom for one hour remain alive, regardless of applied *MLO* concentrations (Fig.17B). Importantly, survivability of these cells did not correlate with their attachment. More specifically, NRCMs treated with 10ug/ml of *MLO* venom for 1 hour, remained 100% live, but demonstrated 40-50% detachment (Fig.17C). Interestingly when identically treated parallel cultures were kept for additional 23 hours (total of 24 hours of incubation), cell viability was severely lessened (Fig.21B). Specifically, at 24 hours of incubation, all cells treated with 10ug/ml and higher, lost up to 70-80% of their viability. This phenomenon was correlated with 100% detachment of NRCMs treated with high doses of *MLO* venom (Fig.21C).

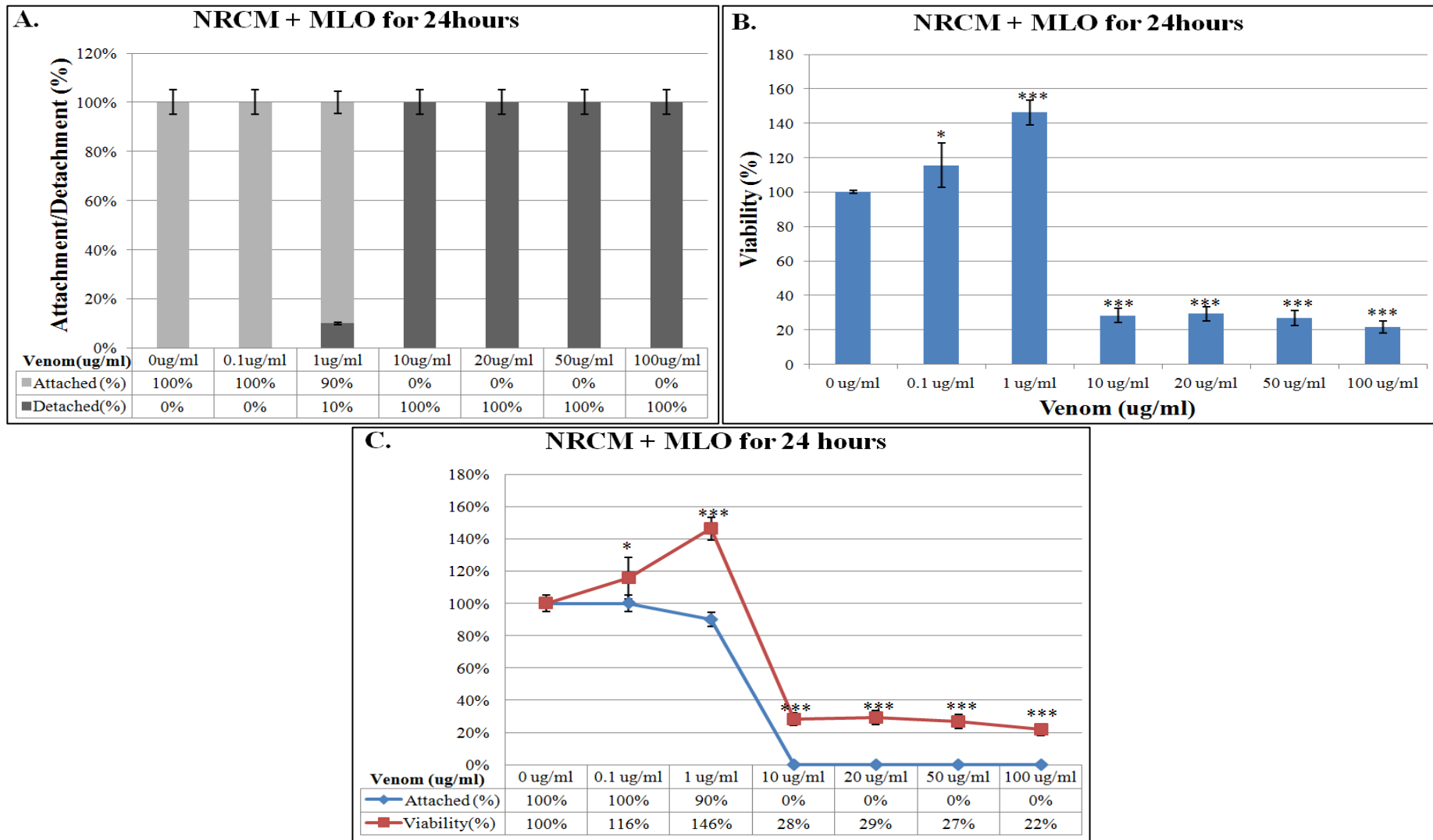


Figure 21. Attachment and Viability of NRCM is affected by MLO in a dose- and time- dependent manner. (A) The ratio of covered areas (dark gray columns) to uncovered areas (light gray columns) of NRCMs cultured for 24hours at indicated concentrations. (B) Effect of MLO venom on NRCMs viability after 24hours of treatment. (C) Attachment (blue line) and Viability (red line) of NRCMs treated with indicated concentrations of whole venom were assessed after 24hours of treatment.

3.1.2. MLO venom effect on CF

Cardiac fibroblasts are an essential part of the myocardium. Therefore, the next set of experiments was conducted to evaluate the effects of *MLO* venom on this type of cells. Toward that goal, cell culture media was removed from cultured CFs and the diluted *MLO* venom was added at the final concentrations of 0.1ug/ml; 1ug/ml; 10ug/ml; 20ug/ml; 50ug/ml; 100ug/ml in triplicates. Cells were incubated for 1 hour. The data demonstrated that CFs treated with the lowest dose (0.1ug/ml) for 1 and 24 hours show no visible effects of detachment whereas parallel cultures treated with 100ug/ml were detached even after 1min post-treatment (Fig.22) and more so after 24h incubation.

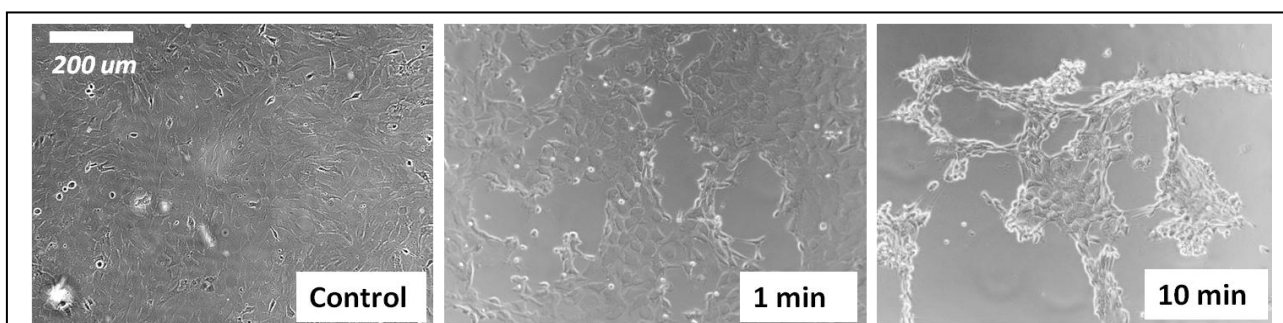


Fig. 22. High concentration of MLO venom is detrimental for CFs attachment to a substrate. CFs (Control) were exposed 100ug/ml of MLO for 1min and 10min.

In order to quantitatively evaluate the detaching effects of indicated concentrations of *MLO* crude venom on CFs, areas covered with cells were compared with the areas without cells after exposure to *MLO* venom for 1 (Fig.23A) and 24hours (Fig.24A). The attachment of CF was affected by *MLO* crude venom starting at 1ug/ml concentration and reaching 100% detachment at 100ug/ml concentration. Quantitated data of the attachment properties show that CFs were affected both in dose and in a time-dependent manner.

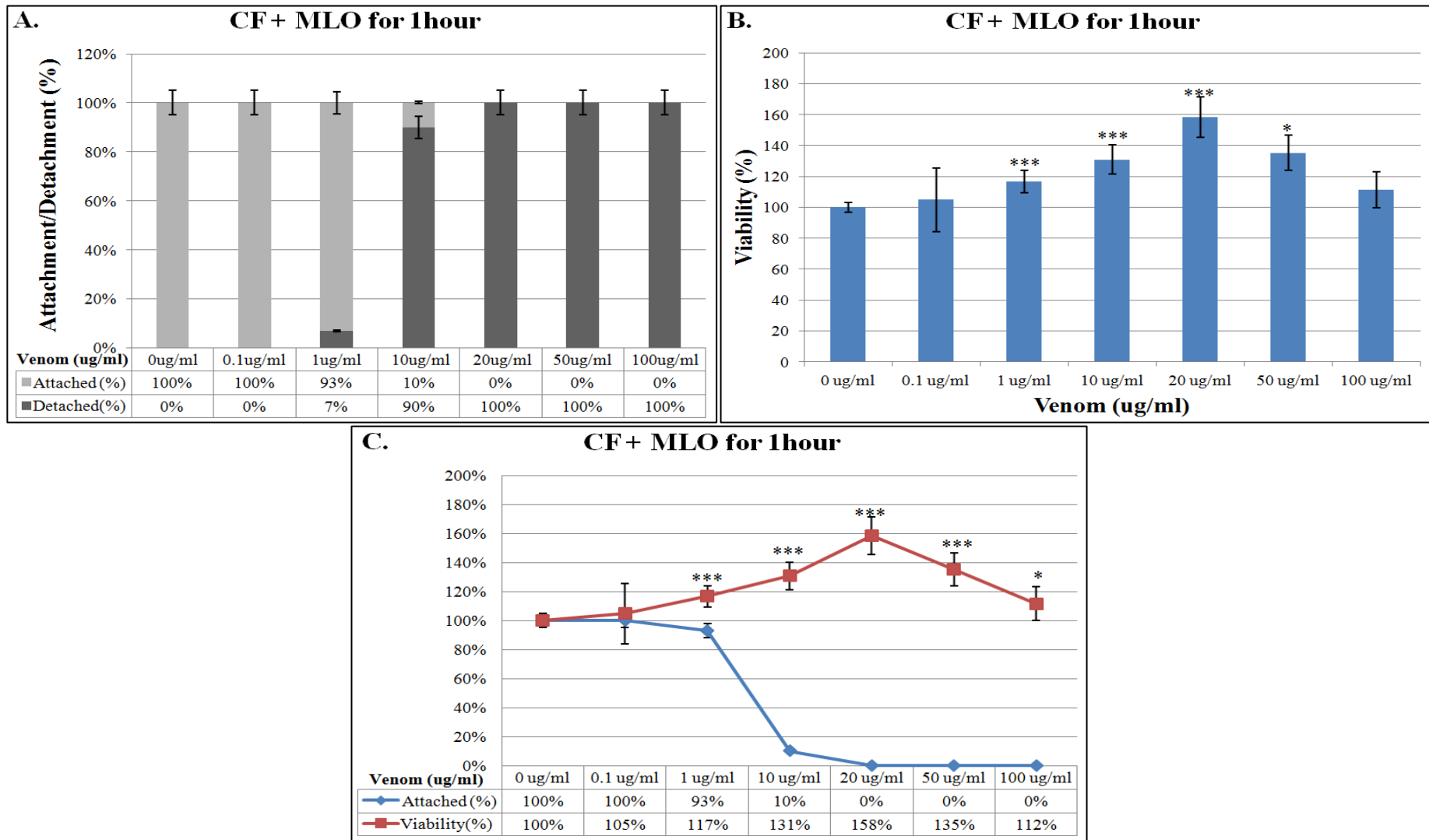


Figure 23. Attachment and Viability of CF is affected by MLO in a dose- and time- dependent manner. (A) The ratio of covered areas (dark gray columns) to uncovered areas (light gray columns) of CFs cultured for 1hour at indicated concentrations. (B) Effect of MLO venom on CFs viability after 1hour of treatment. (C) Attachment (blue line) and Viability (red line) of CFs treated with indicated concentrations of whole venom were assessed after 1hour of treatment.

In order to differentiate between the cytotoxic effect of *MLO* venom (causing cell death) and its effect on attachment properties of CFs, the viability of described cultures was assessed by MTT viability assay. When viability of treated cells was tested after one-hour exposure to the venom, most cells remain alive, regardless of applied *MLO* concentrations (Fig.23B). Similarly to NRCMs, survivability of CFs did not correlate with their attachment. More specifically, CFs treated with 10ug/ml of *MLO* venom for 1 hour, remained 100% live (with slight growth up to 130%), but demonstrated 40-50% detachment (Fig.23C). Interestingly when identically treated parallel cultures were incubated for 24 hours, cell viability was dramatically decreased (Fig.23B). More specifically, the first significant difference was observed starting from 10ug/ml and higher concentration, the cells lost up to 60-70% of their viability. This phenomenon was correlated with 100% detachment of CFs treated with high doses of *MLO* venom (Fig.24C).

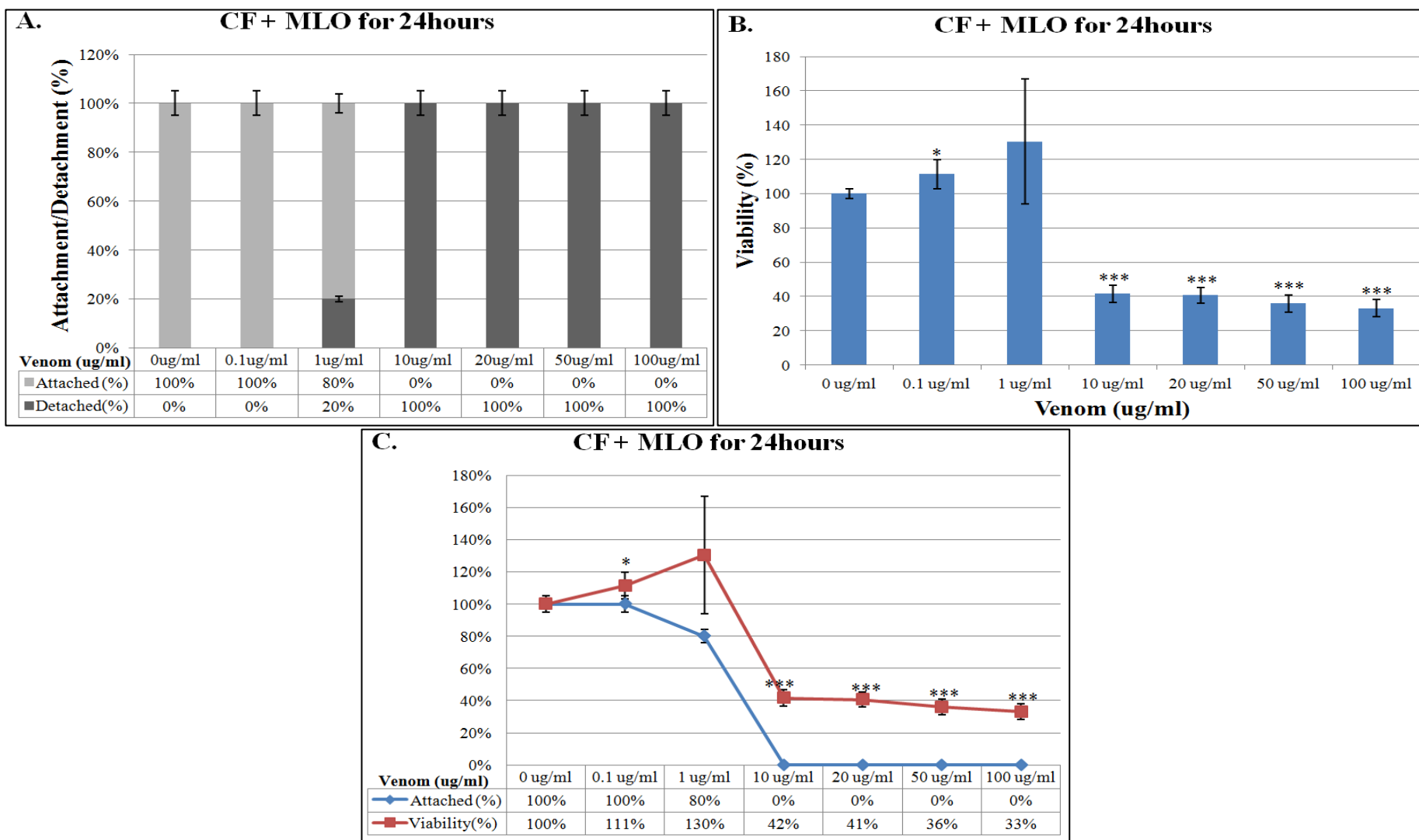
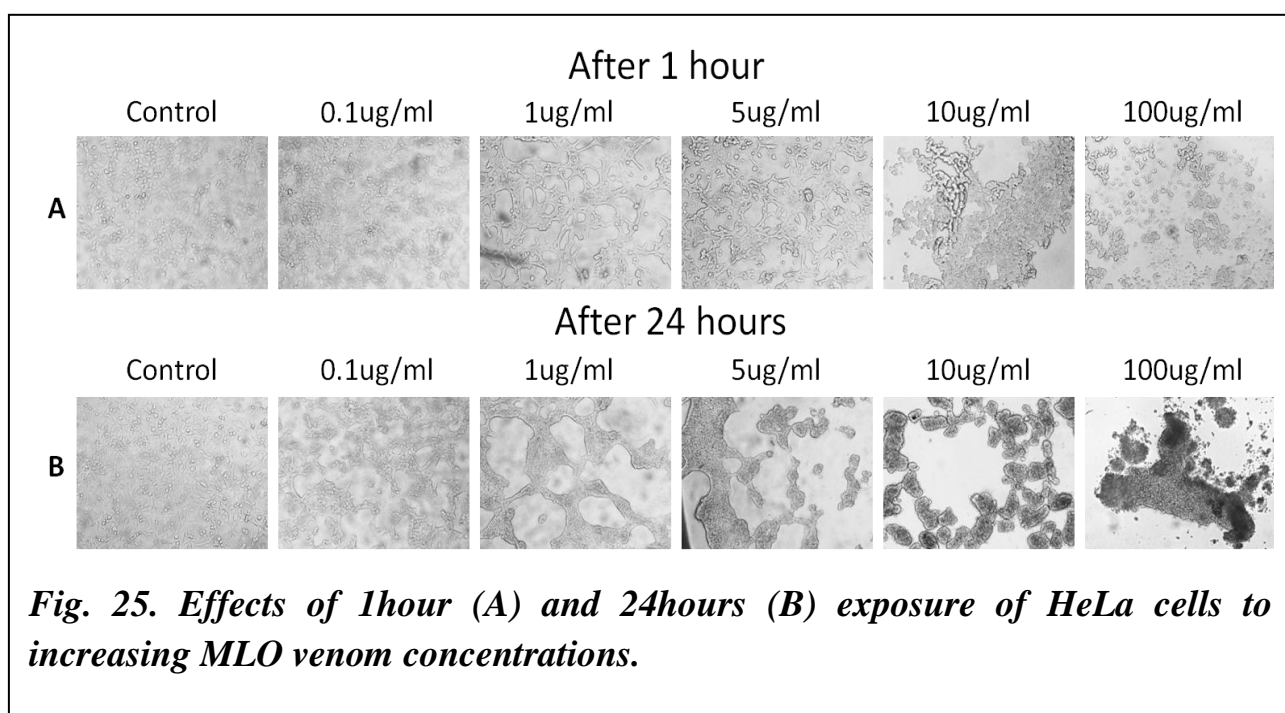


Figure 24. Attachment and Viability of CF is affected by MLO in a dose- and time- dependent manner. (A) The ratio of covered areas (dark gray columns) to uncovered areas (light gray columns) of CFs cultured for 24hours at indicated concentrations. (B) Effect of MLO venom on CFs viability after 24hours of treatment. (C) Attachment (blue line) and Viability (red line) of CFs treated with indicated concentrations of whole venom were assessed after 24hours of treatment.

3.1.3. *MLO* crude venom effect On HeLa cells

Throughout the study, we used HeLa cells as a model of epithelial cells. Since myocardium is heavily vascularized and endothelial cells are the first type of cells within cardiac muscle which are exposed to the venom, it was important to identify the effect of *MLO* venom on these types of cells. For investigation of the effect of *MLO* venom on HeLa cells, culture media was removed and the diluted *MLO* venom was added to the cultured HeLa cells at the final concentrations of 0.1ug/ml; 1ug/ml; 10ug/ml; 20ug/ml; 50ug/ml; 100ug/ml in triplicates. Cells were incubated for 1 hour. The data indicate that HeLa cells treated with the lowest dose (0.1ug/ml) for 1 hour show no visible effects of detachment whereas parallel cultures treated with 10ug/ml and higher concentration reaching 100% detachment after 1 hour of post-treatment (Fig.25A vs 25B.). In order to quantitatively evaluate the detaching effects of indicated concentrations of *MLO* crude venom on HeLa's, areas covered with cells were compared with the areas w/o cells after exposure to *MLO* venom for 1 (Fig.26A) and 24hours (Fig.27A). Quantitated data of the attachment properties show that HeLa cells were affected both in dose and in a time-dependent manner.



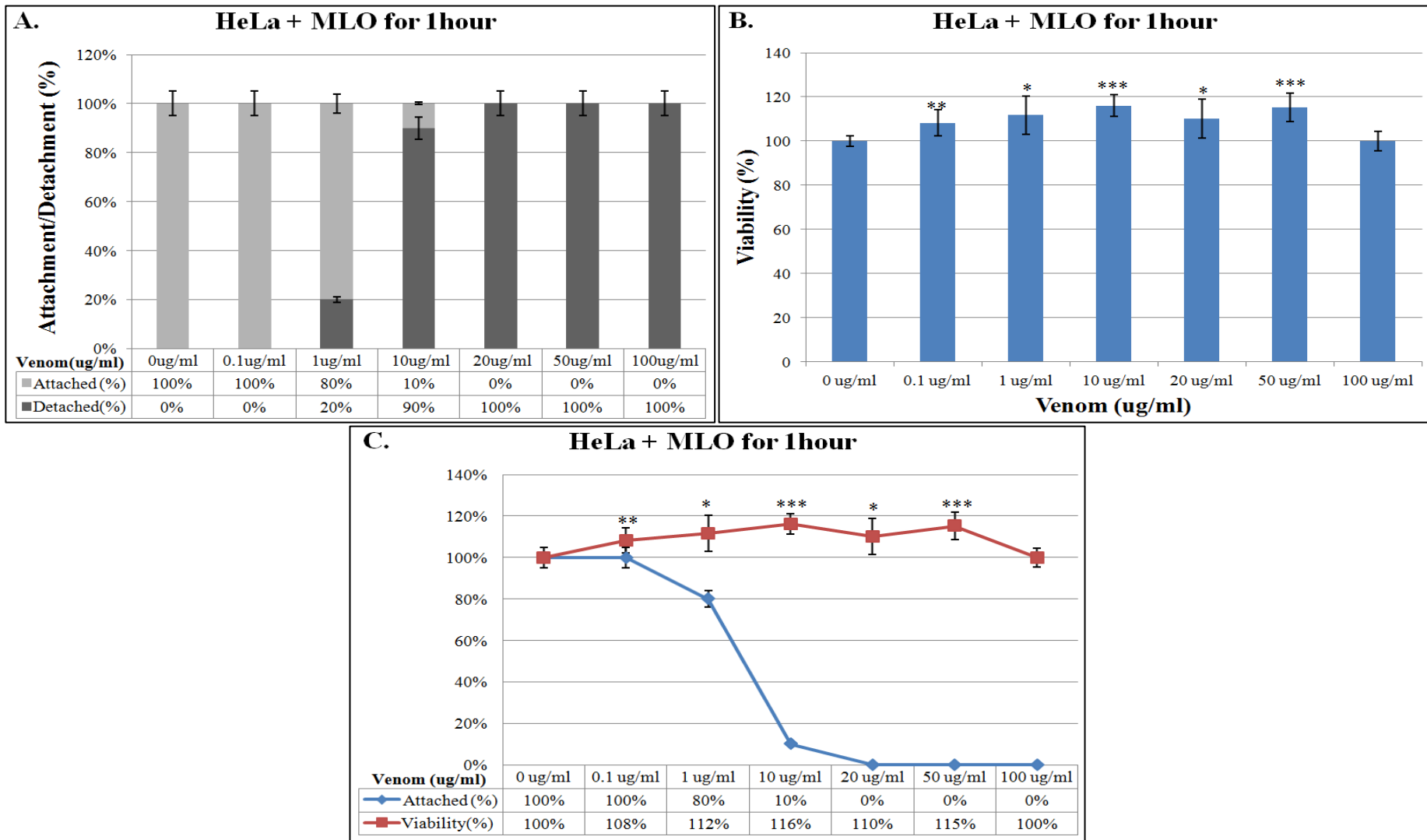


Figure 26. Attachment and Viability of HeLa cells is affected by MLO in a dose- and time- dependent manner. (A) The ratio of covered areas (dark gray columns) to uncovered areas (light gray columns) of HeLa cells cultured for 1 hour at indicated concentrations. (B) Effect of MLO venom on HeLa cells viability after 1 hour of treatment. (C) Attachment (blue line) and Viability (red line) of HeLa cells treated with indicated concentrations of whole venom were assessed after 1 hour of treatment.

As before, to distinguish between the cytotoxic effect of *MLO* venom (causing cell death) and its effect on attachment properties of HeLa cells, the viability of described cultures was assessed by MTT viability assay. When viability of treated cells was tested after one-hour exposure to the venom, most cells remain alive, under all applied *MLO* venom concentrations (Fig.26B). Importantly, survivability of these cells did not correlate with their attachment. More specifically, HeLa cells treated with 10ug/ml of *MLO* venom for 1 hour, remained 100% live, but demonstrated 90% detachment (Fig.26C). Interestingly when identically treated parallel cultures were kept for a total of 24 hours of incubation, cell viability was severely lessened (Fig.27B). Specifically, all cells treated with 20ug/ml and higher lost up to 50-60% of their viability. This phenomenon was correlated with 100% detachment of HeLa cells treated with high doses of *MLO* venom (Fig.27C).

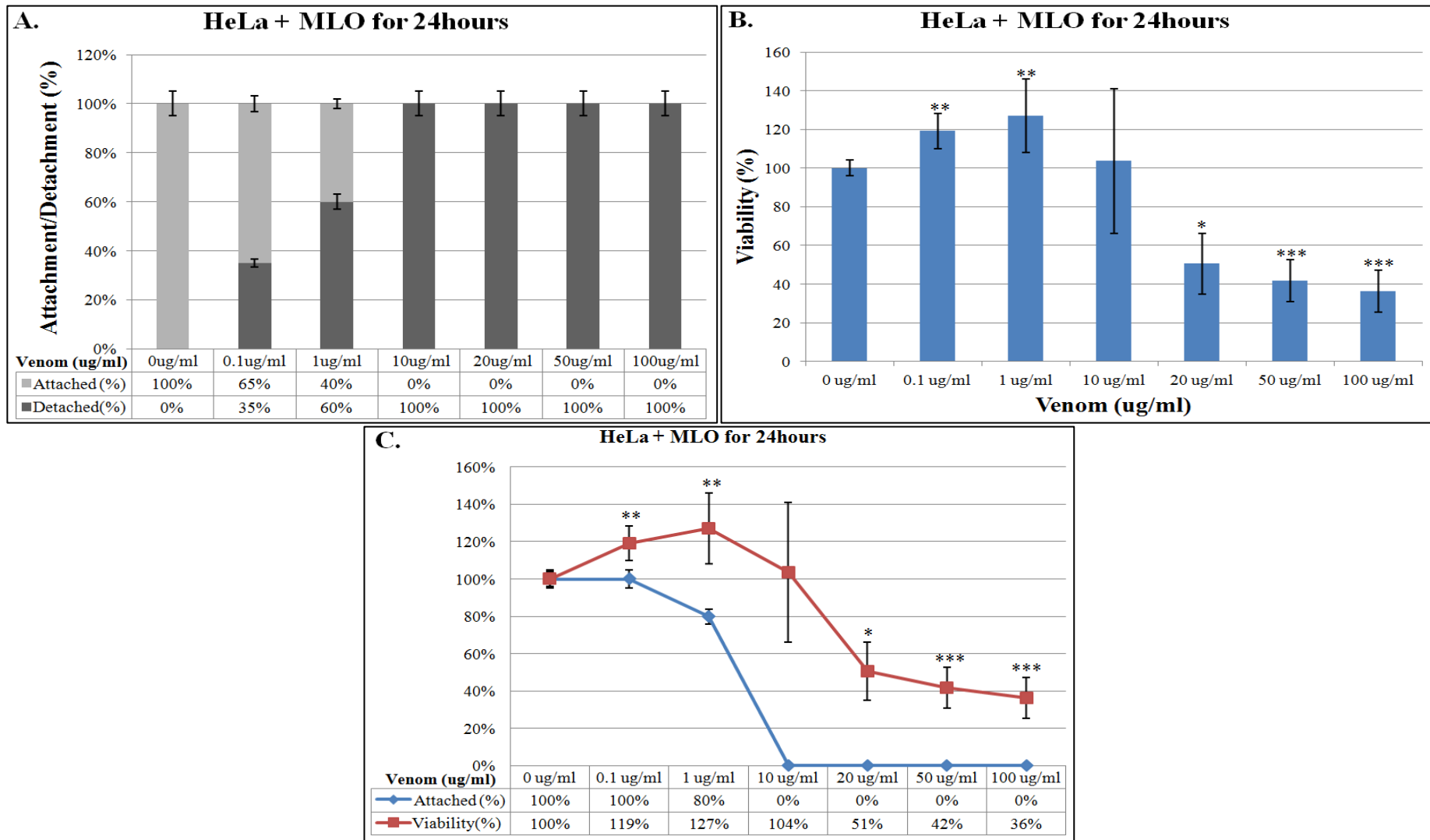


Figure 27. Attachment and Viability of HeLa cells is affected by MLO in a dose- and time- dependent manner. (A) The ratio of covered areas (dark gray columns) to uncovered areas (light gray columns) of HeLa cells cultured for 24hours at indicated concentrations. (B) Effect of MLO venom on HeLa cells viability after 24hours of treatment. (C) Attachment (blue line) and Viability (red line) of HeLa cells treated with indicated concentrations of whole venom were assessed after 24hours of treatment.

3.2. Unraveling the mechanisms of *MLO* detaching effects

In order to understand the mechanism of detachment and how it affects the viability of the cells, we have to try to inhibit individual enzymatic components of the *MLO* venom. For this reason, we use 2 main inhibitors: one of them BPB was used to inhibit the PLA2 of *MLO* snake venom, the second inhibitor which used in this study was EDTA-Na², which inhibits the metalloproteinases of the *MLO* crude venom.

3.2.1. Effect of MLO+BPB mixture on NRCM

PLA2 activity was inhibited with the use of bromophenacyl bromide (BPB) as described in Materials and Methods section. NRCM treated with MLO+BPB mixture for one hour demonstrated 40-50% detachment under exposure to 10ug/ml the mix (Fig.28A). This trend continued and reached 80-90% detachment rate at 100ug/ml concentration of MLO+BPB mix, while the cell viability remained at 100% (Fig.28B). After incubation of parallel cultures for a total of 24 hours, attachment of NRCMs remained unaffected up to the 1ug/ml venom concentration. This result proves that at least a part of the *MLO* venom activity was inhibited by BPB and attachment of NRCMs was improved compared with the effect of the same concentration of uninhibited *MLO* (Fig.29A compared with Fig.21A).

Furthermore, the viability of the same culture treated with MLO+BPB for 24 hours was also slightly improved for lower venom concentrations, but starting from 10ug/ml MLO+BPB mixture the viability significantly dropped to 20-30% viable cells (Fig.29B).

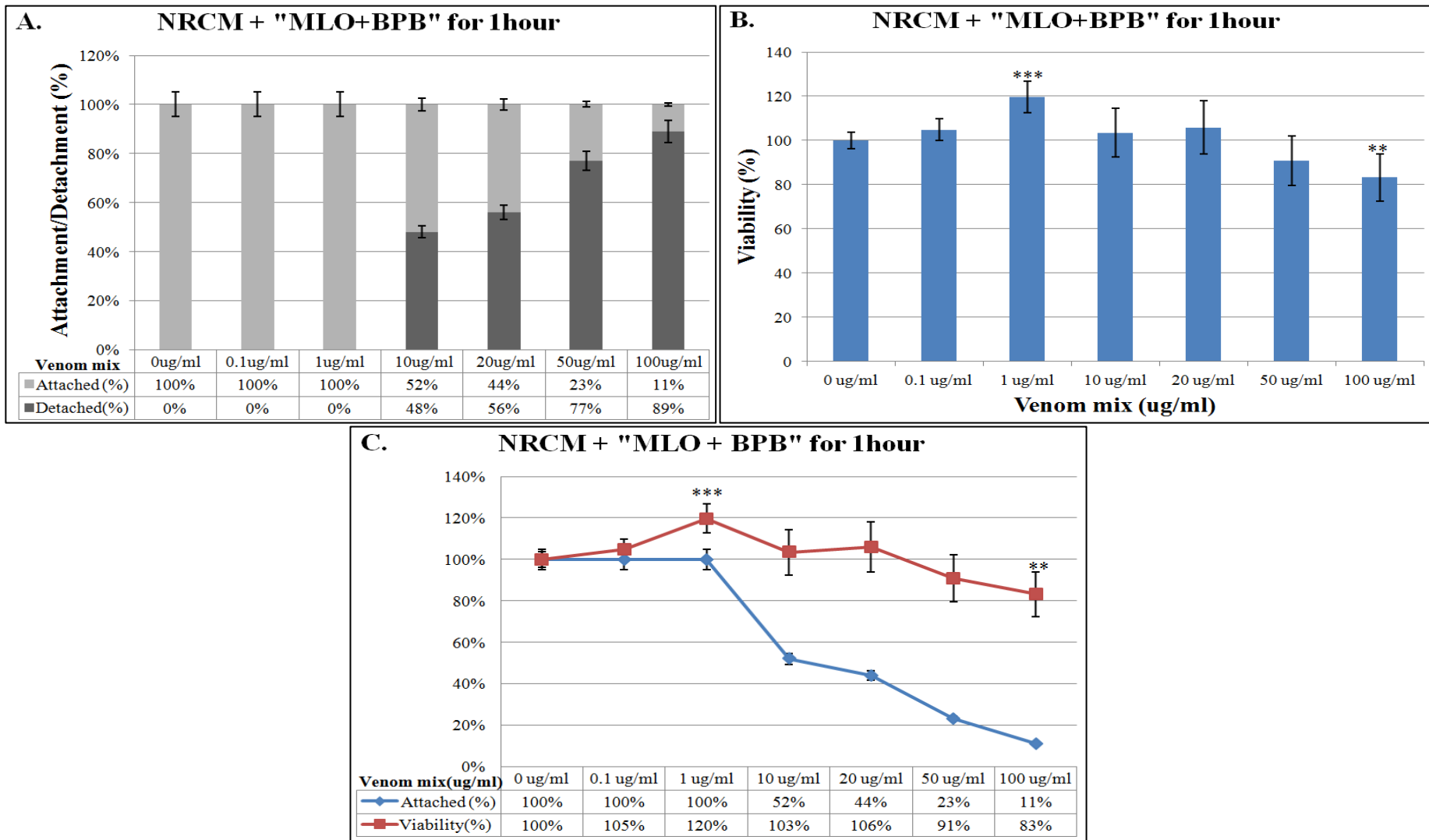


Figure 28. Inhibition of PLA2 enzyme activity within MLO venom results in slight increase viability and attachment of NRCMs at low concentrations. (A) The ratio of covered areas (dark gray columns) to uncovered areas (light gray columns) of NRCMs cultured for 1hour at indicated concentrations. (B) Effect of MLO+BPB mix on NRCMs viability after 1hour of treatment. (C) Attachment (blue line) and Viability (red line) of NRCMs treated with indicated concentrations of MLO+BPB mix were assessed after 1hour of treatment.

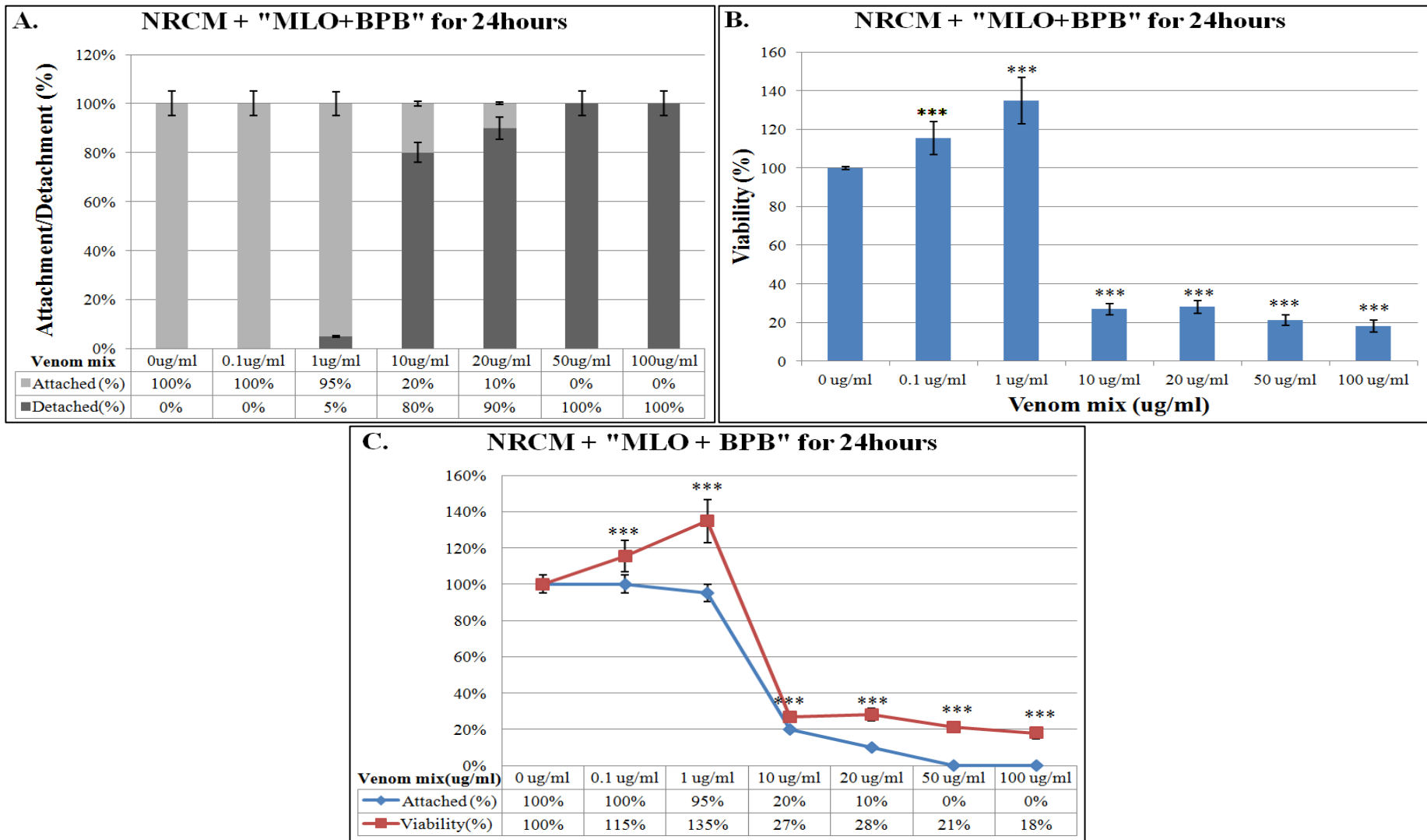


Figure 29. Inhibition of PLA2 enzyme activity within MLO venom results in slight increase viability and attachment of NRCMs at low concentrations. (A) The ratio of covered areas (dark gray columns) to uncovered areas (light gray columns) of NRCMs cultured for 24hours at indicated concentrations. (B) Effect of MLO+BPB mix on NRCMs viability after 24hours of treatment. (C) Attachment (blue line) and Viability (red line) of NRCMs treated with indicated concentrations of MLO+BPB mix were assessed after 24hours of treatment.

3.2.2. Effect of MLO+BPB mixture on CF

Similar experiments were performed to assess the BPB inhibitory effects on the action of a PLA2 enzyme of *MLO* venom. As can be seen in Figure 30A and 31A, no changes in attachment were detected at 1 and 24 hours of when cells were exposed to up to 1 ug/ml MLO+BPB mixture. Once CFs have treated 1ug/ml concentration with MLO+BPB for 1 or 24 hours, the detachment was determined to be 5% which is similar to the effect of uninhibited venom (Fig.30A & 31A compared with Fig.20A & 21A). Comparing these results with the parallel effects of uninhibited *MLO* venom on CFs proves that detachment level of CFs was moderated by the presence of BPB as follows. Starting from a concentration of 10ug/ml of MLO+BPB mixture detachment rate reached 80-100% both after 1 and 24 hours of exposure (Fig.30B and Fig.31B). Remarkably, the cell viability rate remained 100% for the 1-hour treatment; therefore no correlation exists between detachment and cell viability (Fig.30C). After incubation of parallel cultures for a total of 24 hours cell viability dropped by 60-70% (Fig.31C). Taken together this indicates that attachment of CF's is governed by molecules, which are not significantly affected by the PLA2 enzyme, whereas survivability of the same cells is.

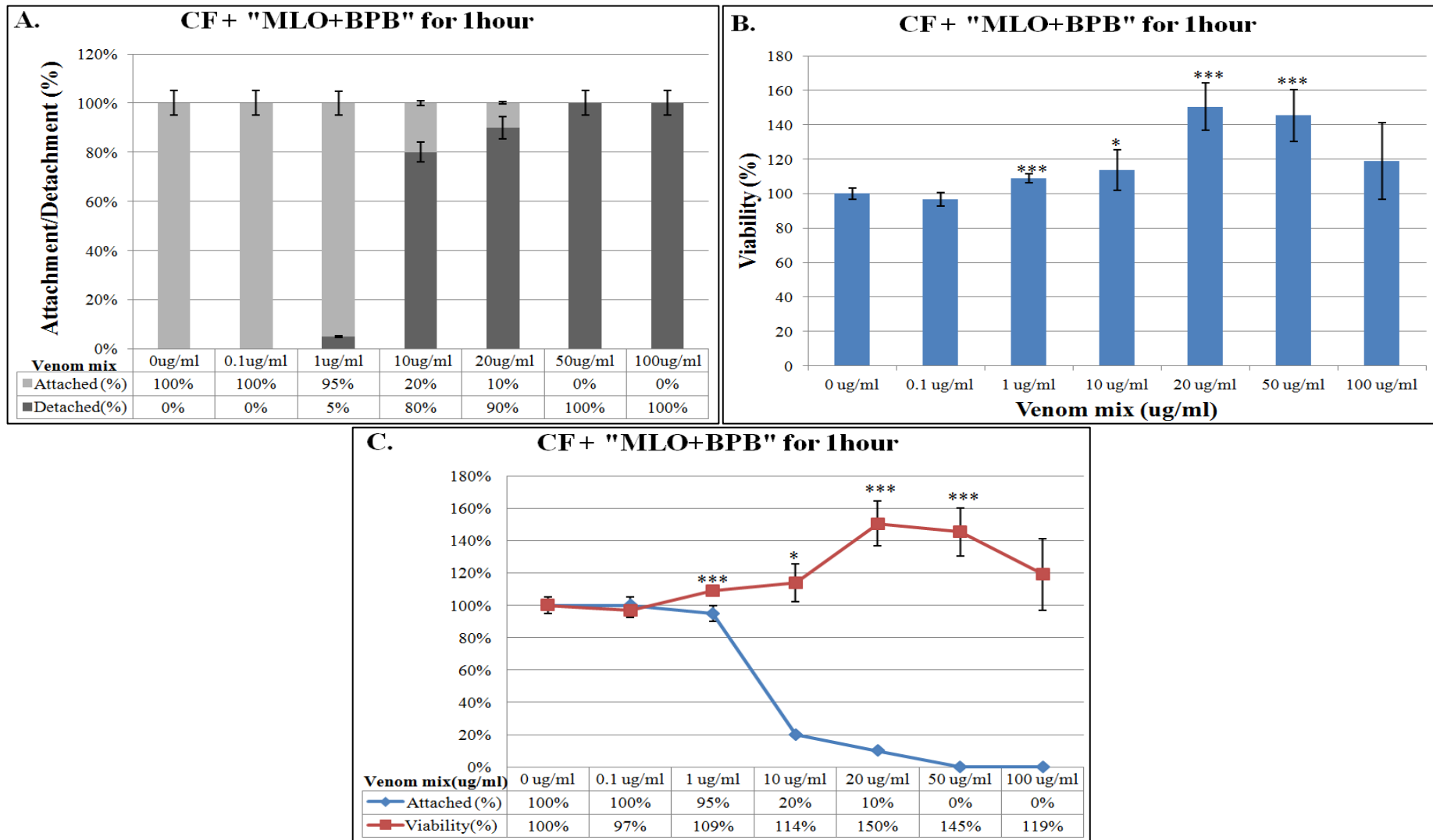


Figure 30. MLO venom with inhibited PLA2 activity (MLO+BPB mix) demonstrated negligible difference in effects of detachment of CFs after 1hour exposure compared to whole venom effects. (A) The ratio of covered areas (dark gray columns) to uncovered areas (light gray columns) of CFs cultured for 1hour at indicated concentrations. (B) Effect of MLO+BPB mix on CFs viability after 1hour of treatment. (C) Attachment (blue line) and Viability (red line) of CFs treated with indicated concentrations of MLO+BPB mix were assessed after 1hour of treatment.

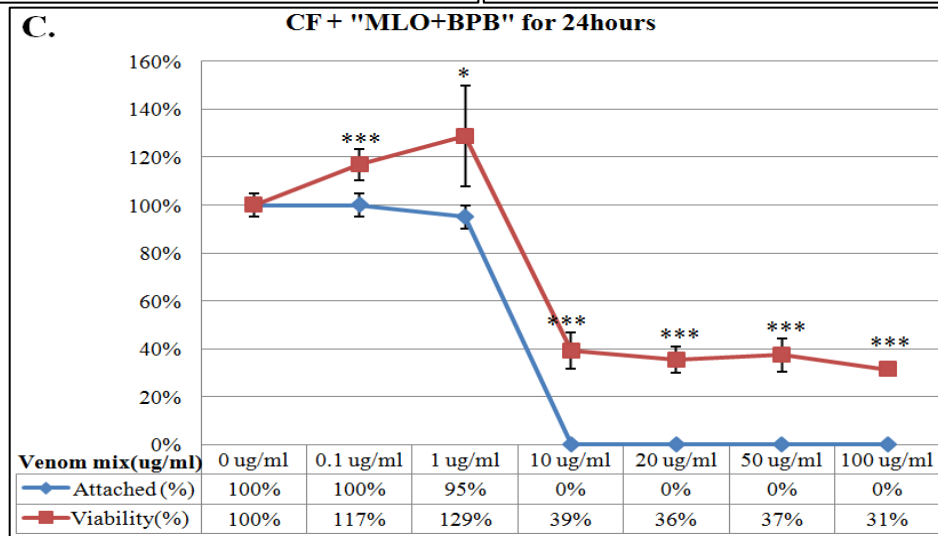
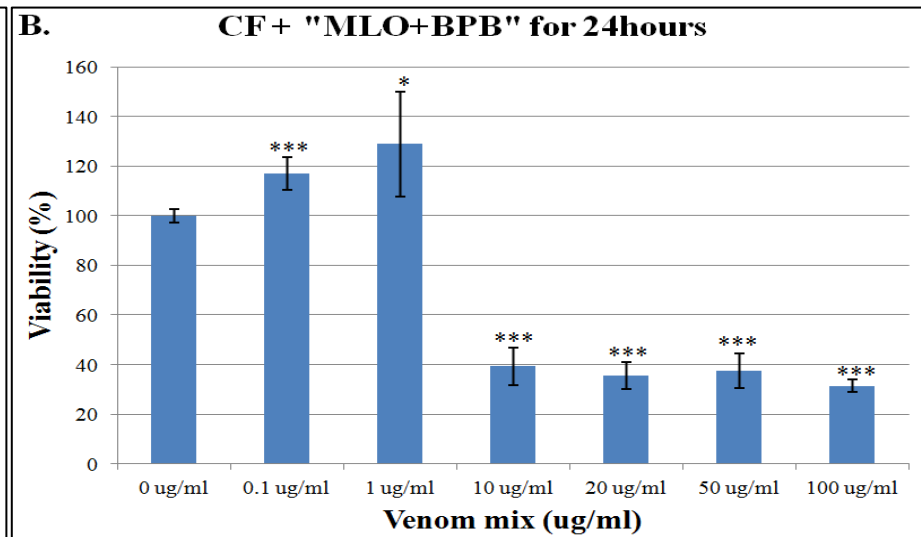
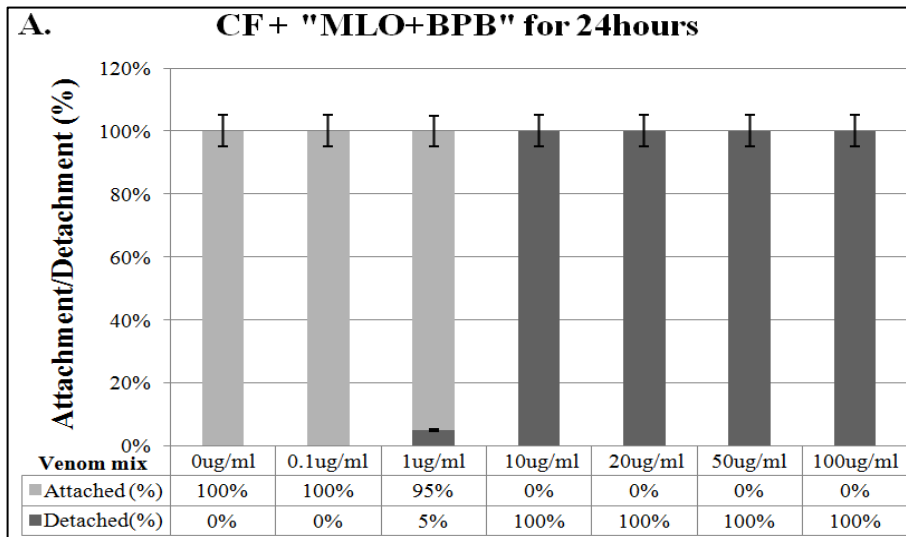


Figure 31. MLO venom with inhibited PLA2 activity (MLO+BPB mix) demonstrated negligible difference in effects of detachment of CFs after 24hours exposure compared to whole venom effects. (A) The ratio of covered areas (dark gray columns) to uncovered areas (light gray columns) of NRCMs cultured for 24hours at indicated concentrations. (B) Effect of MLO+BPB mix on NRCMs viability after 24hours of treatment. (C) Attachment (blue line) and Viability (red line) of NRCMs treated with indicated concentrations of MLO+BPB mix were assessed after 24hours of treatment.

3.2.3. Effect of MLO+BPB mixture on HeLa

HeLa cells treated with MLO+BPB mixture for one hour demonstrated 5% detachment under exposure to 1ug/ml of the mix for 1 and 24 hours (Fig.32A and 33A). When put in comparison with uninhibited *MLO* venom, the degree of detachment of HeLa cells was altered by the presence of BPB. This result confirms that at least a part of the *MLO* venom activity was inhibited by BPB and attachment of HeLa cells was improved compared with the effect of the same concentration of uninhibited *MLO* (Fig.32A & 33A compared with Fig.20A & 21A). Starting from 10ug/ml MLO+BPB mixture detachment rate reached 50-90%, while the cell viability remained 100% (Fig.32C).

Furthermore, the viability of the same culture treated with MLO+BPB for 24 hours was also slightly improved for lower venom concentrations, but starting from 10ug/ml MLO+BPB mixture the viability significantly dropped to 30-60% viable cells (Fig.33C).

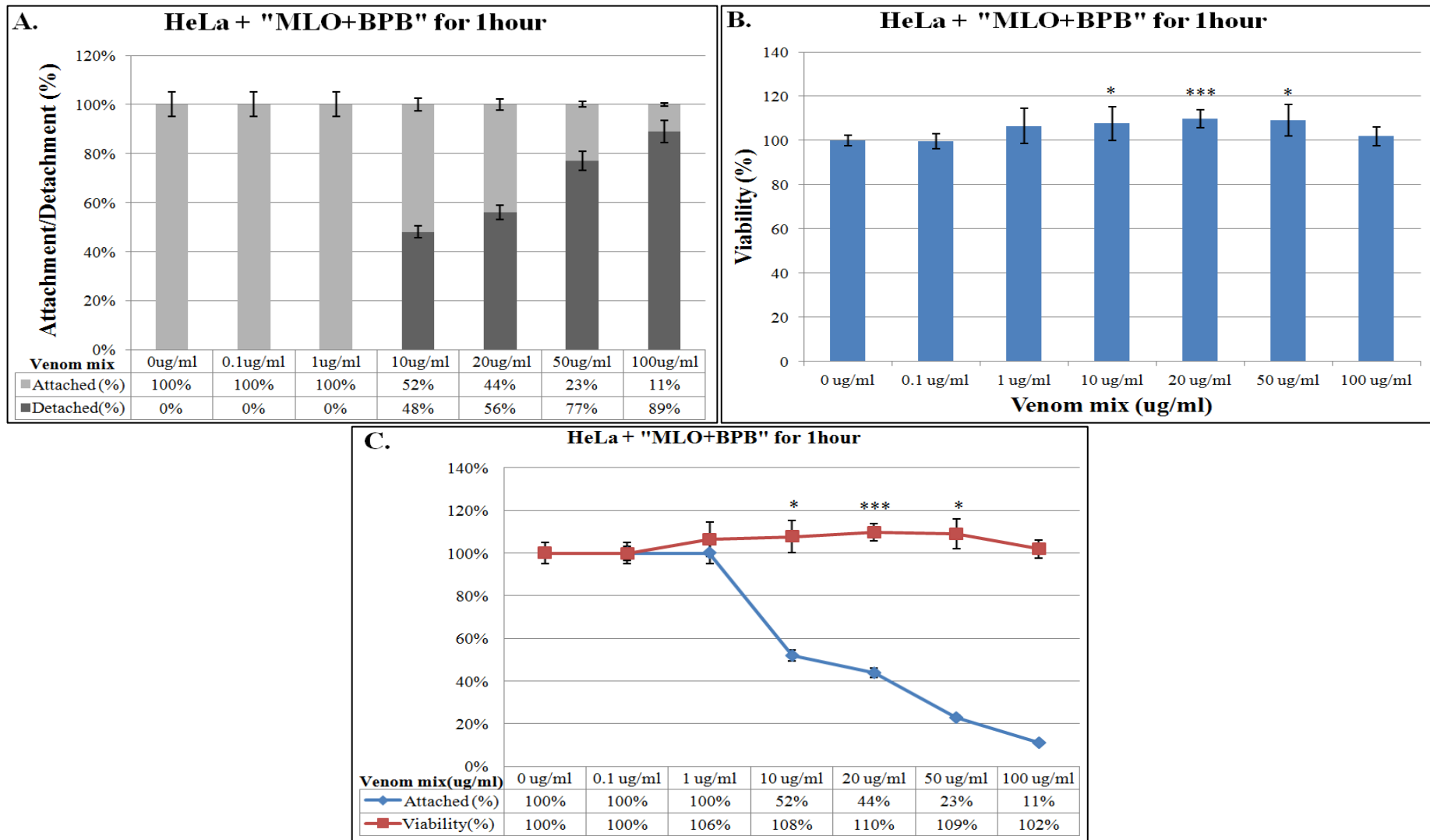


Figure 32. Attachment of HeLa cells treated with MLO+BPB mixture was improved compared with the effect of the same concentration of uninhibited MLO at 1hour exposure. (A) The ratio of covered areas (dark gray columns) to uncovered areas (light gray columns) of HeLa cells cultured for 1hour at indicated concentrations. (B) Effect of MLO+BPB mix on HeLa cells viability after 1hour of treatment. (C) Attachment (blue line) and Viability (red line) of HeLa cells treated with indicated concentrations of MLO+BPB mix were assessed after 1hour of treatment.

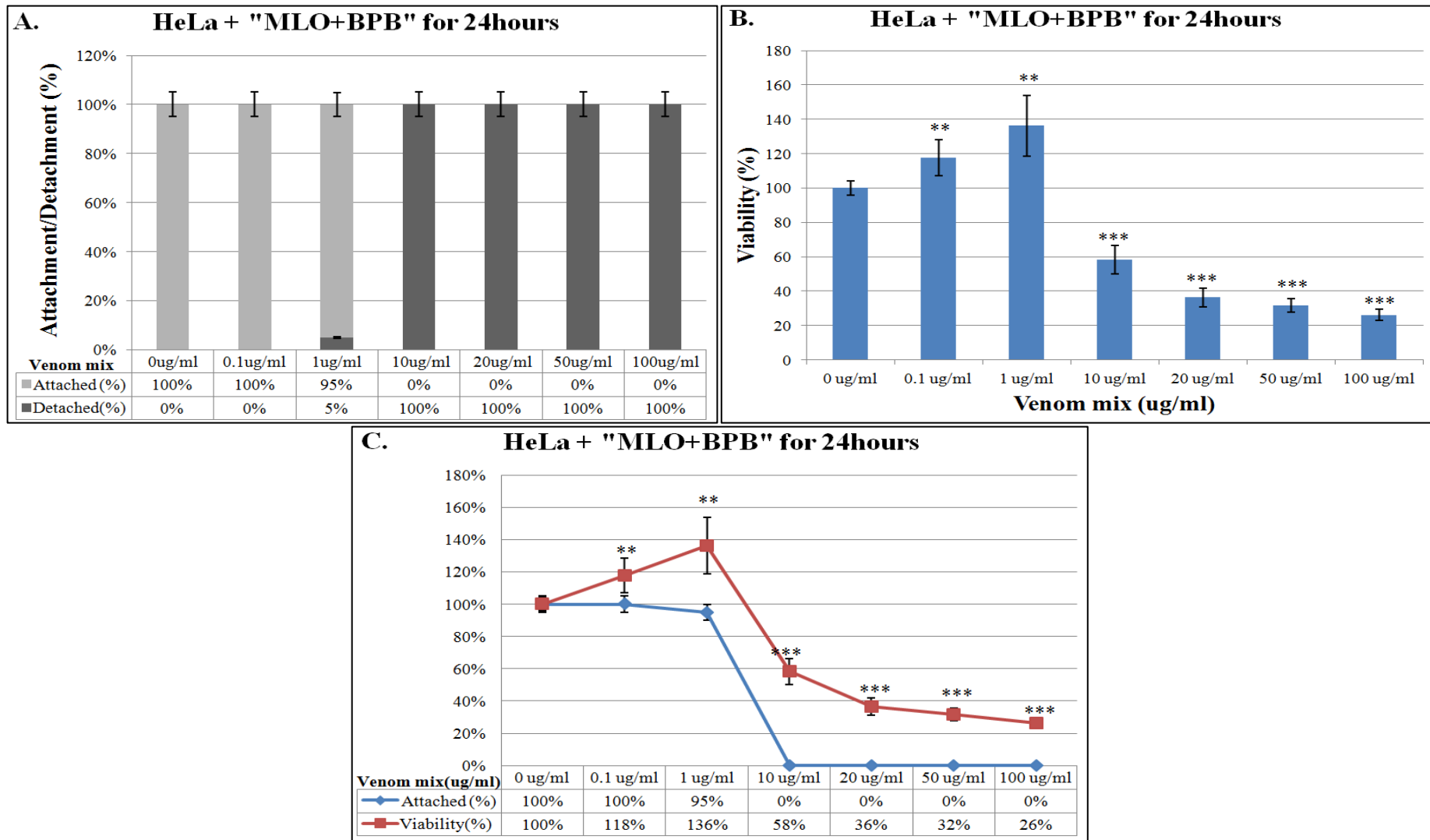


Figure 33. Inhibition of PLA2 enzyme activity within MLO venom results in slight increase viability and attachment of HeLa cells at low concentrations. (A) The ratio of covered areas (dark gray columns) to uncovered areas (light gray columns) of HeLa cells cultured for 24hours at indicated concentrations. (B) Effect of MLO+BPB mix on HeLa cells viability after 24hours of treatment. (C) Attachment (blue line) and Viability (red line) of HeLa cells treated with indicated concentrations of MLO+BPB mix were assessed after 24hours of treatment.

3.3. Effect of metalloproteinases inhibited MLO venom

Ethylenediaminetetraacetic acid disodium (EDTA- Na_2) is known the chelating agent. As such it acts as an effective inhibitor of all metalloproteinases. Therefore to inhibit the metalloproteinases of the *MLO* venom we prepared MLO+EDTA- Na_2 mixture, incubated it for 2hours to allow for the chelating reaction to take place and test the effects of this mixture on attachment properties and viability of NRCM, CFs and HeLa cells.

3.3.1. Effect of MLO+EDTA- Na_2 mixture on NRCM

Metalloproteinases activity was inhibited with the use of Ethylenediaminetetraacetic acid disodium (EDTA- Na_2) as described in Materials and Methods section. NRCM treated with MLO+EDTA- Na_2 mixture for one hour demonstrated 30-40% detachment under exposure to 10ug/ml the mix (Fig.34A). This trend continued and reached 50-60% detachment rate at 100ug/ml concentration of MLO+EDTA- Na_2 mix. This result proves that at least a part of the *MLO* venom metalloproteinases activity was inhibited by EDTA- Na_2 and attachment of NRCMs was improved compared with the effect of the same concentration of uninhibited *MLO* (Fig.34A compared with Fig.20A). In the meantime cell viability remained at 100% (Fig.34B). After incubation of parallel cultures for a total of 24 hours, attachment of NRCMs remained unaffected up to the 1ug/ml venom concentration. This result proves that attachment of NRCMs was improved compared with the effect of the same concentration of uninhibited *MLO* (Fig.35A compared with Fig.21A).

Furthermore, the viability of the same culture treated with MLO+EDTA- Na_2 for 24 hours was also slightly improved for lower venom concentrations, but starting from 10ug/ml MLO+EDTA- Na_2 mixture the viability significantly dropped to 20-30% viable cells (Fig.35B).

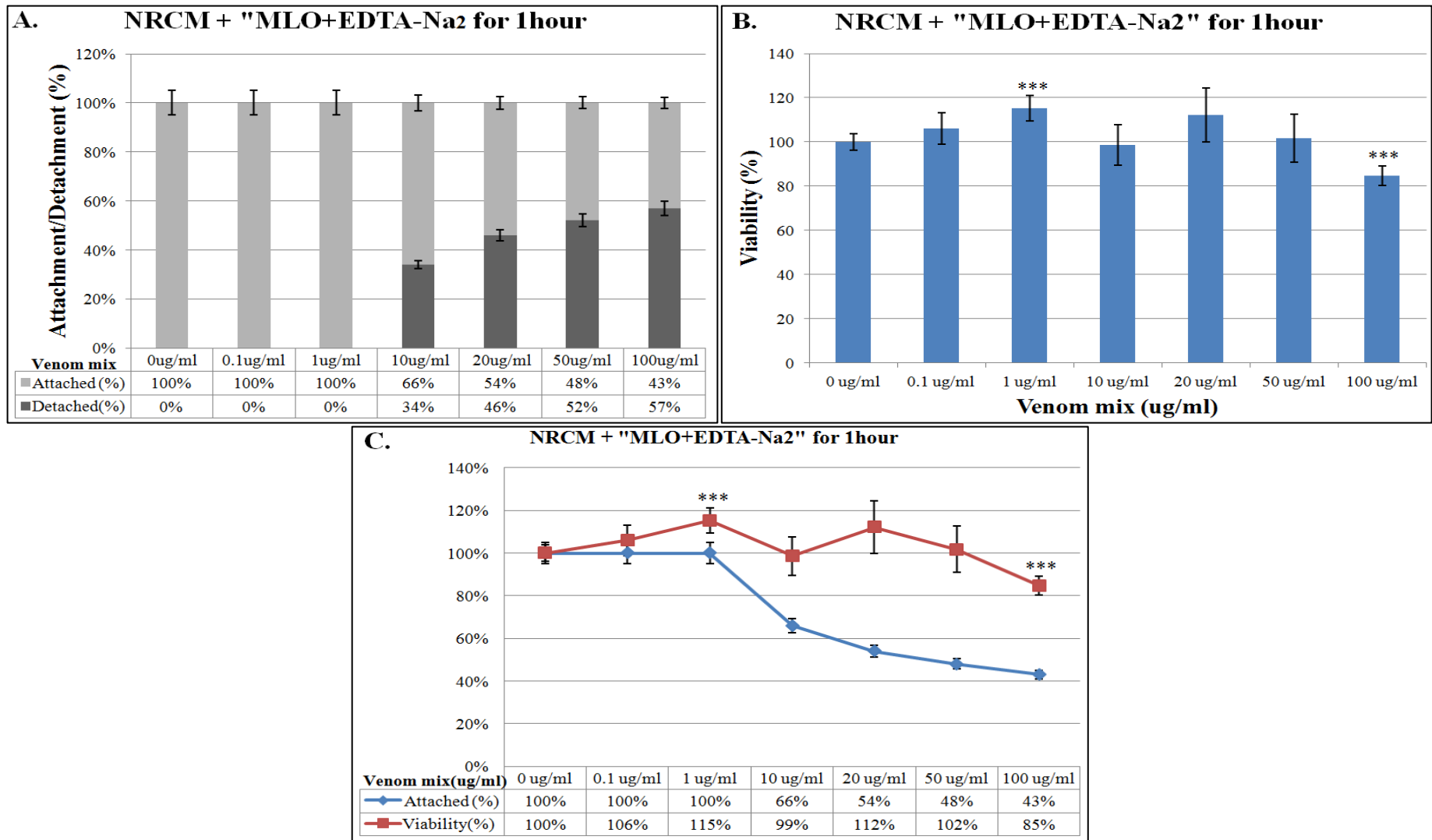


Figure 34. Attachment and viability of NRCMs were improved when MLO venom was inhibited with EDTA-Na₂. (A) The ratio of covered areas (dark gray columns) to uncovered areas (light gray columns) of NRCMs cultured for 1hour at indicated concentrations. (B) Effect of MLO+EDTA-Na₂ mix on NRCMs viability after 1hour of treatment. (C) Attachment (blue line) and Viability (red line) of NRCMs treated with indicated concentrations of MLO+EDTA-Na₂ mix were assessed after 1hour of treatment.

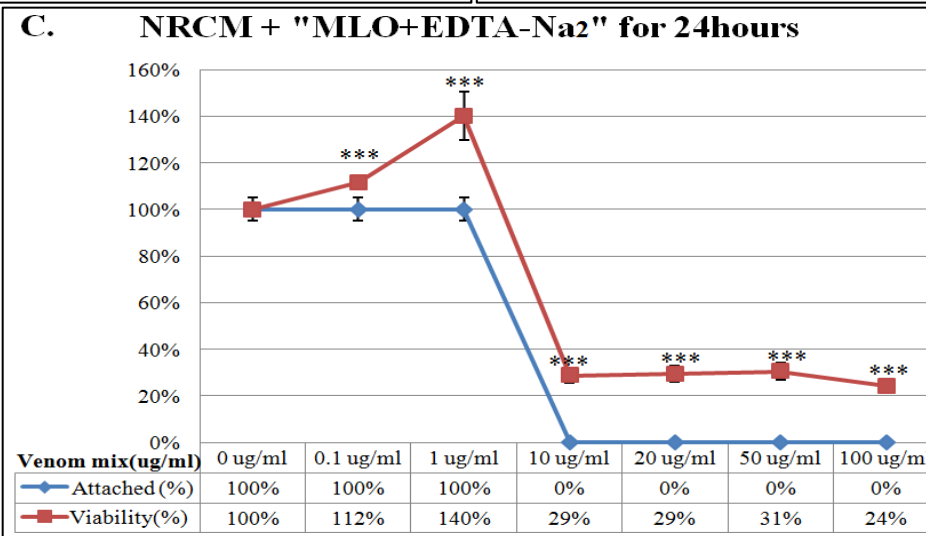
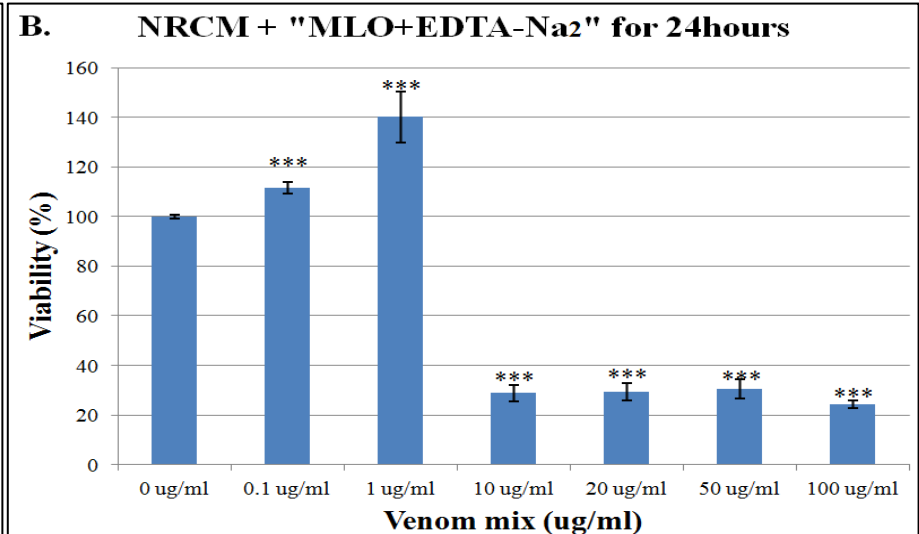
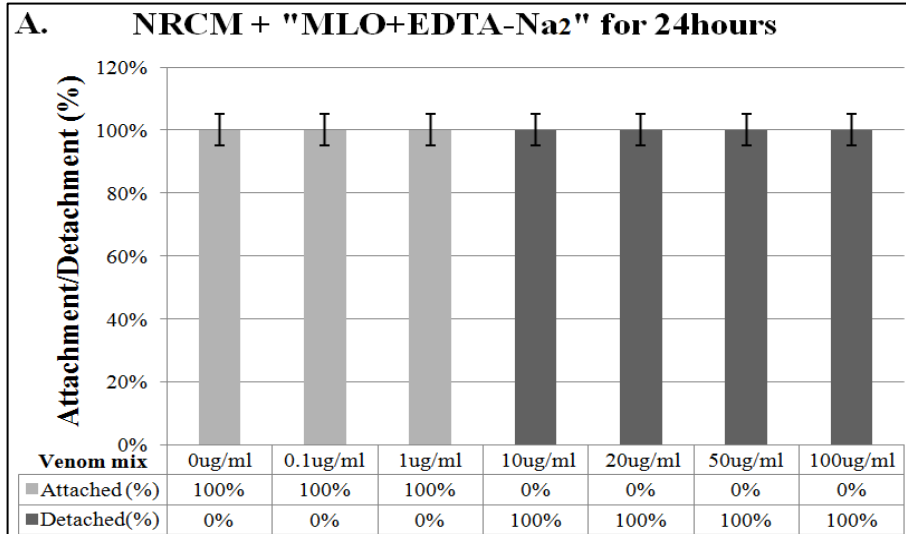


Figure 35. Attachment and viability of NRCMs were improved when MLO venom was inhibited with EDTA-Na₂. (A) The ratio of covered areas (dark gray columns) to uncovered areas (light gray columns) of NRCMs cultured for 24hours at indicated concentrations. (B) Effect of MLO+EDTA-Na₂ mix on NRCMs viability after 24hours of treatment. (C) Attachment (blue line) and Viability (red line) of NRCMs treated with indicated concentrations of MLO+EDTA-Na₂ mix were assessed after 24hours of treatment.

3.3.2. Effect of MLO+EDTA-Na₂ mixture on CF

CFs treated with MLO+EDTA-Na₂ mixture demonstrated no changes in attachment properties at 1 and 24 hours of when cells were exposed to up to 1 ug/ml MLO +EDTA-Na₂ mixture (Fig.36A and Fig.37A). This result proves that at least a part of the *MLO* venom metalloproteinases activity was inhibited by EDTA-Na₂ and attachment of HeLa cells was significantly increased compared with the effect of the same concentration of uninhibited *MLO* (Fig.36A&37A compared with Fig.20A&21A). Remarkably, the cell viability rate remained 100% for 1 and 24 hours of treatment for the indicated concentrations (Fig.36B and Fig.37B respectively); therefore correlation exists between detachment and cell viability (Fig.36C and Fig.37C respectively). CFs treated with MLO+EDTA-Na₂ mixture for one hour demonstrated 50% detachment under exposure to 10ug/ml the mix (Fig.36A). This trend continued and reached 100% detachment rate at 100ug/ml concentration of MLO+EDTA-Na₂ mix both after 1 and 24 hours of exposure (Fig.36A and Fig.37A). Remarkably, the cell viability rate remained 100% for all the concentrations of 1-hour treatment (Fig.36B). Starting from 10ug/ml concentration of MLO+EDTA-Na₂ mixture, the viability rate of 24hour treatment culture dropped by 60-70% (Fig.37B).

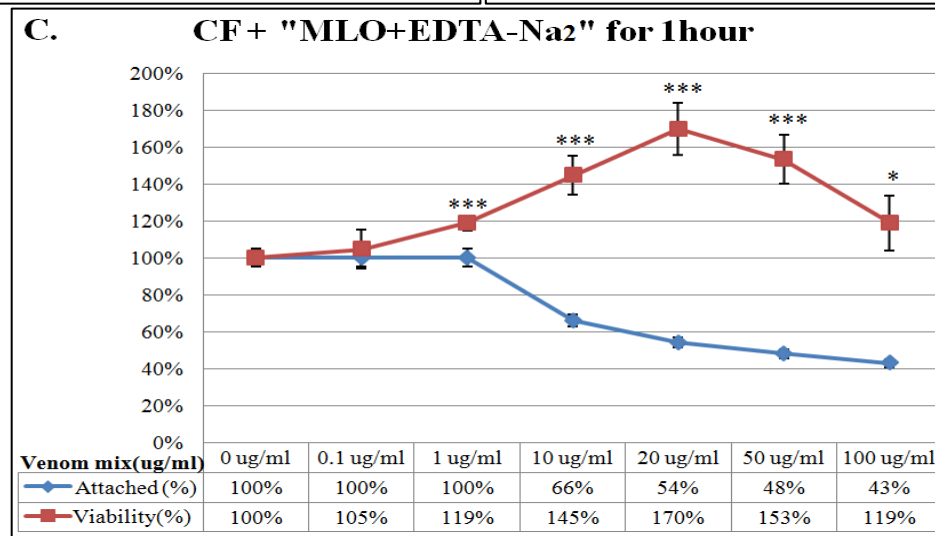
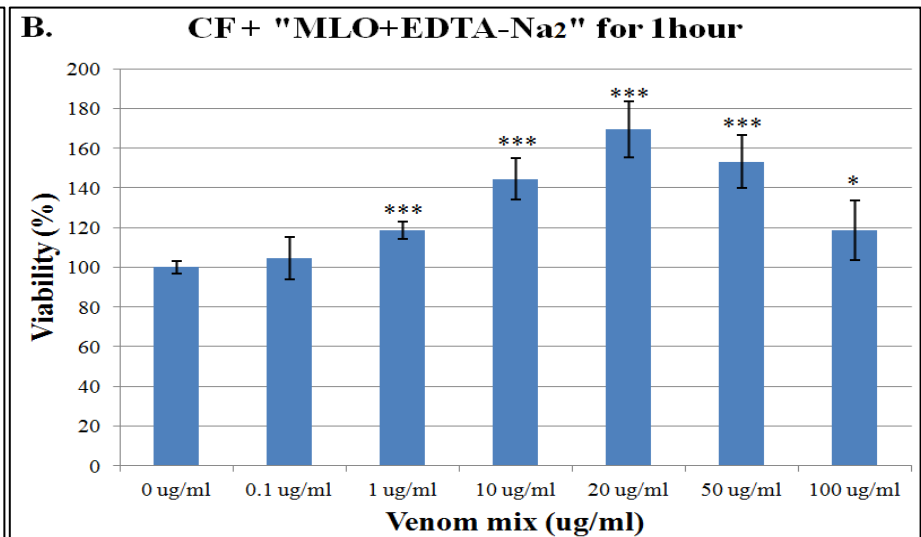
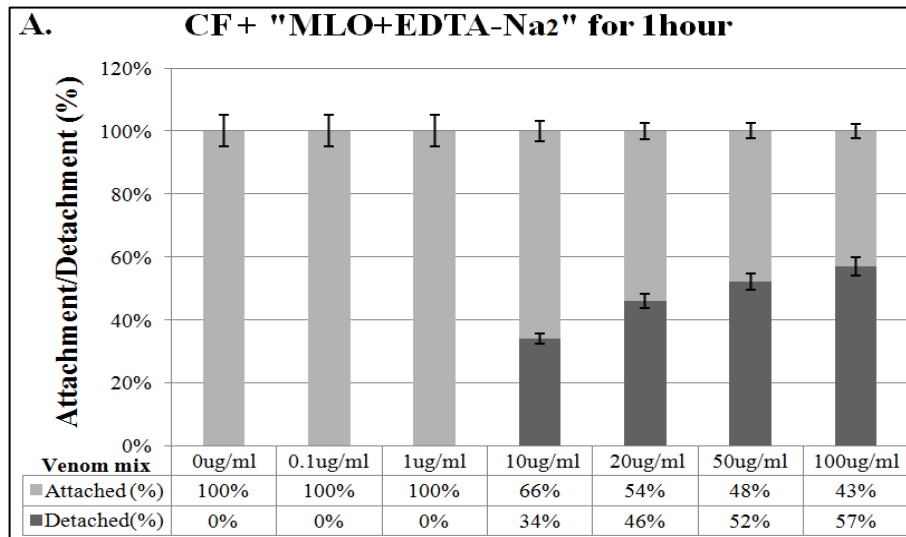


Figure 36. Attachment but not viability of CFs was positively affected by inhibiting metalloproteinases of MLO venom. (A) The ratio of covered areas (dark gray columns) to uncovered areas (light gray columns) of CFs cultured for 1hour at indicated concentrations. (B) Effect of MLO+EDTA-Na₂ mix on CFs viability after 1hour of treatment. (C) Attachment (blue line) and Viability (red line) of CFs treated with indicated concentrations of MLO+EDTA-Na₂ mix were assessed after 1hour of treatment.

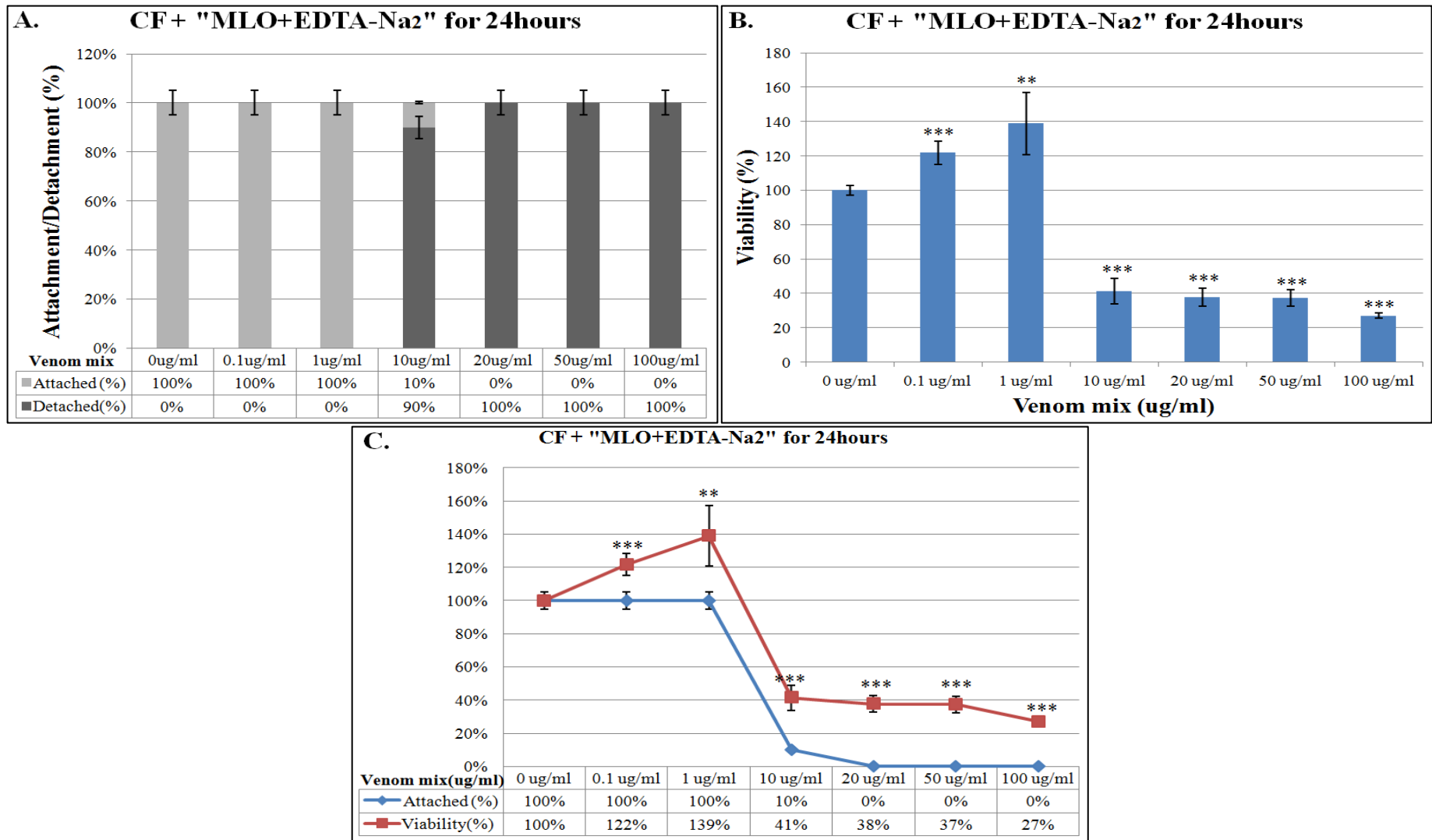


Figure 37. Attachment but not viability of CFs was positively affected by inhibiting metalloproteinases of MLO venom. (A) The ratio of covered areas (dark gray columns) to uncovered areas (light gray columns) of CFs cultured for 24hours at indicated concentrations. (B) Effect of MLO+EDTA-Na₂ mix on CFs viability after 24hours of treatment. (C) Attachment (blue line) and Viability (red line) of CFs treated with indicated concentrations of MLO+EDTA-Na₂ mix were assessed after 24hours of treatment.

3.3.3. Effect of MLO+EDTA-Na₂ mixture on HeLa cells

Parallel experiments were performed to assess the EDTA-Na₂ inhibitory effects on the action of metalloproteinases enzyme of *MLO* venom. Interestingly when dealing with HeLa cells, no changes in viability were detected at 1 and 24 hours across all tested concentrations of MLO+EDTA-Na₂ mixture (Fig.38A and Fig.39A respectively). The cell viability rate remained 100% for 1 and 24 hours of treatment for the indicated concentrations (Fig.38B and Fig.39B respectively). Similarly to CFs, when metalloproteinases activity was inhibited by EDTA-Na₂ and attachment of HeLa cells was significantly increased compared with the effect of the same concentration of uninhibited *MLO* (Fig.38A&39A compared with Fig.20A&21A). Therefore, we hypothesize that metalloproteinases are directly affected adhesion of HeLa cells to the substrate and to each other. HeLa cells, treated with MLO+EDTA-Na₂ mixture for one hour, demonstrated 50% detachment under exposure to 10ug/ml the mix (Fig.38C). This trend continued and reached 100% detachment rate at 100ug/ml concentration of MLO+EDTA-Na₂ mix both after 1 and 24 hours of exposure (Fig.38C and Fig.39C). Starting from 20ug/ml concentration of MLO+EDTA-Na₂ mixture, the viability rate of 24hours treatment culture dropped by 30-50% (Fig.39C).

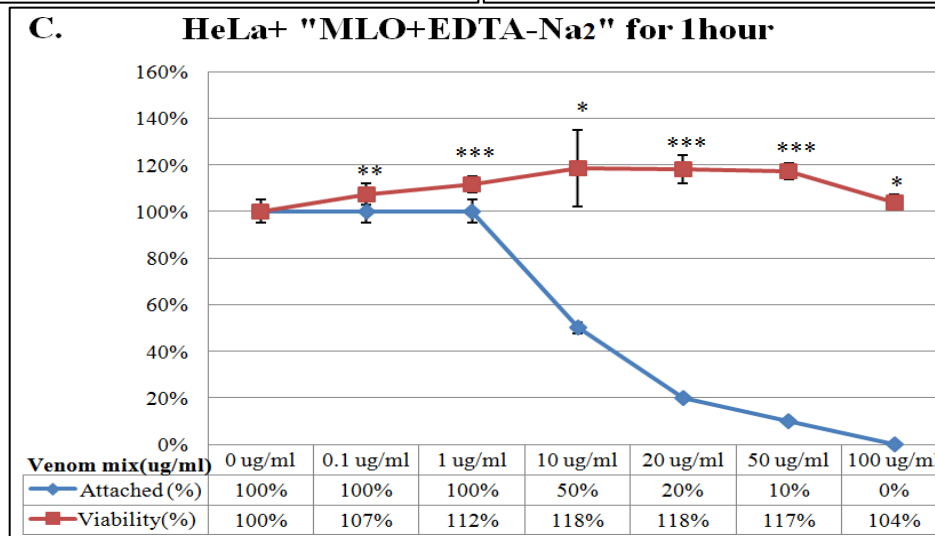
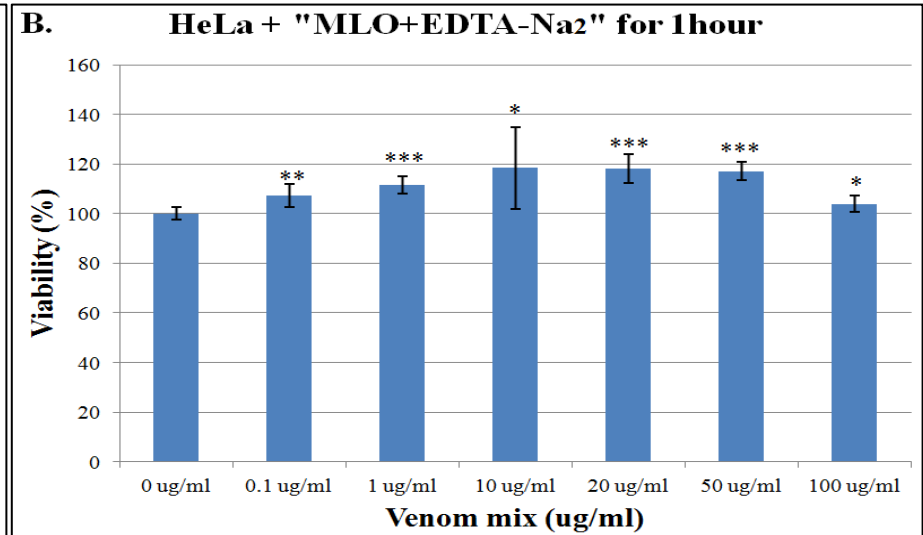
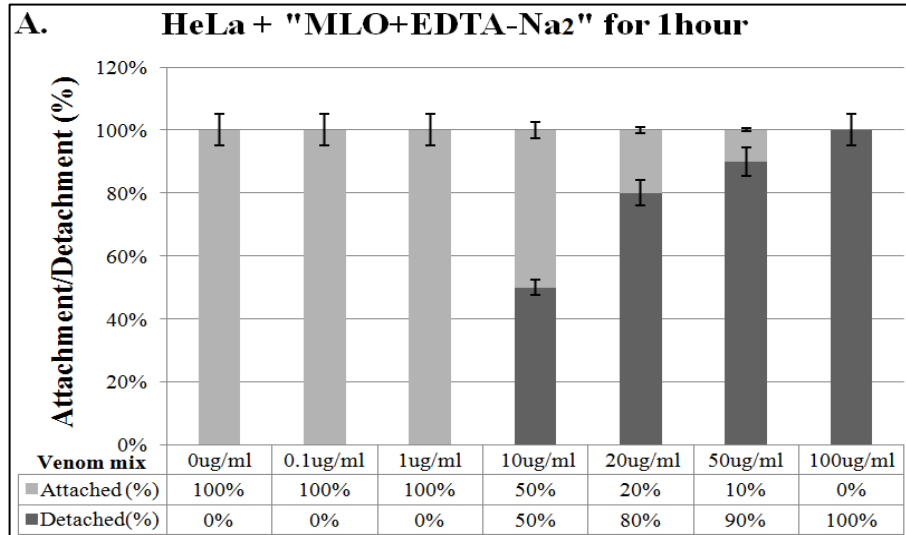


Figure 38. An increase in HeLa cells attachment is detected when MLO venom metalloproteinases are inhibited by EDTA-Na₂. (A) The ratio of covered areas (dark gray columns) to uncovered areas (light gray columns) of HeLa cells cultured for 1hour at indicated concentrations. (B) Effect of MLO+EDTA-Na₂ mix on HeLa cells viability after 1hour of treatment. (C) Attachment (blue line) and Viability (red line) of HeLa cells treated with indicated concentrations of MLO+EDTA-Na₂ mix were assessed after 1hour of treatment.

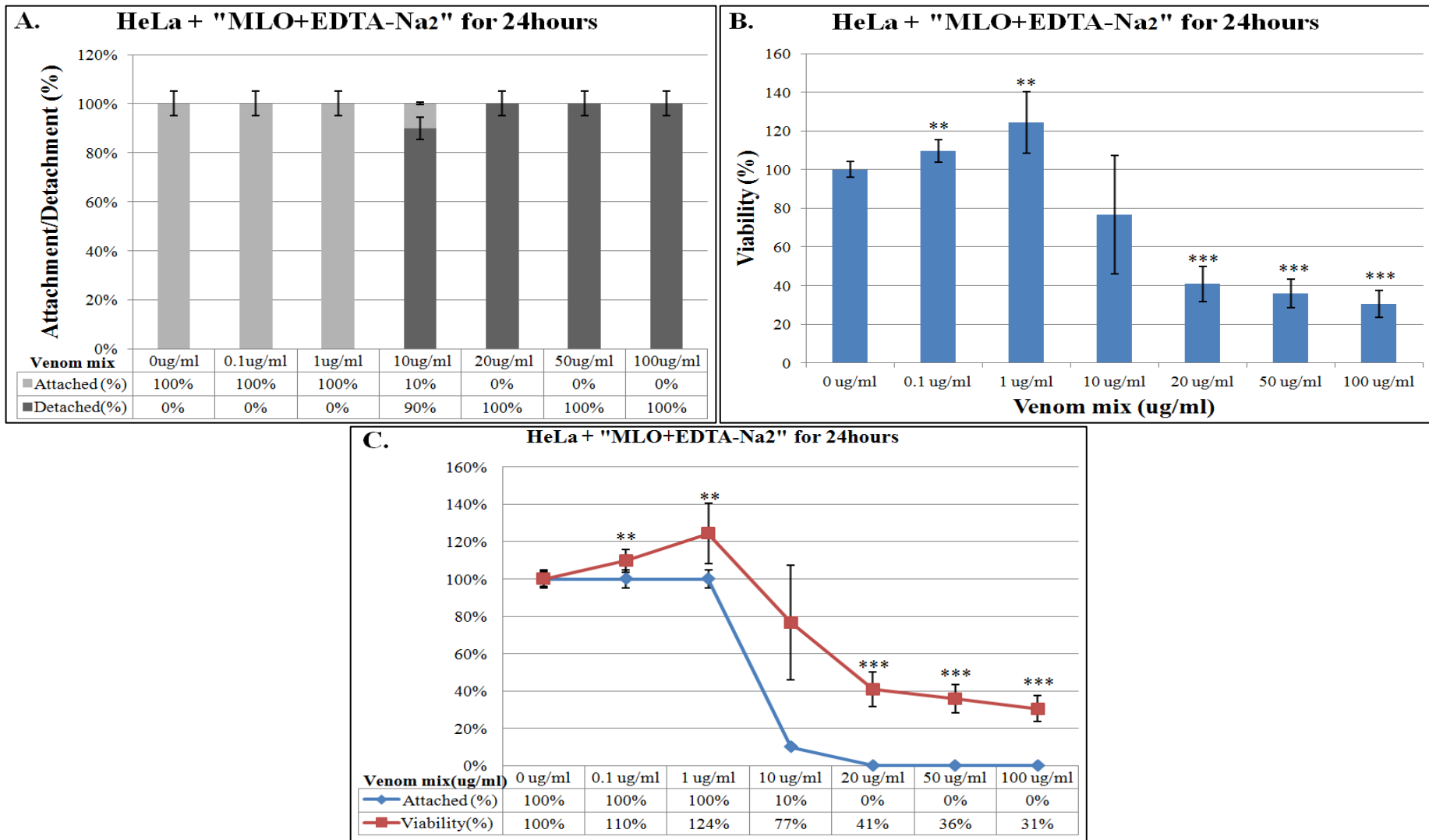


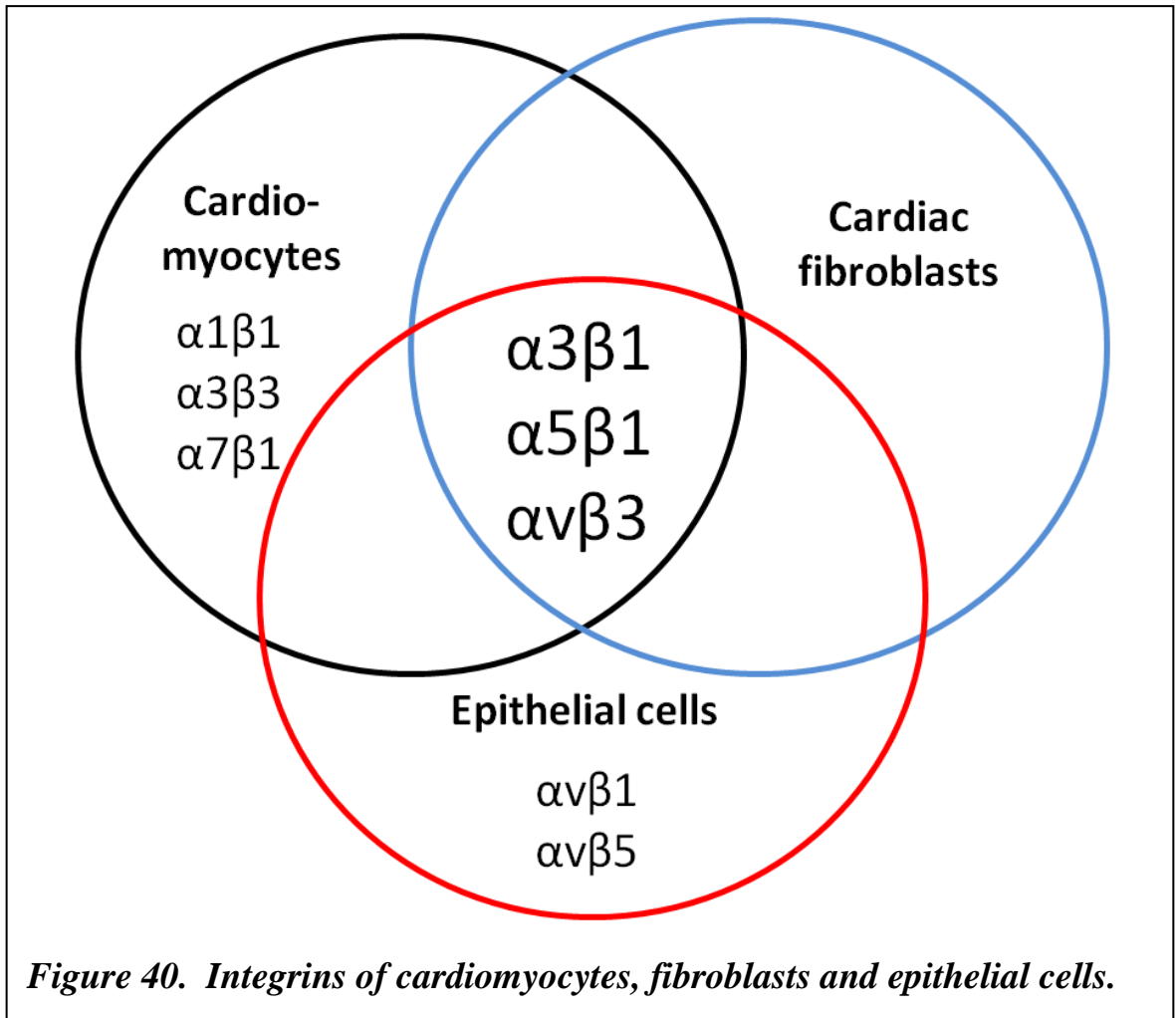
Figure 39. An increase in HeLa cells attachment is detected when MLO venom metalloproteinases are inhibited by EDTA-Na₂. (A) The ratio of covered areas (dark gray columns) to uncovered areas (light gray columns) of HeLa cells cultured for 24hours at indicated concentrations. (B) Effect of MLO+EDTA-Na₂ mix on HeLa cells viability after 24hours of treatment. (C) Attachment (blue line) and Viability (red line) of HeLa cells treated with indicated concentrations of MLO+EDTA-Na₂ mix were assessed after 24hours of treatment.

Chapter 4 Discussion

Snake venoms are quite diverse in individual components, but most of them are complex and deadly cocktails. The unique mixtures of enzymes, peptides and other components customized by natural selection affect vital functions and/or organ's systems of prey. These toxic effects include perturbation of the activity of critical enzymes, receptors, or ion channels, which can thwart the central and peripheral nervous systems, affect cardiovascular and the neuromuscular systems and modify blood coagulation and homeostasis pathways [184]–[188]. Molecular mechanisms behind both myolysis and coagulopathy caused by MLO venom can be linked to its direct effect on integrins that are critical for adhesion, extracellular matrix organization, signaling, survival, and proliferation [127], [189]. Integrins are a major class of cell surface transmembrane type I heterodimeric receptors that mediate a wide variety of cell-cell and cell-extracellular matrix interactions. As of today, there are 18 α and 8 β subunits identified in mammals, which combine to make 24 pairs of different integrin combinations [190]. In the cardiac myocytes and fibroblasts, the most highly expressed integrin heterodimers are $\alpha_1\beta_1$, $\alpha_3\beta_1$, $\alpha_5\beta_1$, $\alpha_7\beta_1$, $\alpha_v\beta_1$, which can bind to collagen I, fibronectin, and laminin, whereas $\alpha_1\beta_1$, $\alpha_5\beta_1$, and $\alpha_7\beta_1$ are predominantly collagen, fibronectin, and laminin-binding receptors, respectively. The presented Venn diagram summarizes the information of the known integrins involved in adhesion of NRCM, CF, and EC (Fig.40).

Snake venom includes disintegrins, that are low molecular weight proteins which interact with specific integrins blocking their functional ability to bind endogenous ligands [191], [192]. Functionally disintegrins are divided into 3 groups based on the active motif present in the integrin binding site which determines their selectivity. The first group includes disintegrins that interact with RGD-dependent integrins ($\alpha_{IIb}\beta_3$, α_v -integrins, and $\alpha_5\beta_1$) and is mainly represented by the disintegrins that contain the RGD tripeptide in their active site. The second group consists of heterodimeric disintegrins containing MLD sequence in the active site and blocks the function of certain leukocyte integrins (α_4 -integrins and $\alpha_9\beta_1$). Lastly, the third

functional group of disintegrins includes selective inhibitors of $\alpha 1\beta 1$ integrin, which contain KTS motif in the active site [193].



Obtustatin and lebestatin (known shortest disintegrins from KTS-family) have been shown to interact specifically with the $\alpha 1\beta 1$ integrin leading to inhibition of adhesion and migration of cells [5], [153], [194]. Expression of disintegrin metalloproteinases has been directly linked to increased matrix degradation in cardiac cells [195]. All these findings suggest that disintegrins from *MLO* venom can have a direct inhibitory effect on formation and function of the cardiac cell network. The exact mechanism of *MLO* venom effects on cell beating rate is outside the scope of these studies as it remains to be determined whether *MLO* venom directly affects and/or changes the balance of excitatory ion currents or if decreased degree of cell attachment to the substrate causes cells to alter their spontaneous beating rate.

Scientific novelty. In this study, we demonstrated that crude venom from *MLO* is affecting adhesion properties of NRCM, CF, and HeLa cells. The LD₅₀ of *MLO* venom in mice is 18.4 ug per 1 mouse [196]. To date, there is no information about the concentration of the venom that is reaching the heart after the bite. We estimate it to be in 5-10ug/ml range based on an average adult mouse weight (20-25 grams) and its volume of blood (being about 6-8% of total body weight or 1.5-2ml of blood). These estimates suggest that concentrations of the venom used in this study can be in fact encountered in vivo. Therefore, in this study, we systematically investigated the effects of low concentrations of *MLO* venom on aforementioned myocardial cells and epithelial cells.

In an attempt to understand the mechanisms of such activity, we used inhibitors specific for individual components of *MLO* venom. Among those were an EDTA-Na₂ chelating agent, which effectively neutralized metalloproteinases of *MLO* venom. The adhesion of tested cells was slightly improved when EDTA-Na₂ inhibited venom was applied to cardiomyocytes, cardiac fibroblasts, and HeLa cells. Similar results were obtained with bromophenacyl bromide (BPB)-inhibited venom, where PLA2 enzyme activity was completely blocked. These results indicate that the aggressive detaching activity of *MLO* venom is not delivered by an individual component of the venom, but rather is a combinatorial effect of several active ingredients.

All in all our data proves the direct effects of *MLO* venom to adherent properties of myocardial cells and HeLa cells. It influences both the adhesion to the extracellular matrix and, differently, the adhesion of cells to each other. In our working model, closely resembling the estimated concentrations of the venom in the bloodstream of a prey, we found that 1ug/ml concentrations demonstrate the most obvious changes in the tested characteristics of studied cells, namely attachment, and viability. This concentration was also found to be the one that does not cause mortality of the cells, but rather simulates a lower level of venom, that is associated with the morbidity of a prey and thus is more important to be studied. Table 2 summarizes the results of exposure of all tested cells to whole *MLO* and its inhibited forms for one and 24-hour

periods obtained under 1ug/ml venom concentrations to illustrate the most significant results of our studies.

Table 2. Summary of attachment and viability data for all types of cells treated with 1ug/ml of each treatment.

Cell type		Exposure time	Treatment type at 1 ug/ml MLO				
			Attachment	MLO-Thermo	MLO	MLO+EDTA-Na ₂	MLO + BPB
Cell type	NRCM	1 hour	Attachment	100%	99%	100%	100%
			Viability	110%	125%	115%	120%
		24 hours	Attachment	100%	90%	100%	95%
			Viability	108%	146%	140%	135%
	CF	1 hour	Attachment	100%	93%	100%	95%
			Viability	103%	117%	119%	109%
		24 hours	Attachment	100%	80%	100%	95%
			Viability	110%	130%	139%	129%
	HeLa	1 hour	Attachment	100%	80%	100%	100%
			Viability	114%	112%	112%	106%
		24 hours	Attachment	100%	80%	100%	95%
			Viability	116%	127%	124%	136%

In another attempt to understand underlying mechanisms of adhesion of NRCM to the substrate, we tested different coatings for attachment of studied cells to well surface. Among those coatings were gelatin, laminin, and fibronectin. Gelatin is a water-soluble natural polymer which is derived from collagen (Collagen Type I). The key adhesion components of gelatin are α_1 , α_3 , α_5 , and β_1 integrin subunits. Laminin is an important and major component of basal lamina, which has a direct effect on cell differentiation, migration, and adhesion. The main adhesion molecules of laminin are α_1 , α_3 , α_5 , α_7 , and β_1 . Fibronectin has numerous important functions, such as cell adhesion, growth, differentiation, and migration. It is also secreted by a variety of cells, in particular, primary fibroblasts and contains the binding part for α_3 , α_5 , α_v , and

β_1 integrin subunits. However, despite the differences of coatings, in these experiments, no visual differences were detected in effects of *MLO* crude venom on adhesive properties of aforementioned cells. This indicates that the mechanism of investigated venom action is more general, superseding specific differences in integrins composition of ECM proteins we have tested.

Conclusions

Macrovipera lebetina obtusa is one of the most poisonous snakes in Armenia, which bites causes unavoidable morbidity and sometimes mortality of a prey. The cardiovascular system is one of the neglected targets of this venom. In our studies, we develop a model for investigating *MLO* venom effects on cultured myocardial and endothelial cells. In this study, we used neonatal rat cardiomyocyte preparation method to address the toxicity of this venom considering the organization of cardiac muscle. Based on the results of presented investigation we made the following conclusions:

- 1) *MLO* venom has a direct affect on cultured myocardial cells such as cardiomyocytes and cardiac fibroblast and epithelial cells, by severely altering their attachment properties.
- 2) *MLO* venom-induced detachment is dose and time dependent in all tested cell types.
- 3) The tolerable dose of *MLO* exposure is the optimal dose for investigating adhesive properties of myocardial and epithelial cells. This was estimated to be in 0.1 and 1 ug/ml range.
- 4) Cardiomyocytes exposed to tolerable doses of the *MLO* venom demonstrates a dramatic increase in contraction frequency, due to a C-type natriuretic peptide, which in turn results in significant decrease of contraction amplitude.
- 5) Identified detachment is characterized by specific order of events: Initially, cells detach from culturing substrate and later cells detach from each other.
- 6) Chelated *MLO* venom causes less detachment in all tested cells types, indicating the involvement of venom metalloproteinases.
- 7) BPB inhibited *MLO* venom is also less detaching for cells, indicating the involvement of PLA2 enzyme of the venom in this process.

Future directions

The results of our studies set off a series of questions that we are planning to address in future. First of all, we are planning to investigate a novel phenomenon – initiation of tachycardia in cardiomyocytes under exposure to non-lethal doses of *MLO* venom. It is known that C-type natriuretic protein (CNP) is a part of *MLO* whole venom. CNP promotes natriuresis and diuresis resulting in loss of sodium and water thereby lowering blood volume and blood pressure. These properties of CNP make it a prime suspect in altering the physiology of cardiomyocytes, but direct studies are yet to be done.

During the course of our investigations, we identified a dose of *MLO* venom that affects adhesion properties of aforementioned cells but does not cause this death. This model provides a unique opportunity to study molecular interactions of lasting cellular culture and work out conditions for testing components of *MLO* venom for drug development.

The severe detachment was detected as a consequence of *MLO* venom on all three tested cell types. Similar effects were detected on other cells, such as skeletal muscle cells, endothelial cells, when other types of snake venoms were used (Borkow et al., 1995). We discovered that detachment from the substrate occurs prior to cell-to-cell detachments. We are intending to unravel the mechanisms of this phenomenon. Attachment of cells to culture substrates, which stimulates extracellular matrix, is mostly provided by integrins. *MLO* venom contains a series of disintegrins in their multiple forms, the most important being obtustatin. Interaction of each tested cell type with culture substrate and with each other will be the focus of future experiments. On the other hand, the network of synchronously beating cardiomyocytes is created by desmosomes and tight junctions, which have complex composition. Understanding of delayed action of *MLO* venom on these connections will be another focus of future studies.

Unexpectedly, we discovered that very low concentrations of *MLO* venom induce an increase in survivability of cardiomyocytes, cardiac fibroblasts and HeLa

cells as detected by MTT assay. This is important to decipher for at least two reasons. First, we plan to investigate whether or not there is a real increase in a number of cells under these conditions. It is possible that at low levels of stress the proliferative mechanisms are stimulated. If that is the case, this will provide a unique opportunity to stimulate the growth of otherwise proliferatively-limited cardiomyocytes for tissue engineering purposes. Second, considering the nature of MTT assay, which measures mitochondrial activity, it is possible that non-lethal doses of *MLO* venom simply accelerate metabolism. We are planning to investigate both of these possibilities.

In addition, we are planning to definitively demonstrate the mechanism of action of individual venom components on detachment, by blocking distinct components of *MLO* venom or their combinations. Our initial experiments indicated the involvement of both PLA2 and metalloproteinases in these processes. However, we detected only slight alterations in venom action when the venom was inhibited by particularized inhibitors. In addition, there are other enzymatic components present in *MLO* venom such as serine proteases. These enzymes are not directly involved in adhesion mechanisms; however, they might play a facilitating/combinatorial role in the detected phenomenon and thus will be included in our future studies. Systematic application of all possible inhibitors and testing the effects of their combination will shed more light on *MLO* venom action mechanisms.

Lastly, more cell types will be incorporated in our studies including endothelial cells (HUVEC), as they are exposed to venom before other cells buried deeper in the tissues, liver cells and others in order to evaluate the commonality of *MLO* venom effects.

References

- [1] J. C. Daltry, W. Wüster, and R. S. Thorpe, "Diet and snake venom evolution," *Nature*, vol. 379, no. 6565, pp. 537–540, Feb. 1996.
- [2] W.-B. Wu and T.-F. Huang, "Activation of MMP-2, cleavage of matrix proteins, and adherens junctions during a snake venom metalloproteinase-induced endothelial cell apoptosis," *Exp. Cell Res.*, vol. 288, no. 1, pp. 143–57, Aug. 2003.
- [3] C.-Y. Lee, *Snake Venoms*. Springer Berlin Heidelberg, 1979.
- [4] K. Trummal, K. T?nism?gi, E. Siigur, A. Aasp?llu, A. Lopp, T. Sillat, R. Saat, L. Kasak, I. Tammiste, P. Kogerman, N. Kalkkinen, and J. Siigur, "A novel metalloprotease from *Vipera lebetina* venom induces human endothelial cell apoptosis," *Toxicon*, vol. 46, no. 1, pp. 46–61, Jul. 2005.
- [5] K.-Z. Olfa, L. José, D. Salma, B. Amine, S. A. Najet, A. Nicolas, L. Maxime, Z. Raoudha, M. Kamel, M. Jacques, S. Jean-Marc, E. A. Mohamed, and M. Naziha, "Lebestatin, a disintegrin from *Macrovipera* venom, inhibits integrin-mediated cell adhesion, migration and angiogenesis," *Lab. Invest.*, vol. 85, no. 12, pp. 1507–16, Dec. 2005.
- [6] L. Sanz, N. Ayvazyan, and J. J. Calvete, "Snake venomomics of the Armenian mountain vipers *Macrovipera lebetina obtusa* and *Vipera raddei*," *J. Proteomics*, vol. 71, no. 2, pp. 198–209, Jul. 2008.
- [7] I. Limam, A. Bazaa, N. Srairi-Abid, S. Taboubi, J. Jebali, R. Zouari-Kessentini, O. Kallech-Ziri, H. Mejdoub, A. Hammami, M. El Ayeb, J. Luis, and N. Marrakchi, "Leberagin-C, A disintegrin-like/cysteine-rich protein from *Macrovipera lebetina transmediterranea* venom, inhibits alphavbeta3 integrin-mediated cell adhesion," *Matrix Biol.*, vol. 29, no. 2, 2010.
- [8] J. M. Gutiérrez and A. Rucavado, "Snake venom metalloproteinases: their role in the pathogenesis of local tissue damage," *Biochimie*, vol. 82, no. 9–10, pp. 841–50.
- [9] B. C. Zychar, C. S. Dale, D. S. Demarchi, and L. R. C. Gonçalves, "Contribution of metalloproteases, serine proteases and phospholipases A2 to the inflammatory reaction induced by *Bothrops jararaca* crude venom in mice," *Toxicon*, vol. 55, no. 2–3, pp. 227–234, Feb. 2010.
- [10] H. W. Vliegen, A. van der Laarse, C. J. Cornelisse, and F. Eulerink, "Myocardial changes in pressure overload-induced left ventricular hypertrophy. A study on tissue composition, polyploidization and multinucleation," *Eur. Heart J.*, vol. 12, no. 4, pp. 488–94, Apr. 1991.
- [11] C. P. Adler, W. P. Ringlage, and N. Böhm, "DNA Content and Cell Number in Heart and Liver of Children: Comparable Biochemical, Cytophotometric and Histological Investigations," *Pathol. - Res. Pract.*, vol. 172, no. 1–2, pp. 25–41, Jul. 1981.
- [12] E. A. Woodcock and S. J. Matkovich, "Cardiomyocytes structure, function and associated pathologies," *Int. J. Biochem. Cell Biol.*, vol. 37, no. 9, pp. 1746–1751, Sep. 2005.
- [13] P. Camelliti, T. K. Borg, and P. Kohl, "Structural and functional characterisation of cardiac fibroblasts," *Cardiovasc. Res.*, vol. 65, no. 1, pp. 40–51, Jan. 2005.
- [14] P. Camelliti, G. P. Devlin, K. G. Matthews, P. Kohl, and C. R. Green, "Spatially and temporally distinct expression of fibroblast connexins after sheep ventricular infarction," *Cardiovasc. Res.*, vol. 62, no. 2, pp. 415–25, May 2004.
- [15] P. Camelliti, C. R. Green, I. LeGrice, and P. Kohl, "Fibroblast network in rabbit sinoatrial node: structural and functional identification of homogeneous and heterogeneous cell coupling," *Circ. Res.*, vol. 94, no. 6, pp. 828–35, Apr. 2004.
- [16] P. Kohl and D. Noble, "Mechanosensitive connective tissue: potential influence on heart rhythm," *Cardiovasc. Res.*, vol. 32, no. 1, pp. 62–8, Jul. 1996.
- [17] C. S. Long, R. D. Brown, T. Ueland, G. Freeman, S. Sasayama, and R. Wilder, "The cardiac fibroblast, another therapeutic target for mending the broken heart?," *J. Mol. Cell. Cardiol.*, vol. 34, no. 10, pp. 1273–8, Oct. 2002.
- [18] D. MacKenna, S. R. Summerour, and F. J. Villarreal, "Role of mechanical factors in modulating cardiac fibroblast function and extracellular matrix synthesis," *Cardiovasc. Res.*,

- vol. 46, no. 2, pp. 257–63, May 2000.
- [19] Y. Sun, M. F. Kiani, A. E. Postlethwaite, and K. T. Weber, “Infarct scar as living tissue.,” *Basic Res. Cardiol.*, vol. 97, no. 5, pp. 343–7, Sep. 2002.
- [20] Y. Sun and K. T. Weber, “Infarct scar: a dynamic tissue.,” *Cardiovasc. Res.*, vol. 46, no. 2, pp. 250–6, May 2000.
- [21] K. R. Junqueira CL, Carneiro J, *Basic histology*, 8th ed. Norwalk: Appleton & Lange, 1992.
- [22] W. A. Hsueh, R. E. Law, and Y. S. Do, “Integrins, adhesion, and cardiac remodeling.,” *Hypertens. (Dallas, Tex. 1979)*, vol. 31, no. 1 Pt 2, pp. 176–80, Jan. 1998.
- [23] Katz AM, *Physiology of the heart*. New York: Raven Press, 1992.
- [24] J. Pinnell, S. Turner, and S. Howell, “Cardiac muscle physiology,” *Contin. Educ. Anaesthesia, Crit. Care Pain*, vol. 7, no. 3, pp. 85–88, Jun. 2007.
- [25] J. P. Reeves, M. Condrescu, G. Chernaya, and J. P. Gardner, “Na⁺/Ca²⁺ antiport in the mammalian heart.,” *J. Exp. Biol.*, vol. 196, pp. 375–88, Nov. 1994.
- [26] L. V Hryshko and K. D. Philipson, “Sodium-calcium exchange: recent advances.,” *Basic Res. Cardiol.*, vol. 92 Suppl 1, pp. 45–51, 1997.
- [27] C. W. Balke and S. R. Shorofsky, “Alterations in calcium handling in cardiac hypertrophy and heart failure.,” *Cardiovasc. Res.*, vol. 37, no. 2, pp. 290–9, Feb. 1998.
- [28] R. Mukherjee and F. G. Spinale, “L-type calcium channel abundance and function with cardiac hypertrophy and failure: a review.,” *J. Mol. Cell. Cardiol.*, vol. 30, no. 10, pp. 1899–916, Oct. 1998.
- [29] H. B. Nuss, D. C. Johns, S. Kääb, G. F. Tomaselli, D. Kass, J. H. Lawrence, and E. Marban, “Reversal of potassium channel deficiency in cells from failing hearts by adenoviral gene transfer: a prototype for gene therapy for disorders of cardiac excitability and contractility.,” *Gene Ther.*, vol. 3, no. 10, pp. 900–12, Oct. 1996.
- [30] T. K. Borg and L. Terracio, “Interaction of the extracellular matrix with cardiac myocytes during development and disease.” S. Karger AG, 1990.
- [31] T. F. Robinson, L. Cohen-Gould, and S. M. Factor, “Skeletal framework of mammalian heart muscle. Arrangement of inter- and pericellular connective tissue structures.,” *Lab. Invest.*, vol. 49, no. 4, pp. 482–98, Oct. 1983.
- [32] R. Horowitz, E. S. Kempner, M. E. Bisher, and R. J. Podolsky, “A physiological role for titin and nebulin in skeletal muscle.,” *Nature*, vol. 323, no. 6084, pp. 160–4, Sep. 1986.
- [33] I. Morano, K. Hädicke, S. Grom, A. Koch, R. H. Schwinger, M. Böhm, S. Bartel, E. Erdmann, and E. G. Krause, “Titin, myosin light chains and C-protein in the developing and failing human heart.,” *J. Mol. Cell. Cardiol.*, vol. 26, no. 3, pp. 361–8, Mar. 1994.
- [34] D. M. Eble and F. G. Spinale, “Contractile and cytoskeletal content, structure, and mRNA levels with tachycardia-induced cardiomyopathy.,” *Am. J. Physiol.*, vol. 268, no. 6 Pt 2, pp. H2426-39, Jun. 1995.
- [35] H. Tsutsui, K. Ishihara, and G. Cooper, “Cytoskeletal role in the contractile dysfunction of hypertrophied myocardium.,” *Science*, vol. 260, no. 5108, pp. 682–7, Apr. 1993.
- [36] W. J. Katz AM, Takenaka H, “The sarcoplasmic reticulum,” *Hear. Cardiovasc. Syst. Sci. Found.*, pp. 61–100, 1986.
- [37] V. J. Kadambi and E. G. Kranias, “Phospholamban: a protein coming of age.,” *Biochem. Biophys. Res. Commun.*, vol. 239, no. 1, pp. 1–5, Oct. 1997.
- [38] M. Aubier and N. Viires, “Calcium ATPase and respiratory muscle function.,” *Eur. Respir. J.*, vol. 11, no. 3, pp. 758–66, Mar. 1998.
- [39] A. J. Williams, “The functions of two species of calcium channel in cardiac muscle excitation-contraction coupling.,” *Eur. Heart J.*, vol. 18 Suppl A, pp. A27-35, Jan. 1997.
- [40] W. H. Barry and J. H. Bridge, “Intracellular calcium homeostasis in cardiac myocytes.,” *Circulation*, vol. 87, no. 6, pp. 1806–15, Jun. 1993.
- [41] R. M. Berne and M. N. Levy, *Cardiovascular physiology*. Mosby, 2001.
- [42] M. Tada and T. Toyofuku, “SR Ca(2⁺)-ATPase/phospholamban in cardiomyocyte function.,”

- J. Card. Fail.*, vol. 2, no. 4 Suppl, pp. S77-85, Dec. 1996.
- [43] V. J. Kadambi, S. Ponniah, J. M. Harrer, B. D. Hoit, G. W. Dorn, R. A. Walsh, and E. G. Kranias, "Cardiac-specific overexpression of phospholamban alters calcium kinetics and resultant cardiomyocyte mechanics in transgenic mice.," *J. Clin. Invest.*, vol. 97, no. 2, pp. 533–9, Jan. 1996.
- [44] C. Franzini-Armstrong and F. Protasi, "Ryanodine receptors of striated muscles: a complex channel capable of multiple interactions.," *Physiol. Rev.*, vol. 77, no. 3, pp. 699–729, Jul. 1997.
- [45] M. J. Berridge, "Elementary and global aspects of calcium signalling.," *J. Physiol.*, no. Pt 2, pp. 291–306, Mar. 1997.
- [46] G. Hasenfuss, M. Meyer, W. Schillinger, M. Preuss, B. Pieske, and H. Just, "Calcium handling proteins in the failing human heart.," *Basic Res. Cardiol.*, vol. 92 Suppl 1, pp. 87–93, 1997.
- [47] D. M. Bers, J. W. Bassani, and R. A. Bassani, "Na-Ca exchange and Ca fluxes during contraction and relaxation in mammalian ventricular muscle.," *Ann. N. Y. Acad. Sci.*, vol. 779, pp. 430–42, Apr. 1996.
- [48] D. M. Bers, "Excitation-Contraction Coupling," 2001, pp. 203–244.
- [49] B. Alberts, A. Johnson, J. Lewis, M. Raff, K. Roberts, and P. Walter, *Molecular biology of the cell*, 4th ed. New York: Garland Science, 2002.
- [50] G. H. Pollack, *Muscles and molecules : uncovering the principles of biological motion*. Seattle: Ebner & Sons Publishers, 1990.
- [51] D. M. Bers, "Cardiac excitation-contraction coupling.," *Nature*, vol. 415, no. 6868, pp. 198–205, Jan. 2002.
- [52] F. G. Spinale, R. Mukherjee, B. M. Fulbright, J. Hu, F. A. Crawford, and M. R. Zile, "Contractile properties of isolated porcine ventricular myocytes.," *Cardiovasc. Res.*, vol. 27, no. 2, pp. 304–11, Feb. 1993.
- [53] F. G. Spinale, B. M. Fulbright, R. Mukherjee, R. Tanaka, J. Hu, F. A. Crawford, and M. R. Zile, "Relation between ventricular and myocyte function with tachycardia-induced cardiomyopathy.," *Circ. Res.*, vol. 71, no. 1, pp. 174–87, Jul. 1992.
- [54] R. B. New, J. L. Zellner, L. Hebbbar, R. Mukherjee, A. C. Sampson, J. W. Hendrick, J. R. Handy, F. A. Crawford, and F. G. Spinale, "Isolated left ventricular myocyte contractility in patients undergoing cardiac operations.," *J. Thorac. Cardiovasc. Surg.*, vol. 116, no. 3, pp. 495–502, Sep. 1998.
- [55] C. A. Walker and F. G. Spinale, "The structure and function of the cardiac myocyte: a review of fundamental concepts.," *J. Thorac. Cardiovasc. Surg.*, vol. 118, no. 2, pp. 375–82, Aug. 1999.
- [56] P. W. Reddien and A. S. Alvarado, "FUNDAMENTALS OF PLANARIAN REGENERATION," *Annu. Rev. Cell Dev. Biol.*, vol. 20, no. 1, pp. 725–757, Nov. 2004.
- [57] J. J. V. McMurray, S. Adamopoulos, S. D. Anker, A. Auricchio, M. Böhm, K. Dickstein, V. Falk, G. Filippatos, C. Fonseca, M. A. Gomez-Sanchez, T. Jaarsma, L. Køber, G. Y. H. Lip, A. Pietro Maggioni, A. Parkhomenko, B. M. Pieske, B. A. Popescu, P. K. Rønnevik, F. H. Rutten, J. Schwitter, P. Seferovic, J. Stepinska, P. T. Trindade, A. A. Voors, F. Zannad, A. Zeiher, J. J. Bax, H. Baumgartner, C. Ceconi, V. Dean, C. Deaton, R. Fagard, C. Funck-Brentano, D. Hasdai, A. Hoes, P. Kirchhof, J. Knuuti, P. Kolh, T. McDonagh, C. Moulin, B. A. Popescu, Ž. Reiner, U. Sechtem, P. A. Sirnes, M. Tendera, A. Torbicki, A. Vahanian, S. Windecker, T. McDonagh, U. Sechtem, L. A. Bonet, P. Avraamides, H. A. Ben Lamin, M. Brignole, A. Coca, P. Cowburn, H. Dargie, P. Elliott, F. A. Flachskampf, G. F. Guida, S. Hardman, B. Iung, B. Merkely, C. Mueller, J. N. Nanas, O. W. Nielsen, S. Ørn, J. T. Parissis, and P. Ponikowski, "ESC Guidelines for the diagnosis and treatment of acute and chronic heart failure 2012," *Eur. J. Heart Fail.*, vol. 14, no. 8, pp. 803–869, Aug. 2012.
- [58] T. C. G. Bosch, "Why polyps regenerate and we don't: Towards a cellular and molecular

- framework for Hydra regeneration,” *Dev. Biol.*, vol. 303, no. 2, pp. 421–433, Mar. 2007.
- [59] J. P. Brockes and A. Kumar, “Comparative Aspects of Animal Regeneration,” *Annu. Rev. Cell Dev. Biol.*, vol. 24, no. 1, pp. 525–549, Nov. 2008.
- [60] K. D. Poss, “Advances in understanding tissue regenerative capacity and mechanisms in animals,” *Nat. Rev. Genet.*, vol. 11, no. 10, pp. 710–22, Oct. 2010.
- [61] A. P. Beltrami, L. Barlucchi, D. Torella, M. Baker, F. Limana, S. Chimenti, H. Kasahara, M. Rota, E. Musso, K. Urbanek, A. Leri, J. Kajstura, B. Nadal-Ginard, and P. Anversa, “Adult cardiac stem cells are multipotent and support myocardial regeneration,” *Cell*, vol. 114, no. 6, pp. 763–76, Sep. 2003.
- [62] G. M. Ellison, C. Vicinanza, A. J. Smith, I. Aquila, A. Leone, C. D. Waring, B. J. Henning, G. G. Stirparo, R. Papait, M. Scarfò, V. Agosti, G. Viglietto, G. Condorelli, C. Indolfi, S. Ottolenghi, D. Torella, and B. Nadal-Ginard, “Adult c-kitpos Cardiac Stem Cells Are Necessary and Sufficient for Functional Cardiac Regeneration and Repair,” *Cell*, vol. 154, no. 4, pp. 827–842, Aug. 2013.
- [63] J. H. van Berlo and J. D. Molkentin, “An emerging consensus on cardiac regeneration,” *Nat. Med.*, vol. 20, no. 12, pp. 1386–1393, Dec. 2014.
- [64] J. H. van Berlo, O. Kanisicak, M. Maillet, R. J. Vagnozzi, J. Karch, S.-C. J. Lin, R. C. Middleton, E. Marbán, and J. D. Molkentin, “c-kit+ cells minimally contribute cardiomyocytes to the heart,” *Nature*, vol. 509, no. 7500, pp. 337–341, May 2014.
- [65] K. U. Hong, Y. Guo, Q.-H. Li, P. Cao, T. Al-Maqtari, B. N. Vajravelu, J. Du, M. J. Book, X. Zhu, Y. Nong, A. Bhatnagar, and R. Bolli, “c-kit+ Cardiac Stem Cells Alleviate Post-Myocardial Infarction Left Ventricular Dysfunction Despite Poor Engraftment and Negligible Retention in the Recipient Heart,” *PLoS One*, vol. 9, no. 5, p. e96725, May 2014.
- [66] M. Gneocchi, Z. Zhang, A. Ni, and V. J. Dzau, “Paracrine Mechanisms in Adult Stem Cell Signaling and Therapy,” *Circ. Res.*, vol. 103, no. 11, pp. 1204–1219, Nov. 2008.
- [67] A. Behfar, R. Crespo-Diaz, A. Terzic, and B. J. Gersh, “Cell therapy for cardiac repair—lessons from clinical trials,” *Nat. Rev. Cardiol.*, vol. 11, no. 4, pp. 232–246, Mar. 2014.
- [68] M. A. Laflamme and C. E. Murry, “Heart regeneration,” *Nature*, vol. 473, no. 7347, pp. 326–335, May 2011.
- [69] J. X. Chen, M. Krane, M.-A. Deutsch, L. Wang, M. Rav-Acha, S. Gregoire, M. C. Engels, K. Rajarajan, R. Karra, E. D. Abel, J. C. Wu, D. Milan, and S. M. Wu, “Inefficient Reprogramming of Fibroblasts into Cardiomyocytes Using Gata4, Mef2c, and Tbx5,” *Circ. Res.*, vol. 111, no. 1, pp. 50–55, Jun. 2012.
- [70] M. Ieda, J.-D. Fu, P. Delgado-Olguin, V. Vedantham, Y. Hayashi, B. G. Bruneau, and D. Srivastava, “Direct Reprogramming of Fibroblasts into Functional Cardiomyocytes by Defined Factors,” *Cell*, vol. 142, no. 3, pp. 375–386, Aug. 2010.
- [71] K. Song, Y.-J. Nam, X. Luo, X. Qi, W. Tan, G. N. Huang, A. Acharya, C. L. Smith, M. D. Tallquist, E. G. Neilson, J. A. Hill, R. Bassel-Duby, and E. N. Olson, “Heart repair by reprogramming non-myocytes with cardiac transcription factors,” *Nature*, vol. 485, no. 7400, pp. 599–604, May 2012.
- [72] T. Sadahiro, S. Yamanaka, and M. Ieda, “Direct Cardiac Reprogramming: Progress and Challenges in Basic Biology and Clinical Applications,” *Circ. Res.*, vol. 116, no. 8, pp. 1378–1391, Apr. 2015.
- [73] M. H. Soonpaa, K. K. Kim, L. Pajak, M. Franklin, and L. J. Field, “Cardiomyocyte DNA synthesis and binucleation during murine development,” *Am. J. Physiol.*, vol. 271, no. 5 Pt 2, pp. H2183-9, Nov. 1996.
- [74] I. Flink, “Cell cycle reentry of ventricular and atrial cardiomyocytes and cells within the epicardium following amputation of the ventricular apex in the axolotl, *Amblystoma mexicanum* : confocal microscopic immunofluorescent image analysis of bromodeoxyuridine-labeled nuclei,” *Anat. Embryol. (Berl.)*, vol. 205, no. 3, pp. 235–244, Jun. 2002.

- [75] K. D. Poss, L. G. Wilson, and M. T. Keating, “Heart Regeneration in Zebrafish,” *Science* (80-.), vol. 298, no. 5601, pp. 2188–2190, Dec. 2002.
- [76] N. Witman, B. Murtuza, B. Davis, A. Arner, and J. I. Morrison, “Recapitulation of developmental cardiogenesis governs the morphological and functional regeneration of adult newt hearts following injury,” *Dev. Biol.*, vol. 354, no. 1, pp. 67–76, Jun. 2011.
- [77] E. R. Porrello, A. I. Mahmoud, E. Simpson, J. A. Hill, J. A. Richardson, E. N. Olson, and H. A. Sadek, “Transient Regenerative Potential of the Neonatal Mouse Heart,” *Science* (80-.), vol. 331, no. 6020, pp. 1078–1080, Feb. 2011.
- [78] M. J. Foglia and K. D. Poss, “Building and re-building the heart by cardiomyocyte proliferation,” *Development*, vol. 143, no. 5, pp. 729–40, Mar. 2016.
- [79] M. Jessup and S. Brozena, “Heart Failure,” *N. Engl. J. Med.*, vol. 348, no. 20, pp. 2007–2018, May 2003.
- [80] M. G. Sutton and N. Sharpe, “Left ventricular remodeling after myocardial infarction: pathophysiology and therapy,” *Circulation*, vol. 101, no. 25, pp. 2981–8, Jun. 2000.
- [81] P. Z. Gerczuk and R. A. Kloner, “An Update on Cardioprotection,” *J. Am. Coll. Cardiol.*, vol. 59, no. 11, pp. 969–978, Mar. 2012.
- [82] R. Zak, D. Gershon, D. Kahn, and et al., “Cell proliferation during cardiac growth,” *Am. J. Cardiol.*, vol. 31, no. 2, pp. 211–9, Feb. 1973.
- [83] O. Bergmann, R. D. Bhardwaj, S. Bernard, S. Zdunek, F. Barnabé-Heider, S. Walsh, J. Zupicich, K. Alkass, B. A. Buchholz, H. Druid, S. Jovinge, and J. Frisén, “Evidence for Cardiomyocyte Renewal in Humans,” *Science* (80-.), vol. 324, no. 5923, pp. 98–102, Apr. 2009.
- [84] O. Bergmann, S. Zdunek, A. Felker, M. Salehpour, K. Alkass, S. Bernard, S. L. Sjostrom, M. Szewczykowska, T. Jackowska, C. dos Remedios, T. Malm, M. Andrä, R. Jashari, J. R. Nyengaard, G. Possnert, S. Jovinge, H. Druid, and J. Frisén, “Dynamics of Cell Generation and Turnover in the Human Heart,” *Cell*, vol. 161, no. 7, pp. 1566–1575, Jun. 2015.
- [85] K. Kikuchi and K. D. Poss, “Cardiac Regenerative Capacity and Mechanisms,” *Annu. Rev. Cell Dev. Biol.*, vol. 28, no. 1, pp. 719–741, Nov. 2012.
- [86] P. P. Rumyantsev, “Interrelations of the proliferation and differentiation processes during cardiac myogenesis and regeneration,” *Int. Rev. Cytol.*, vol. 51, pp. 186–273, 1977.
- [87] H. E. Macmahon, “Hyperplasia and Regeneration of the Myocardium in Infants and in Children,” *Am. J. Pathol.*, vol. 13, no. 5, p. 845–854.5, Sep. 1937.
- [88] A. S. Warthin, “The myocardial lesions of diphtheria,” *J. Infect. Dis.*, vol. 35, no. 1, pp. 32–66, Jul. 1924.
- [89] S. Fratz, A. Hager, C. Schreiber, M. Schwaiger, J. Hess, and H. C. Stern, “Long-Term Myocardial Scarring After Operation for Anomalous Left Coronary Artery From the Pulmonary Artery,” *Ann. Thorac. Surg.*, vol. 92, no. 5, pp. 1761–1765, Nov. 2011.
- [90] B. J. Haubner, J. Schneider, U. Schweigmann, T. Schuetz, W. Dichtl, C. Velik-Salchner, J.-I. Stein, and J. M. Penninger, “Functional Recovery of a Human Neonatal Heart After Severe Myocardial Infarction Novelty and Significance,” *Circ. Res.*, vol. 118, no. 2, pp. 216–221, Jan. 2016.
- [91] B. J. Haubner, M. Adamowicz-Brice, S. Khadayate, V. Tiefenthaler, B. Metzler, T. Aitman, and J. M. Penninger, “Complete cardiac regeneration in a mouse model of myocardial infarction,” *Aging (Albany. NY)*, vol. 4, no. 12, pp. 966–77, Dec. 2012.
- [92] S. A. Jesty, M. A. Steffey, F. K. Lee, M. Breitbach, M. Hesse, S. Reining, J. C. Lee, R. M. Doran, A. Y. Nikitin, B. K. Fleischmann, and M. I. Kotlikoff, “c-kit+ precursors support postinfarction myogenesis in the neonatal, but not adult, heart,” *Proc. Natl. Acad. Sci. U. S. A.*, vol. 109, no. 33, pp. 13380–5, Aug. 2012.
- [93] E. G. Strungs, E. L. Ongstad, M. P. O’Quinn, J. A. Palatinus, L. J. Jourdan, and R. G. Gourdie, “Cryoinjury models of the adult and neonatal mouse heart for studies of scarring and regeneration,” *Methods Mol. Biol.*, vol. 1037, pp. 343–53, 2013.

- [94] D. M. Bryant, C. C. O'Meara, N. N. Ho, J. Gannon, L. Cai, and R. T. Lee, "A systematic analysis of neonatal mouse heart regeneration after apical resection," *J. Mol. Cell. Cardiol.*, vol. 79, pp. 315–318, Feb. 2015.
- [95] A. Uygun and R. T. Lee, "Mechanisms of Cardiac Regeneration.," *Dev. Cell*, vol. 36, no. 4, pp. 362–74, Feb. 2016.
- [96] E. R. Porrello, A. I. Mahmoud, E. Simpson, B. A. Johnson, D. Grinsfelder, D. Canseco, P. P. Mammen, B. A. Rothermel, E. N. Olson, and H. A. Sadek, "Regulation of neonatal and adult mammalian heart regeneration by the miR-15 family.," *Proc. Natl. Acad. Sci. U. S. A.*, vol. 110, no. 1, pp. 187–92, Jan. 2013.
- [97] C. Jopling, E. Sleep, M. Raya, M. Martí, A. Raya, and J. C. I. Belmonte, "Zebrafish heart regeneration occurs by cardiomyocyte dedifferentiation and proliferation," *Nature*, vol. 464, no. 7288, pp. 606–609, Mar. 2010.
- [98] A. Lepilina, A. N. Coon, K. Kikuchi, J. E. Holdway, R. W. Roberts, C. G. Burns, and K. D. Poss, "A dynamic epicardial injury response supports progenitor cell activity during zebrafish heart regeneration.," *Cell*, vol. 127, no. 3, pp. 607–19, Nov. 2006.
- [99] D. C. Andersen, S. Ganesalingam, C. H. Jensen, and S. P. Sheikh, "Do Neonatal Mouse Hearts Regenerate following Heart Apex Resection?," *Stem Cell Reports*, vol. 2, no. 4, pp. 406–413, Apr. 2014.
- [100] C. Han, Y. Nie, H. Lian, R. Liu, F. He, H. Huang, and S. Hu, "Acute inflammation stimulates a regenerative response in the neonatal mouse heart.," *Cell Res.*, vol. 25, no. 10, pp. 1137–51, Oct. 2015.
- [101] A. Darehzereshki, N. Rubin, L. Gamba, J. Kim, J. Fraser, Y. Huang, J. Billings, R. Mohammadzadeh, J. Wood, D. Warburton, V. Kaartinen, and C.-L. Lien, "Differential regenerative capacity of neonatal mouse hearts after cryoinjury.," *Dev. Biol.*, vol. 399, no. 1, pp. 91–9, Mar. 2015.
- [102] B. M. Gumbiner, "Cell adhesion: the molecular basis of tissue architecture and morphogenesis.," *Cell*, vol. 84, no. 3, pp. 345–57, Feb. 1996.
- [103] M. Bernfield, M. T. Hinkes, and R. L. Gallo, "Developmental expression of the syndecans: possible function and regulation.," *Dev. Suppl.*, pp. 205–12, 1993.
- [104] B. M. Gumbiner, "Proteins associated with the cytoplasmic surface of adhesion molecules.," *Neuron*, vol. 11, no. 4, pp. 551–64, Oct. 1993.
- [105] R. O. Hynes, "Integrins: versatility, modulation, and signaling in cell adhesion.," *Cell*, vol. 69, no. 1, pp. 11–25, Apr. 1992.
- [106] R. O. Hynes and A. D. Lander, "Contact and adhesive specificities in the associations, migrations, and targeting of cells and axons.," *Cell*, vol. 68, no. 2, pp. 303–22, Jan. 1992.
- [107] D. F. Mosher, J. Sottile, C. Wu, and J. A. McDonald, "Assembly of extracellular matrix.," *Curr. Opin. Cell Biol.*, vol. 4, no. 5, pp. 810–8, Oct. 1992.
- [108] T. A. Springer, "Traffic signals for lymphocyte recirculation and leukocyte emigration: the multistep paradigm.," *Cell*, vol. 76, no. 2, pp. 301–14, Jan. 1994.
- [109] C. E. Turner and K. Burridge, "Transmembrane molecular assemblies in cell-extracellular matrix interactions.," *Curr. Opin. Cell Biol.*, vol. 3, no. 5, pp. 849–53, Oct. 1991.
- [110] M. Takeichi, "Cadherin cell adhesion receptors as a morphogenetic regulator.," *Science*, vol. 251, no. 5000, pp. 1451–5, Mar. 1991.
- [111] W. Birchmeier and J. Behrens, "Cadherin expression in carcinomas: role in the formation of cell junctions and the prevention of invasiveness.," *Biochim. Biophys. Acta*, vol. 1198, no. 1, pp. 11–26, May 1994.
- [112] M. Takeichi, "Cadherins in cancer: implications for invasion and metastasis.," *Curr. Opin. Cell Biol.*, vol. 5, no. 5, pp. 806–11, Oct. 1993.
- [113] L. Larue, M. Ohsugi, J. Hirchenhain, and R. Kemler, "E-cadherin null mutant embryos fail to form a trophectoderm epithelium.," *Proc. Natl. Acad. Sci. U. S. A.*, vol. 91, no. 17, pp. 8263–7, Aug. 1994.

- [114] R. Kemler, M. Ozawa, and M. Ringwald, "Calcium-dependent cell adhesion molecules.," *Curr. Opin. Cell Biol.*, vol. 1, no. 5, pp. 892–7, Oct. 1989.
- [115] D. L. Rimm, E. R. Koslov, P. Kebriaei, C. D. Cianci, and J. S. Morrow, "Alpha 1(E)-catenin is an actin-binding and -bundling protein mediating the attachment of F-actin to the membrane adhesion complex.," *Proc. Natl. Acad. Sci. U. S. A.*, vol. 92, no. 19, pp. 8813–7, Sep. 1995.
- [116] A. Nagafuchi, S. Ishihara, and S. Tsukita, "The roles of catenins in the cadherin-mediated cell adhesion: functional analysis of E-cadherin-alpha catenin fusion molecules.," *J. Cell Biol.*, vol. 127, no. 1, pp. 235–45, Oct. 1994.
- [117] M. S. Kinch, G. J. Clark, C. J. Der, and K. Burridge, "Tyrosine phosphorylation regulates the adhesions of ras-transformed breast epithelia.," *J. Cell Biol.*, vol. 130, no. 2, pp. 461–71, Jul. 1995.
- [118] D. R. Garrod, "Desmosomes and hemidesmosomes.," *Curr. Opin. Cell Biol.*, vol. 5, no. 1, pp. 30–40, Feb. 1993.
- [119] S. M. Troyanovsky, L. G. Eshkind, R. B. Troyanovsky, R. E. Leube, and W. W. Franke, "Contributions of cytoplasmic domains of desmosomal cadherins to desmosome assembly and intermediate filament anchorage.," *Cell*, vol. 72, no. 4, pp. 561–74, Feb. 1993.
- [120] B. Gumbiner, "Structure, biochemistry, and assembly of epithelial tight junctions.," *Am. J. Physiol.*, vol. 253, no. 6 Pt 1, pp. C749–58, Dec. 1987.
- [121] J. L. Madara, "Tight junction dynamics: is paracellular transport regulated?," *Cell*, vol. 53, no. 4, pp. 497–8, May 1988.
- [122] M. Furuse, M. Itoh, T. Hirase, A. Nagafuchi, S. Yonemura, S. Tsukita, and S. Tsukita, "Direct association of occludin with ZO-1 and its possible involvement in the localization of occludin at tight junctions.," *J. Cell Biol.*, vol. 127, no. 6 Pt 1, pp. 1617–26, Dec. 1994.
- [123] S. K. Kim, "Tight junctions, membrane-associated guanylate kinases and cell signaling.," *Curr. Opin. Cell Biol.*, vol. 7, no. 5, pp. 641–9, Oct. 1995.
- [124] F. G. Giancotti and E. Ruoslahti, "Integrin signaling.," *Science*, vol. 285, no. 5430, pp. 1028–32, Aug. 1999.
- [125] N. A. Hotchin and A. Hall, "Regulation of the actin cytoskeleton, integrins and cell growth by the Rho family of small GTPases.," *Cancer Surv.*, vol. 27, pp. 311–22, 1996.
- [126] R. O. Hynes, "Cell adhesion: old and new questions.," *Trends Cell Biol.*, vol. 9, no. 12, pp. M33–7, Dec. 1999.
- [127] H. Okada, N. C. Lai, Y. Kawaraguchi, P. Liao, J. Copps, Y. Sugano, S. Okada-Maeda, I. Banerjee, J. M. Schilling, A. R. Gingras, E. K. Asfaw, J. Suarez, S.-M. Kang, G. A. Perkins, C. G. Au, S. Israeli-Rosenberg, A. M. Manso, Z. Liu, D. J. Milner, S. J. Kaufman, H. H. Patel, D. M. Roth, H. K. Hammond, S. S. Taylor, W. H. Dillmann, J. I. Goldhaber, and R. S. Ross, "Integrins protect cardiomyocytes from ischemia/reperfusion injury.," *J. Clin. Invest.*, vol. 123, no. 10, pp. 4294–308, Oct. 2013.
- [128] L. Osborn, C. Hession, R. Tizard, C. Vassallo, S. Luhowskyj, G. Chi-Rosso, and R. Lobb, "Direct expression cloning of vascular cell adhesion molecule 1, a cytokine-induced endothelial protein that binds to lymphocytes.," *Cell*, vol. 59, no. 6, pp. 1203–11, Dec. 1989.
- [129] M. J. Elices, L. Osborn, Y. Takada, C. Crouse, S. Luhowskyj, M. E. Hemler, and R. R. Lobb, "VCAM-1 on activated endothelium interacts with the leukocyte integrin VLA-4 at a site distinct from the VLA-4/fibronectin binding site.," *Cell*, vol. 60, no. 4, pp. 577–84, Feb. 1990.
- [130] M. P. Bevilacqua, "Endothelial-Leukocyte Adhesion Molecules," *Annu. Rev. Immunol.*, vol. 11, no. 1, pp. 767–804, Apr. 1993.
- [131] G. L. Kukiela, H. K. Hawkins, L. Michael, A. M. Manning, K. Youker, C. Lane, M. L. Entman, C. W. Smith, and D. C. Anderson, "Regulation of intercellular adhesion molecule-1 (ICAM-1) in ischemic and reperfused canine myocardium.," *J. Clin. Invest.*, vol. 92, no. 3, pp. 1504–1516, Sep. 1993.

- [132] T. Yamazaki, Y. Seko, T. Tamatani, M. Miyasaka, H. Yagita, K. Okumura, R. Nagai, and Y. Yazaki, "Expression of intercellular adhesion molecule-1 in rat heart with ischemia/reperfusion and limitation of infarct size by treatment with antibodies against cell adhesion molecules.," *Am. J. Pathol.*, vol. 143, no. 2, pp. 410–8, Aug. 1993.
- [133] K. A. Youker, H. K. Hawkins, G. L. Kukielka, J. L. Perrard, L. H. Michael, C. M. Ballantyne, C. W. Smith, and M. L. Entman, "Molecular evidence for induction of intracellular adhesion molecule-1 in the viable border zone associated with ischemia-reperfusion injury of the dog heart.," *Circulation*, vol. 89, no. 6, pp. 2736–46, Jun. 1994.
- [134] Y. Seko, H. Yagita, K. Okumura, and Y. Yazaki, "Expression of vascular cell adhesion molecule-1 in murine hearts with acute myocarditis caused by coxsackievirus B3.," *J. Pathol.*, vol. 180, no. 4, pp. 450–4, Dec. 1996.
- [135] M. L. Entman, K. Youker, S. B. Shappell, C. Siegel, R. Rothlein, W. J. Dreyer, F. C. Schmalstieg, and C. W. Smith, "Neutrophil adherence to isolated adult canine myocytes. Evidence for a CD18-dependent mechanism.," *J. Clin. Invest.*, vol. 85, no. 5, pp. 1497–506, May 1990.
- [136] C. W. Smith, M. L. Entman, C. L. Lane, A. L. Beaudet, T. I. Ty, K. Youker, H. K. Hawkins, and D. C. Anderson, "Adherence of neutrophils to canine cardiac myocytes in vitro is dependent on intercellular adhesion molecule-1.," *J. Clin. Invest.*, vol. 88, no. 4, pp. 1216–1223, Oct. 1991.
- [137] K. Ban, U. Ikeda, M. Takahashi, T. Kanbe, T. Kasahara, and K. Shimada, "Expression of intercellular adhesion molecule-1 on rat cardiac myocytes by monocyte chemoattractant protein-1.," *Cardiovasc. Res.*, vol. 28, no. 8, pp. 1258–62, Aug. 1994.
- [138] U. Ikeda, M. Ikeda, S. Kano, and K. Shimada, "Neutrophil adherence to rat cardiac myocyte by proinflammatory cytokines.," *J. Cardiovasc. Pharmacol.*, vol. 23, no. 4, pp. 647–52, Apr. 1994.
- [139] Y. Hattori and K. Kasai, "Induction of mRNAs for ICAM-1, VCAM-1, and ELAM-1 in cultured rat cardiac myocytes and myocardium in vivo.," *Biochem. Mol. Biol. Int.*, vol. 41, no. 5, pp. 979–86, Apr. 1997.
- [140] M. L. Dustin, R. Rothlein, A. K. Bhan, C. A. Dinarello, and T. A. Springer, "Induction by IL 1 and interferon-gamma: tissue distribution, biochemistry, and function of a natural adherence molecule (ICAM-1).," *J. Immunol.*, vol. 137, no. 1, pp. 245–54, Jul. 1986.
- [141] P. Angel, M. Imagawa, R. Chiu, B. Stein, R. J. Imbra, H. J. Rahmsdorf, C. Jonat, P. Herrlich, and M. Karin, "Phorbol ester-inducible genes contain a common cis element recognized by a TPA-modulated trans-acting factor.," *Cell*, vol. 49, no. 6, pp. 729–39, Jun. 1987.
- [142] P. A. Baeuerle and T. Henkel, "Function and Activation of NF-kappaB in the Immune System," *Annu. Rev. Immunol.*, vol. 12, no. 1, pp. 141–179, Apr. 1994.
- [143] T. Collins, M. A. Read, A. S. Neish, M. Z. Whitley, D. Thanos, and T. Maniatis, "Transcriptional regulation of endothelial cell adhesion molecules: NF-kappa B and cytokine-inducible enhancers.," *FASEB J.*, vol. 9, no. 10, pp. 899–909, Jul. 1995.
- [144] P. Ghezzi, C. A. Dinarello, M. Bianchi, M. E. Rosandich, J. E. Repine, and C. W. White, "Hypoxia increases production of interleukin-1 and tumor necrosis factor by human mononuclear cells.," *Cytokine*, vol. 3, no. 3, pp. 189–94, May 1991.
- [145] R. Shreeniwas, S. Koga, M. Karakurum, D. Pinsky, E. Kaiser, J. Brett, B. A. Wolitzky, C. Norton, J. Plocinski, and W. Benjamin, "Hypoxia-mediated induction of endothelial cell interleukin-1 alpha. An autocrine mechanism promoting expression of leukocyte adhesion molecules on the vessel surface.," *J. Clin. Invest.*, vol. 90, no. 6, pp. 2333–9, Dec. 1992.
- [146] K. Yamauchi-Takahara, Y. Ihara, A. Ogata, K. Yoshizaki, J. Azuma, and T. Kishimoto, "Hypoxic stress induces cardiac myocyte-derived interleukin-6.," *Circulation*, vol. 91, no. 5, pp. 1520–4, Mar. 1995.
- [147] S. L. Hempel, M. M. Monick, and G. W. Hunninghake, "Effect of hypoxia on release of IL-1 and TNF by human alveolar macrophages.," *Am. J. Respir. Cell Mol. Biol.*, vol. 14, no. 2, pp.

- 170–6, Feb. 1996.
- [148] N. Yoshida, D. N. Granger, D. C. Anderson, R. Rothlein, C. Lane, and P. R. Kvietys, “Anoxia/reoxygenation-induced neutrophil adherence to cultured endothelial cells.,” *Am. J. Physiol.*, vol. 262, no. 6 Pt 2, pp. H1891-8, Jun. 1992.
- [149] D. C. Hess, W. Zhao, J. Carroll, M. McEachin, and K. Buchanan, “Increased expression of ICAM-1 during reoxygenation in brain endothelial cells.,” *Stroke*, vol. 25, no. 7, p. 1463–7; discussion 1468, Jul. 1994.
- [150] T. S. Kang, D. Georgieva, N. Genov, M. T. Murakami, M. Sinha, R. P. Kumar, P. Kaur, S. Kumar, S. Dey, S. Sharma, A. Vrieling, C. Betzel, S. Takeda, R. K. Arni, T. P. Singh, and R. M. Kini, “Enzymatic toxins from snake venom: structural characterization and mechanism of catalysis,” *FEBS J.*, vol. 278, no. 23, pp. 4544–4576, Dec. 2011.
- [151] T. M. R. Manjunatha Kini, Kenneth J Clemetson, Francis S. Markland, Mary Ann McLane, *Toxins and Hemostasis*. Dordrecht: Springer Netherlands, 2011.
- [152] W.-K. You, H.-J. Seo, K.-H. Chung, and D.-S. Kim, “A novel metalloprotease from *Gloydius halys* venom induces endothelial cell apoptosis through its protease and disintegrin-like domains.,” *J. Biochem.*, vol. 134, no. 5, pp. 739–49, Nov. 2003.
- [153] J. J. Calvete, M. P. Moreno-Murciano, R. D. G. Theakston, D. G. Kisiel, and C. Marcinkiewicz, “Snake venom disintegrins: novel dimeric disintegrins and structural diversification by disulphide bond engineering.,” *Biochem. J.*, vol. 372, no. Pt 3, pp. 725–34, Jun. 2003.
- [154] Y. Wang, M. C. de Waard, A. Sterner-Kock, H. Stepan, H.-P. Schultheiss, D. J. Duncker, and T. Walther, “Cardiomyocyte-restricted over-expression of C-type natriuretic peptide prevents cardiac hypertrophy induced by myocardial infarction in mice.,” *Eur. J. Heart Fail.*, vol. 9, no. 6–7, pp. 548–57, Jun. 2007.
- [155] T. Soeki, I. Kishimoto, H. Okumura, T. Tokudome, T. Horio, K. Mori, and K. Kangawa, “C-type natriuretic peptide, a novel antifibrotic and antihypertrophic agent, prevents cardiac remodeling after myocardial infarction,” *J. Am. Coll. Cardiol.*, vol. 45, no. 4, pp. 608–616, Feb. 2005.
- [156] N. A. Santos-Filho and C. T. Santos, “Alpha-type phospholipase A2 inhibitors from snake blood,” *J. Venom. Anim. Toxins Incl. Trop. Dis.*, vol. 23, no. 1, p. 19, Dec. 2017.
- [157] R. Schezaro-Ramos, R. de C. O. Collaço, P. Randazzo-Moura, T. Rocha, J. C. Cogo, and L. Rodrigues-Simioni, “Influence of phospholipase inhibition on neuromuscular activity of *Bothrops fonsecai* snake venom,” *Toxicon*, vol. 130, pp. 35–43, May 2017.
- [158] D. C. Achê, M. S. R. Gomes, D. L. N. de Souza, M. A. Silva, M. I. H. Brandeburgo, K. A. G. Yoneyama, R. S. Rodrigues, M. H. Borges, D. S. Lopes, and V. de M. Rodrigues, “Biochemical properties of a new PI SVMP from *Bothrops pauloensis*: Inhibition of cell adhesion and angiogenesis,” *Int. J. Biol. Macromol.*, vol. 72, pp. 445–453, Jan. 2015.
- [159] W. E. Louch, K. A. Sheehan, and B. M. Wolska, “Methods in cardiomyocyte isolation, culture, and gene transfer.,” *J. Mol. Cell. Cardiol.*, vol. 51, no. 3, pp. 288–98, Sep. 2011.
- [160] W. F. SCHERER, J. T. SYVERTON, and G. O. GEY, “Studies on the propagation in vitro of poliomyelitis viruses. IV. Viral multiplication in a stable strain of human malignant epithelial cells (strain HeLa) derived from an epidermoid carcinoma of the cervix.,” *J. Exp. Med.*, vol. 97, no. 5, pp. 695–710, May 1953.
- [161] W. F. Kocholaty, E. B. Ledford, J. G. Daly, and T. A. Billings, “Toxicity and some enzymatic properties and activities in the venoms of Crotalidae, Elapidae and Viperidae.,” *Toxicon*, vol. 9, no. 2, pp. 131–8, Apr. 1971.
- [162] M. L. AHUJA and A. G. BROOKS, “A note on the action of heparin on Russell’s viper venom.,” *Indian J. Med. Res.*, vol. 34, no. 2, pp. 317–22, Oct. 1946.
- [163] D. Sket, F. Gubensek, S. Adamic, and D. Lebez, “Action of a partially purified basic protein fraction from *Vipera ammodytes* venom.,” *Toxicon*, vol. 11, no. 1, pp. 47–53, Jan. 1973.
- [164] C. Moroz, A. de Vries, and M. Sela, “Isolation and characterization of a neurotoxin from

- Vipera palestinae venom.," *Biochim. Biophys. Acta*, vol. 124, no. 1, pp. 136–46, Jul. 1966.
- [165] J. Krupnick, H. I. Bicher, and S. Gitter, "Central neurotoxic effects of the venoms of *Naja naja* and *Vipera palestinae*," *Toxicon*, vol. 6, no. 1, pp. 11–6, Aug. 1968.
- [166] R. W. MASTER and S. S. RAO, "Starch-gel electrophoresis of venoms of Indian krait and saw-scaled viper and identification of enzymes and toxins," *Biochim. Biophys. Acta*, vol. 71, pp. 416–21, May 1963.
- [167] F. KORNALIK and P. PUDLAK, "Coagulation defect following non-toxic doses of *Echis viper* venom," *Experientia*, vol. 18, pp. 381–2, Aug. 1962.
- [168] M. L. AHUJA, N. VEERARAGHAVAN, and I. G. K. MENON, "Action of heparin on the venom of *Echis carinatus*," *Nature*, vol. 158, no. 4024, p. 878, Dec. 1946.
- [169] J. RECHNIC, P. TRACHTENBERG, J. CASPER, C. MOROZ, and A. DE VRIES, "Afibrinogenemia and thrombocytopenia in guinea pigs following injection of *Echis colorata* venom," *Blood*, vol. 20, pp. 735–49, Dec. 1962.
- [170] U. Sandbank and M. Djaldetti, "Effect of *Echis colorata* venom inoculation on the nervous system of the dog and guinea pig," *Acta Neuropathol.*, vol. 6, no. 1, pp. 61–9, Jan. 1966.
- [171] U. Sandbank, Z. Jerushalmy, E. Ben-David, and A. De Vries, "Effect of *Echis coloratus* venom on brain vessels," *Toxicon*, vol. 12, no. 3, pp. 267–71, May 1974.
- [172] S. GITTER, G. LEVI, S. KOCHWA, A. DE VRIES, J. RECHNIC, and J. CASPER, "Studies on the venom of *Echis colorata*," *Am. J. Trop. Med. Hyg.*, vol. 9, pp. 391–9, Jul. 1960.
- [173] O. H. Osman and K. A. Gumaa, "Pharmacological studies of snake (*Bitis arietans*) venom," *Toxicon*, vol. 12, no. 6, pp. 569–75, Dec. 1974.
- [174] S. KOCHWA, C. PERLMUTTER, S. GITTER, J. RECHNIC, and A. DE VRIES, "Studies on *Vipera palestinae* venom. Fractionation by ion exchange chromatography," *Am. J. Trop. Med. Hyg.*, vol. 9, pp. 374–80, Jul. 1960.
- [175] R. W. MASTER and S. S. RAO, "Identification of enzymes and toxins in venoms of Indian cobra and Russell's viper after starch gel electrophoresis," *J. Biol. Chem.*, vol. 236, pp. 1986–90, Jul. 1961.
- [176] A. Arutunyan, D. R. Webster, L. M. Swift, and N. Sarvazyan, "Localized injury in cardiomyocyte network: a new experimental model of ischemia-reperfusion arrhythmias," *Am. J. Physiol. Heart Circ. Physiol.*, vol. 280, no. 4, pp. H1905-15, Apr. 2001.
- [177] N. G. Posnack, N. H. Lee, R. Brown, and N. Sarvazyan, "Gene expression profiling of DEHP-treated cardiomyocytes reveals potential causes of phthalate arrhythmogenicity," *Toxicology*, vol. 279, no. 1–3, pp. 54–64, Jan. 2011.
- [178] W. Nieuwenhuizen, H. Kunze, and G. H. de Haas, "Phospholipase A2 (phosphatide acylhydrolase, EC 3.1.1.4) from porcine pancreas," *Methods Enzymol.*, vol. 32, pp. 147–54, 1974.
- [179] C.-Y. Lee, Ed., *Snake Venoms: Handbook of Experimental Pharmacology*, vol. 52. Berlin, Heidelberg: Springer Berlin Heidelberg, 1979.
- [180] C. Eggeling, J. Widengren, R. Rigler, and C. A. M. Seidel, "Photobleaching of Fluorescent Dyes under Conditions Used for Single-Molecule Detection: Evidence of Two-Step Photolysis," *Anal. Chem.*, vol. 70, no. 13, pp. 2651–2659, Jul. 1998.
- [181] T. Mosmann, "Rapid colorimetric assay for cellular growth and survival: application to proliferation and cytotoxicity assays," *J. Immunol. Methods*, vol. 65, no. 1–2, pp. 55–63, Dec. 1983.
- [182] F. Denizot and R. Lang, "Rapid colorimetric assay for cell growth and survival," *J. Immunol. Methods*, vol. 89, no. 2, pp. 271–277, May 1986.
- [183] D. Gerlier and N. Thomasset, "Use of MTT colorimetric assay to measure cell activation," *J. Immunol. Methods*, vol. 94, no. 1–2, pp. 57–63, Nov. 1986.
- [184] J. J. Calvete, L. Sanz, Y. Angulo, B. Lomonte, and J. M. Gutiérrez, "Venoms, venomics, antivenomics," *FEBS Lett.*, vol. 583, no. 11, pp. 1736–43, Jun. 2009.
- [185] S. P. Mackessy, "Evolutionary trends in venom composition in the Western Rattlesnakes

- (*Crotalus viridis sensu lato*): Toxicity vs. tenderizers,” *Toxicon*, vol. 55, no. 8, pp. 1463–1474, Jul. 2010.
- [186] S.P. MacKessy, *Handbook of Venoms and Toxins of Reptiles*. CRC Press, Taylor & Francis Group, 2010.
- [187] R. M. KINI, “Toxins in thrombosis and haemostasis: potential beyond imagination,” *J. Thromb. Haemost.*, vol. 9, pp. 195–208, Jul. 2011.
- [188] R. Kini and C. Koh, “Metalloproteases Affecting Blood Coagulation, Fibrinolysis and Platelet Aggregation from Snake Venoms: Definition and Nomenclature of Interaction Sites,” *Toxins (Basel)*, vol. 8, no. 10, p. 284, Sep. 2016.
- [189] S. Israeli-Rosenberg, A. M. Manso, H. Okada, and R. S. Ross, “Integrins and integrin-associated proteins in the cardiac myocyte,” *Circ. Res.*, vol. 114, no. 3, pp. 572–86, Jan. 2014.
- [190] J. D. Humphries, A. Byron, and M. J. Humphries, “Integrin ligands at a glance,” *J. Cell Sci.*, vol. 119, no. Pt 19, pp. 3901–3, Oct. 2006.
- [191] M. S. Dennis, W. J. Henzel, R. M. Pitti, M. T. Lipari, M. A. Napier, T. A. Deisher, S. Bunting, and R. A. Lazarus, “Platelet glycoprotein IIb-IIIa protein antagonists from snake venoms: evidence for a family of platelet-aggregation inhibitors,” *Proc. Natl. Acad. Sci. U. S. A.*, vol. 87, no. 7, pp. 2471–5, Apr. 1990.
- [192] S. Niewiarowski, M. A. McLane, M. Kloczewiak, and G. J. Stewart, “Disintegrins and other naturally occurring antagonists of platelet fibrinogen receptors,” *Semin. Hematol.*, vol. 31, no. 4, pp. 289–300, Oct. 1994.
- [193] C. Marcinkiewicz, “Functional characteristic of snake venom disintegrins: potential therapeutic implication,” *Curr. Pharm. Des.*, vol. 11, no. 7, pp. 815–27, Jan. 2005.
- [194] D. G. Kisiel, J. J. Calvete, J. Katzhendler, A. Fertala, P. Lazarovici, and C. Marcinkiewicz, “Structural determinants of the selectivity of KTS-disintegrins for the alpha1beta1 integrin,” *FEBS Lett.*, vol. 577, no. 3, pp. 478–82, Nov. 2004.
- [195] Y. Y. Li, C. F. McTiernan, and A. M. Feldman, “Proinflammatory cytokines regulate tissue inhibitors of metalloproteinases and disintegrin metalloproteinase in cardiac cells,” *Cardiovasc. Res.*, vol. 42, no. 1, pp. 162–72, Apr. 1999.
- [196] T. Kurtović, M. Lang Balija, N. Ayvazyan, and B. Halassy, “Paraspecificity of *Vipera ammodytes*-specific antivenom towards *Montivipera raddei* and *Macrovipera lebetina obtusa* venoms,” *Toxicon*, vol. 78, pp. 103–112, Feb. 2014.
- [197] K. A. Y. J. Gordon Betts, OpenStax College, Peter Desaix, Jody E. Johnson, Edward W. Johnson, Oksana Korol, Dean Kruse, Brandon Poe, James Wise, Mark D. Womble, *Anatomy and Physiology - OpenStax*. OpenStax College, 2013.
- [198] F. Martini, J. L. Nath, and E. F. Bartholomew, *Fundamentals of anatomy & physiology*, 10th ed. .
- [199] Y. Ikeda, M. Hoshijima, and K. R. Chien, “Toward biologically targeted therapy of calcium cycling defects in heart failure,” *Physiology (Bethesda)*, vol. 23, no. 1, pp. 6–16, Feb. 2008.
- [200] Boundless, “Mechanism and Contraction Events of Cardiac Muscle Fibers.” Boundless, 21-Oct-2016.